

# A combinatorial approach to Rauzy-type dynamics I: permutations and the Kontsevich–Zorich–Boissy classification theorem

Quentin De Mourgues

*Institut Fourier, Université Grenoble Alpes  
100, rue des Maths, 38610 Gires, France*  
and

*LIPN, Université Paris 13  
99, av. J.-B. Clément, 93430 Villetaneuse, France*  
`quentin.de-mourgues@univ-grenoble-alpes.fr`

Andrea Sportiello

*CNRS, and LIPN, Université Paris 13  
99, av. J.-B. Clément, 93430 Villetaneuse, France*  
`andrea.sportiello@lipn.univ-paris13.fr`

3rd May 2017

**Abstract.** Rauzy-type dynamics are group actions on a collection of combinatorial objects. The first and best known example concerns an action on permutations, associated to interval exchange transformations (IET) for the Poincaré map on compact orientable translation surfaces. The equivalence classes on the objects induced by the group action are related to components of the moduli spaces of Abelian differentials with prescribed singularities, and, in two variants of the problem, have been classified by Kontsevich and Zorich, and by Boissy, through methods involving both combinatorics and algebraic geometry.

We provide here a purely combinatorial proof of both classification theorems, and in passing establish a few previously unnoticed features. As will be shown elsewhere, our methods extend also to other Rauzy-type dynamics, both on labeled and unlabeled structures. Some of these dynamics have a geometrical interpretation (e.g., matchings, related to IET on non-orientable surfaces), while some others do not have one so far.

# Contents

<b>1 Algebraic setting</b>	<b>3</b>
1.1 Permutational diagram monoids and groups . . . . .	3
1.2 Three basic examples of dynamics . . . . .	5
1.3 What kind of results? . . . . .	7
1.4 Definition of the invariants . . . . .	8
1.5 Exceptional classes . . . . .	11
1.6 The classification theorems . . . . .	13
1.7 Surgery operators . . . . .	14
<b>2 Connection with the geometry of translation surfaces</b>	<b>16</b>
2.1 Strata of translation surfaces . . . . .	16
2.2 Geometric interpretation of the invariants . . . . .	24
2.3 Surgery operators . . . . .	28
2.4 A summary of terminology . . . . .	37
<b>3 Some basic facts</b>	<b>38</b>
3.1 Properties of the cycle invariant . . . . .	38
3.2 Standard permutations . . . . .	40
3.3 Standard families . . . . .	42
3.4 Reduced dynamics and boosted dynamics . . . . .	45
3.5 Square constructors for permutations . . . . .	46
<b>4 The sign invariant</b>	<b>48</b>
4.1 Arf functions for permutations . . . . .	48
4.2 Calculating with Arf functions . . . . .	49
<b>5 Surgery operators</b>	<b>53</b>
5.1 Operator $T$ . . . . .	54
5.2 Operators $q_1$ and $q_2$ . . . . .	62
<b>6 The induction</b>	<b>67</b>
6.1 Simple properties of the invariant . . . . .	68
6.2 Fusion lemmas for $T$ . . . . .	69
6.3 Fusion lemmas for $q_1$ and $q_2$ . . . . .	70
6.4 Classification of Rauzy classes . . . . .	72
6.5 Classification of extended Rauzy classes . . . . .	75
<b>A Representation of Cayley graphs</b>	<b>78</b>
<b>B Non-primitive classes</b>	<b>79</b>
<b>C Exceptional classes</b>	<b>81</b>
C.1 Classes $\text{Id}_n$ . . . . .	82
C.2 Classes $\text{Id}'_n$ . . . . .	85
C.3 Synthetic presentation of classes $\text{Id}_n$ and $\text{Id}'_n$ . . . . .	87

# 1 Algebraic setting

## 1.1 Permutational diagram monoids and groups

Let  $X_I$  be a set of labeled combinatorial objects, with elements labeled from the set  $I$ .<sup>1</sup> We use the shortcut  $[n] = \{1, 2, \dots, n\}$ , and  $X_n \equiv X_{[n]}$ . The symmetric group  $\mathfrak{S}_n$  acts naturally on  $X_n$ , by producing the object with permuted labels.<sup>2</sup>

Vertex-labeled graphs (or digraphs, or hypergraphs) are a typical example. Extra structure may be added, e.g. in hypergraphs we can complement hyperedges with a cyclic ordering of the incident vertices, and in both graphs and hypergraphs we can specify a cyclic ordering of the incident edges at each vertex. This provides an embedding of the abstract graph on a surface.

Set partitions are a special case of hypergraphs (all vertices have degree 1). Matchings are a special case of partitions, in which all blocks have size 2. Permutations  $\sigma$  are a special case of matchings, in which each block  $\{i, j\}$  has  $i \in \{1, 2, \dots, n\}$  and  $j = \sigma(i) + n \in \{n + 1, n + 2, \dots, 2n\}$ .

We will consider dynamics over spaces of this type, generated by operators of a special form that we now introduce:

**Definition 1.1** (Monoid and group operators). *We say that  $A$  is a monoid operator on set  $X_n$ , if, for the datum of a finite set  $Y_n$ , a map  $a : X_n \rightarrow Y_n$ , and a map  $\alpha : Y_n \rightarrow \mathfrak{S}_n$ , it consists of the map on  $X_n$  defined by*

$$A(x) = \alpha_{a(x)}x, \quad (1)$$

where the action  $\alpha x$  is in the sense of the symmetric-group action over  $X_n$ . We say that  $A$  is a group operator if, furthermore,  $a(A(x)) = a(x)$ .

Said informally, the function  $a$  ‘‘poses a question’’ to the structure  $x$ . The possible answers are listed in the set  $Y$ . For each answer, there is a different permutation, by which we act on  $x$ . Actually, as anticipated, we only use  $a$  and  $\alpha$  in the combination  $A = \alpha_{a(\cdot)}$ , so that the use of two symbols for the single function  $A$  is redundant. This choice is done for clarity in our applications, where the notation allows to stress that  $Y_n$  has a much smaller cardinality than  $X_n$  and  $\mathfrak{S}_n$ , i.e. very few ‘answers’ are possible. In our main application,  $|X_n| = |\mathfrak{S}_n| = n!$  while  $|Y_n| = n$ . The asymptotic behaviour is similar ( $|X_n|$  at least exponential,  $|Y_n|$  at most linear) in all of our applications.

Clearly we have:

**Proposition 1.2.** *Group operators are invertible.*

*Proof.* The property  $a(A(x)) = a(x)$  implies that, for all  $k \in \mathbb{N}$ ,  $A^k(x) = (\alpha_{a(x)})^k x$ . Thus, for all  $x$  there exists an integer  $d_A(x) \in \mathbb{N}^+$  such that  $A^{d_A(x)}(x) = x$ . More precisely,  $d_A(x)$  is the l.c.m. of the cycle-lengths of  $\alpha_{a(x)}$ . Call  $d_A = \text{lcm}_{x \in X_n} d_A(x)$ . Then  $d_A$  is a finite integer, and we can pose  $A^{-1} = A^{d_A-1}$ . The reasonings above shows that  $A$  is a bijection on  $X_n$ , and  $A^{-1}$  is its inverse.  $\square$

**Definition 1.3** (monoid and group dynamics). *We call a monoid dynamics the datum of a family of spaces  $\{X_n\}_{n \in \mathbb{N}}$  as above, and a finite collection  $\mathcal{A} = \{A_i\}$  of monoid operators. We call a group dynamics the analogous structure, in which all  $A_i$ ’s are group operators.*

*For a monoid dynamics on the datum  $S_n = (X_n, \mathcal{A})$ , we say that  $x, x' \in X_n$  are strongly connected,  $x \sim x'$ , if there exist words  $w, w' \in \mathcal{A}^*$  such that  $wx = x'$  and  $w'x' = x$ .*

*For a group dynamics on the datum  $S_n = (X_n, \mathcal{A})$ , we say that  $x, x' \in X_n$  are connected,  $x \sim x'$ , if there exists a word  $w \in \mathcal{A}^*$  such that  $wx = x'$ .*

<sup>1</sup>In the most general context  $I$  may be a multi-set, i.e. allow for repetitions. However, at the purposes of the present paper, we will mainly concentrate on the case in which each label is repeated exactly once.

<sup>2</sup>For  $I$  a multiset, the natural action would be the one of  $\mathfrak{S}_{|I|}/\text{Aut}(I)$ .

Here the action  $wx$  is in the sense of monoid action. Being connected is clearly an equivalence relation, and coincides with the relation of being graph-connected on the Cayley Graph associated to the dynamics, i.e. the digraph with vertices in  $X_n$ , and edges  $x \longleftrightarrow_i x'$  if  $A_i^{\pm 1}x = x'$ . An analogous statement holds for strong-connectivity, and the associated Cayley Digraph.

**Definition 1.4** (classes of configurations). *Given a dynamics as above, and  $x \in X_n$ , we define  $C(x) \subseteq X_n$ , the class of  $x$ , as the set of configurations connected to  $x$ ,  $C(x) = \{x' : x \sim x'\}$ .*

Two natural distances on the classes of  $X_n$  can be associated to a group dynamics with generators  $\mathcal{A} = \{A_i\}$ .

**Definition 1.5** (distance and alternation distance). *Let  $\sigma, \tau$  configurations of  $X_n$  in the same class. The graph distance  $d_G(\sigma, \tau)$  is the ordinary graph distance in the associated Cayley Graph, i.e.  $d_G(\sigma, \tau)$  is the minimum  $\ell \in \mathbb{N}$  such that there exists a word  $w \in \{A_i, A_i^{-1}\}^*$ , of length  $\ell$ , such that  $\tau = w\sigma$ . A graph geodesic is a  $w$  realising the minimum. We also define the alternation distance  $d(\sigma, \tau)$ , and alternation geodesics, as the analogous quantities, for words in the infinite alphabet  $\{(A_i)^j\}_{j \geq 1}$ .*

**Example 1.6.** *If  $w = a^3 b a^{-2} b^{-3} a$ , and  $wx = x'$ , we know that the distance  $d_G(x, x')$  is at most  $3 + 1 + 2 + 3 + 1 = 10$ , and the alternation distance  $d(x, x')$  is at most 5.*

Contrarily to graph distance, the alternation distance is stable w.r.t. a number of combinatorial operations that we will perform on our configurations, and which are defined later on in the text or in future work (restriction to ‘primitive classes’, study of ‘reduced dynamics’, permutations in  $\mathfrak{S}_\infty, \dots$ ). These facts suggests that alternation distance is a more natural notion in this family of problems.

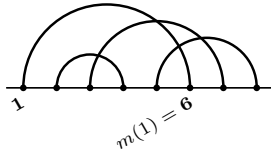
The goal of the series of papers, of which this is the first one, is to provide *classification theorems* for dynamics of this kind.

In this and a companion paper we will be concerned with the classification of classes, and further combinatorial study of their structure, for three special group dynamics. These dynamics are two version of the *Rauzy dynamics*, first introduced by Rauzy [Rau79], and whose study has been pioneered by Veech [Vee82] and Masur [Mas82] (the connected classes are called *Rauzy classes*). In these cases the group action is related to the interval exchange map on translation surfaces. Thus, on one side, its study is motivated by questions in dynamical systems. On the other side, the previously obtained classification of classes relies on notions and known results in algebraic geometry. Section 1.2 describes these three dynamics, and Section 2 gives a short account of these connections.

The classification theorems associated to these families have been provided (with some *caveat* discussed later on) in a series of papers, starting with the seminal work of Kontsevich and Zorich [KZ03], and followed by [Boi12], so our approach provides just an alternative derivation of these results. Nonetheless, it has two points of interest. A first point is that, as our approach is quite different from the previous ones, along the way we happen to extract some extra information on the combinatorial structure of the Rauzy classes. An example, which is mentioned in Section 2.3 and that will be illustrated in more detail in future work, is the construction of ‘many’ representatives for each Rauzy class, extending previous results of Zorich [Zor08]. The second, more methodological point of interest is that our approach is completely combinatorial, self-contained, and in particular it makes no use of any facts from algebraic geometry. In this sense, it answers a question posed by Kontsevich and Zorich in [KZ03]:

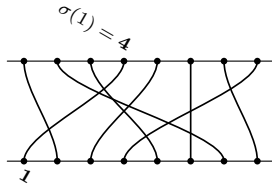
*The extended Rauzy classes can be defined in purely combinatorial terms [...] thus the problem of the description of the extended Rauzy classes, and hence, of the description of connected components of the strata of Abelian differentials, is purely combinatorial. However, it seems very hard to solve it directly. [...] we give a classification of extended Rauzy classes using not only combinatorics but also tools of algebraic geometry, topology and of dynamical systems.*

$$m = ((16)(24)(37)(58)) \in \mathcal{M}_8$$



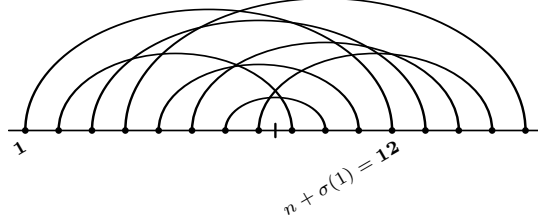
$$\sigma = [41583627] \in \mathfrak{S}_8$$

diagram representation



$$\sigma = [41583627] \in \mathfrak{S}_8 \subseteq \mathcal{M}_{16}$$

matching diagram representation



$$\sigma = [41583627] \in \mathfrak{S}_8$$

matrix representation

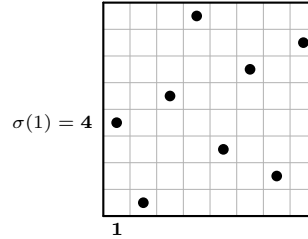


Figure 1: Diagram representations of matchings and permutations, and matrix representation of permutations.

Note that the task of providing a purely combinatorial proof of these classification theorems has been also carried over, with different methods than ours, by [Fic16].

In further papers, we will address also other variants of these group actions on combinatorial structures, that, by analogy, we name *Rauzy-type dynamics*. A number of these other versions do not have at the moment any algebraic or geometric interpretation, nonetheless reasonings on similar grounds of the ones presented here provide a classification theorem also in these other cases.

## 1.2 Three basic examples of dynamics

Let  $\mathfrak{S}_n$  denote the set of permutations of size  $n$ , and  $\mathfrak{M}_n$  the set of matchings over  $[2n]$ , thus with  $n$  arcs. Let us call  $\omega$  the permutation  $\omega(i) = n + 1 - i$ .

A permutation  $\sigma \in \mathfrak{S}_n$  can be seen as a special case of a matching over  $[2n]$ , in which the first  $n$  elements are paired to the last  $n$  ones, i.e. the matching  $m_\sigma \in \mathfrak{M}_n$  associated to  $\sigma$  is  $m_\sigma = \{(i, \sigma(i) + n) \mid i \in [n]\}$ .

We say that  $\sigma \in \mathfrak{S}_n$  is *irreducible* if  $\omega\sigma$  doesn't leave stable any interval  $\{1, \dots, k\}$ , for  $1 \leq k < n$ , i.e. if  $\{\sigma(1), \dots, \sigma(k)\} \neq \{n - k + 1, \dots, n\}$  for any  $k = 1, \dots, n - 1$ . We also say that  $m \in \mathfrak{M}_n$  is *irreducible* if it does not match an interval  $\{1, \dots, k\}$  to an interval  $\{2n - k + 1, \dots, 2n\}$ . Let us call  $\mathfrak{S}_n^{\text{irr}}$  and  $\mathfrak{M}_n^{\text{irr}}$  the corresponding sets of irreducible configurations.

We represent matchings over  $[2n]$  as arcs in the upper half plane, connecting pairwise  $2n$  points on the real line (see figure 1, top left). Permutations, being a special case of matching, can also be represented in this way (see figure 1, top right), however, in order to save space and improve readability, we rather represent them as arcs in a horizontal strip, connecting  $n$  points at the bottom boundary to  $n$  points on the top boundary (as in Figure 1, bottom left). Both sets of points are indicised from left to right. We use the name of *diagram representation* for such representations.

We will also often represent configurations as grids filled with one bullet per row and per column (and call this *matrix representation* of a permutation). We choose here to conform to

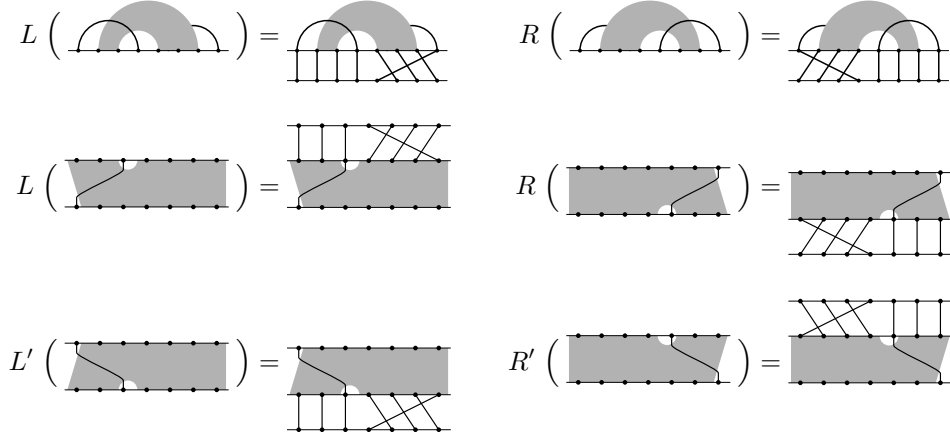


Figure 2: Our three main examples of dynamics, in diagram representation. Top: the  $\mathcal{M}_n$  case. Middle: the  $\mathcal{S}_n$  case. Bottom: in the  $\mathcal{S}_n^{\text{ex}}$  case we have the same operators  $L$  and  $R$  as in the  $\mathcal{S}_n$  case, plus the two operators  $L'$  and  $R'$ .

the customary notation in the field of Permutation Patterns, by adopting the algebraically weird notation, of putting a bullet at the *Cartesian* coordinate  $(i, j)$  if  $\sigma(i) = j$ , so that the identity is a grid filled with bullets on the *anti-diagonal*, instead that on the diagonal. An example is given in figure 1, bottom right.

Let us define a special set of permutations (in cycle notation)

$$\gamma_{L,n}(i) = (i-1 \ i-2 \ \dots \ 1)(i)(i+1) \dots (n); \quad (2a)$$

$$\gamma_{R,n}(i) = (1)(2) \dots (i)(i+1 \ i+2 \ \dots \ n); \quad (2b)$$

i.e., in a picture in which the action is diagrammatic, and acting on structures  $x \in X_n$  from below,



Of course,  $\omega \gamma_{L,n}(i) \omega = \gamma_{R,n}(n+1-i)$ .

The three group dynamics we mainly analyse in this and companion papers are

$\mathcal{M}_n$ : The space of configuration is  $\mathfrak{M}_n^{\text{irr}}$ , irreducible  $n$ -arc matchings. There are two generators,  $L$  and  $R$ , with  $a_L(m)$  being the index paired to 1,  $a_R(m)$  the index paired to  $2n$ ,  $\alpha_{L,i} = \gamma_{L,i,2n}$ , and  $\alpha_{R,i} = \gamma_{R,i,2n}$  ( $a$  and  $\alpha$  are as in Definition 1.1). See Figure 2, top.

$\mathcal{S}_n$ : The space of configuration is  $\mathfrak{S}_n^{\text{irr}}$ , irreducible permutations of size  $n$ . Again, there are two generators,  $L$  and  $R$ . If permutations are seen as matchings such that indices in  $\{1, \dots, n\}$  are paired to indices in  $\{n+1, \dots, 2n\}$ , the dynamics coincide with the one given above. See Figure 2, middle.

$\mathcal{S}_n^{\text{ex}}$ : The space of configuration is  $\mathfrak{S}_n^{\text{irr}}$ . Now we have four generators,  $L$  and  $R$  are as above, and  $L'$  and  $R'$  act as  $L'\sigma = S(L(S\sigma))$ , and  $R'\sigma = S(R(S\sigma))$  where  $S$  is the anti-diagonal axial symmetry in the matrix representation. See Figure 2, middle and bottom.

More precisely, we study  $\mathcal{S}_n$  and  $\mathcal{S}_n^{\text{ex}}$  here, and delay the study of  $\mathcal{M}_n$  to future work.

The motivation for restricting to irreducible permutations and matchings shall be clear at this point: a non-irreducible permutation is a grid with a non-trivial block-decomposition.

The operators  $L$  and  $R$  only act on the first block (say, of size  $k$ ), while, in  $\mathcal{S}_n^{\text{ex}}$ , the operators  $L'$  and  $R'$  only act on the last block (say, of size  $k'$ ), so that the study of the dynamics trivially reduces to the study of the  $\mathcal{S}_k$  dynamics, or of the direct product  $\mathcal{S}_k \times \mathcal{S}_{k'}$ , on these blocks (see figure 4).

This simple observation, however, comes with a disclaimer: in our combinatorial operations on configurations, which produce the required induction steps in the classification theorem, we shall always guarantee that the outcome of our manipulations on irreducible configurations is still irreducible. Proving such a condition will occasionally be a subtle task.

### 1.3 What kind of results?

In the series of papers initiated by the present one, we study collections  $X_n$  of discrete combinatorial objects, where  $n$  is a size parameter, and the cardinality of  $X_n$  is exponential or super-exponential (i.e.,  $\ln X_n = \Theta(n(\ln n)^\gamma)$ ) for some  $\gamma$ ). We introduce two or more bijections, called ‘operators’, like the operators  $L, R, \dots$  of the previous section, and define classes as the connected components of the associated Cayley Graph. It will come out that there is a super-polynomial number of classes (in the examples investigated here, roughly  $\exp(\alpha\sqrt{n})$  for a certain  $\alpha$ ), the majority of them having super-exponential cardinalities, which are not ‘round’ numbers<sup>3</sup>.

Thus, a natural question is: in which form can we expect to ‘solve’ such a problem, if the structure of the problem is apparently so wild, and any possible complete answer is most likely not encompassed by a compact formula?

We may expect, and in fact give here, results of the following forms:

- A *classification* of the classes, i.e., the identification of a natural labeling of the classes, and a criterium that, for a configuration of size  $n$ , gives the label of its class through an algorithm which is polynomial in  $n$  (and possibly linear). As a corollary, this would give an algorithm that, for any two configurations, determines in polynomial time if they are in the same class or not.<sup>4</sup>
- The exact characterisation of the Cayley Graph of the few *exceptional classes* that may exist, which in fact *do* have round formulas, and an intelligible structure. Interestingly,

<sup>3</sup>I.e., numbers which most likely do not have simple factorised formulas, contrarily e.g. to the existence of hook formulas for the number of standard and semi-standard Young tableaux, or MacMahon formulas for the number of plane partitions, and various other examples in Algebraic Combinatorics.

<sup>4</sup>We insist on the algorithm complexity aspect as, if we do not pose a complexity bound, the mere greedy exploration of the Cayley Graph trivialises the question at hand.

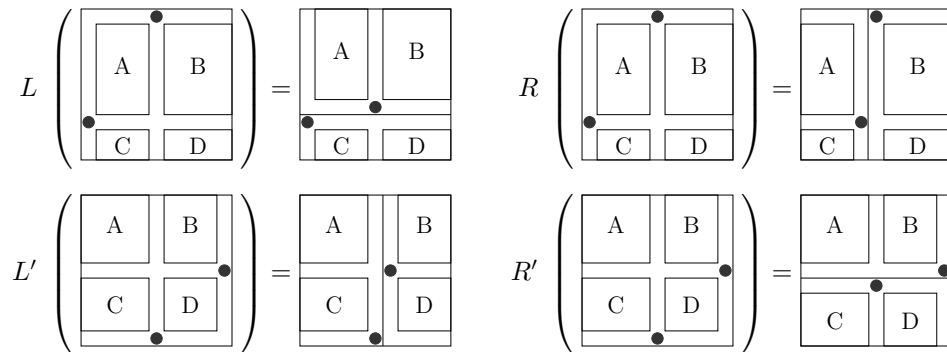


Figure 3: Our two examples of dynamics concerning permutations, in matrix representation. Top: the  $\mathcal{S}_n$  case. Bottom: in the  $\mathcal{S}_n^{\text{ex}}$  case we have the same operators  $L$  and  $R$  as in the  $\mathcal{S}_n$  case, plus the two operators  $L'$  and  $R'$ . See also Figure 2.

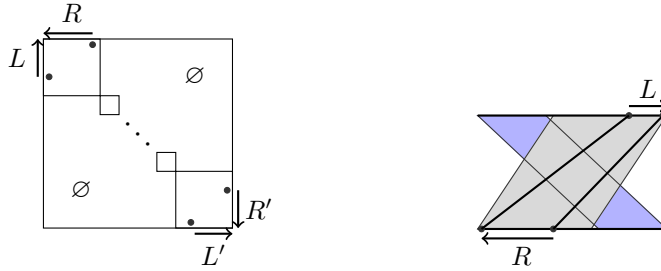


Figure 4: Left: A reducible permutation in matrix representation; the  $\mathcal{S}^{\text{ex}}$  dynamic acts on the first block with  $L$  and  $R$  and on the last block with  $L'$  and  $R'$ . An analogous statement holds for the dynamics  $\mathcal{S}$ . Right: A reducible permutation in diagram representation; the  $\mathcal{S}$  dynamics acts on the gray part with  $L$  and  $R$ , while leaving the blue part unchanged. An analogous statement holds for the dynamics  $\mathcal{S}^{\text{ex}}$ .

in the case of the Rauzy dynamics, we found two exceptional classes: the hyperelliptic one that has been understood since Rauzy [Rau79, sec. 4], and a second one, which is primitive only in the  $\mathcal{S}$  dynamics (not in the  $\mathcal{S}^{\text{ex}}$  one), and, to the best of our knowledge, was never described before. These two classes play an important role in the forementioned classification theorem, and their detailed study is performed in Appendix C.

- Upper/lower bounds on various interesting quantities, e.g. the cardinalities of the classes, or their diameter.
- Finally, what we consider the most important and original contribution of our work, the elucidation of a combinatorial structure which is recursive in  $n$ : even if the structure of the classes at size  $n$  is intrinsically too complex for being described by a simple formula (see [Del13] for the most compact formulas known so far), nothing prevents in principle from the existence of a reasonably explicit description of this structure at size  $n$ , in terms of the structures at sizes  $n' < n$ . This interplay of structures at different sizes, obtained through peculiar “surgery” operations at the level of the corresponding Cayley Graphs (partially analogous to the well-established surgeries at the level of Riemann surfaces of [EMZ03, KZ03], see the following Section 2.3), appears at several stages in our proofs.

## 1.4 Definition of the invariants

The main purpose of this paper, and its first companion, is to characterise the classes appearing in the dynamics introduced above: of  $\mathcal{S}_n$  and  $\mathcal{S}_n^{\text{ex}}$ , in this paper, and of  $\mathcal{M}_n$ , in the companion one. The characterisation is based roughly on three steps: (1) we identify some “exceptional classes”, for which the structure of the configurations is completely elucidated; (2) we identify a collection of data structures which are invariant under the dynamics; (3) we prove, through a complex induction based on surgery, that these invariants are complete, i.e. we characterise the admissible invariant structures, and prove that configurations with the same invariant, and not in an exceptional class, are also in the same class.

In this section we sketch the step (2), i.e. we present the invariants. Some of the proofs are postponed.



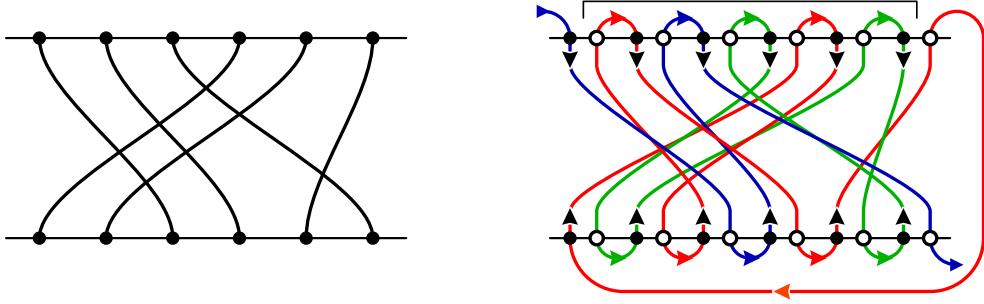


Figure 5: Left: an irreducible permutation,  $\sigma = [451263]$ . Right: the construction of the cycle structure. Different cycles are in different colour. The length of a cycle or path, defined as the number of top (or bottom) arcs, is thus 2 for red and violet, and 1 for blue. The green arrows are the endpoints of the rank path, which is in blue. As a result, in this example  $\lambda(\sigma) = (2, 2)$  (for the cycles of color red and violet),  $r(\sigma) = 1$  (corresponding to the rank path of color blue), and  $\ell(\sigma) = 2$ .

### 1.4.1 Cycle invariant

Let  $\sigma$  be a permutation, identified with its diagram. An edge of  $\sigma$  is a pair  $(i^-, j^+)$ , for  $j = \sigma(i)$ , where  $-$  and  $+$  denote positioning at the bottom and top boundary of the diagram. Perform the following manipulations on the diagram: (1) replace each edge with a pair of crossing edges; more precisely, replace each edge endpoint, say  $i^-$ , by a black and a white endpoint,  $i_b^-$  and  $i_w^-$  (the black on the left), then introduce the edges  $(i_b^-, j_w^+)$  and  $(i_w^-, j_b^+)$ . (2) connect by an arc the points  $i_w^\pm$  and  $(i+1)_b^\pm$ , for  $i = 1, \dots, n-1$ , both on the bottom and the top of the diagram; (3) connect by an arc the top-right and bottom-left endpoints,  $n_w^+$  and  $1_b^-$ . Call this arc the “ $-1$  mark”.

The resulting structure is composed of a number of closed cycles, and one open path connecting the top-left and bottom-right endpoints, that we call the *rank path*. If it is a cycle that goes through the  $-1$  mark (and not the rank path), we call it the *principal cycle*. Define the length of an (open or closed) path as the number of top (or bottom) arcs (connecting a white endpoint to a black endpoint) in the path. These numbers are always positive integers (for  $n > 1$  and irreducible permutations). The length  $r$  of the rank path will be called the *rank* of  $\sigma$ , and  $\lambda = \{\lambda_i\}$ , the collection of lengths of the cycles, will be called the *cycle structure* of  $\sigma$ . Define  $\ell(\sigma)$  as the number of cycles in  $\sigma$  (this does not include the rank). See Figure 5, for an example.

Note that this quantity does *not* coincide with the ordinary path-length of the corresponding paths. The path-length of a cycle of length  $k$  is  $2k$ , unless it goes through the  $-1$  mark, in which case it is  $2k+1$ . Analogously, if the rank is  $r$ , the path-length of the rank path is  $2r+1$ , unless it goes through the  $-1$  mark, in which case it is  $2r+2$ . (This somewhat justifies the name of “ $-1$  mark” for the corresponding arc in the construction of the cycle invariant.)

In the interpretation within the geometry of translation surfaces, the cycle invariant is exactly the collection of conical singularities in the surface (we have a singularity of  $2k\pi$  on the surface, for every cycle of length  $\lambda_i = k$  in the cycle invariant, and the rank corresponds to the ‘marked singularity’ of [Boi12], see Section 2).

It is easily seen that

$$r + \sum_i \lambda_i = n - 1, \quad (3)$$

this formula is called the *dimension formula*. Moreover, in the list  $\{r, \lambda_1, \dots, \lambda_\ell\}$ , there is an even number of even entries (This is part of Lemma 6.1 in Section 6.1, but it could also

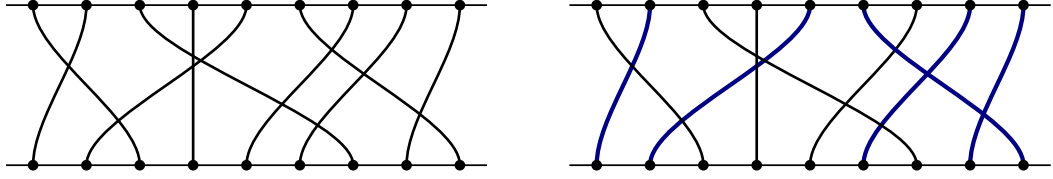


Figure 6: Left: an example of permutation,  $\sigma = [251478396]$ . Right: an example of subset  $I = \{1, 2, 6, 8, 9\}$  (labels are for the bottom endpoints, edges in  $I$  are in blue). There are two crossings, out of the maximal number  $\binom{|I|}{2} = 10$ , thus  $\chi_I = 8$  in this case, and this set contributes  $(-1)^{|I|+\chi_I} = (-1)^{5+8} = -1$  to  $A(\sigma)$ .

be proven easily already at this stage<sup>5</sup>).

We have

**Proposition 1.7.** *The pair  $(\lambda, r)$  is invariant in the  $\mathcal{S}$  dynamics.*

Now connect also the endpoints  $n_{\bar{w}}$  and  $1_b^+$  of the rank path. Call  $\lambda' = \lambda \cup \{r\}$  the resulting collection of cycle lengths. It is easily seen that

$$\sum_i \lambda'_i = n - 1. \quad (4)$$

We have

**Proposition 1.8.** *The quantity  $\lambda'$  is invariant in the  $\mathcal{S}^{\text{ex}}$  dynamics.*

These two propositions are proven in Section 3.1.

#### 1.4.2 Sign invariant

For  $\sigma$  a permutation, let  $[n]$  be identified to the set of edges (e.g., by labeling the edges w.r.t. the bottom endpoints, left to right). For  $I \subseteq [n]$  a set of edges, define  $\chi(I)$  as the number of pairs  $\{i', i''\} \subseteq I$  of non-crossing edges. Call

$$\bar{A}(\sigma) := \sum_{I \subseteq [n]} (-1)^{|I|+\chi(I)} \quad (5)$$

the *Arf invariant* of  $\sigma$  (see Figure 6 for an example). Call  $s(\sigma) = \text{Sign}(\bar{A}(\sigma)) \in \{-1, 0, +1\}$  the *sign* of  $\sigma$ . We have

**Proposition 1.9.** *The sign of  $\sigma$  can be written as  $s(\sigma) = 2^{-\frac{n+\ell}{2}} \bar{A}(\sigma)$ , where  $\ell$  is the number of cycles of  $\sigma$ . The quantity  $s(\sigma)$  is invariant both in the  $\mathcal{S}$  and  $\mathcal{S}^{\text{ex}}$  dynamics.*

The proof of invariance claimed in this proposition is given in Section 4.2, while the proof that  $s(\sigma) = 2^{-\frac{n+\ell}{2}} \bar{A}(\sigma)$  is given in Section 6.1, namely in Lemma 6.1. In section 2 we motivate the name of Arf invariant by making explicit the connection to the associated quantity in the theory of translation surfaces (and, more generally, of Riemann surfaces).

Here we give the main idea in the proof of the invariance. The four operators of  $\mathcal{S}^{\text{ex}}$  are related by a dihedral symmetry of the diagram, and the expression for  $\bar{A}(\sigma)$  is manifestly invariant under these symmetries, so it suffices to consider just one operator, say  $L$ . This operator uses an edge  $e$  of the diagram of  $\sigma$  to determine the permutation, then it moves

<sup>5</sup>This is a simple induction. Adding an edge at any given position changes the cycle invariant either by  $\lambda_i \rightarrow a + 1 \oplus \lambda_i - a$  for some  $a$ , or by  $\lambda_i \oplus \lambda_j \rightarrow \lambda_i + \lambda_j + 1$ . A case analysis on the parity of  $\lambda_i$ ,  $a$  and  $\lambda_j$  leads to our claim.

a number of edge endpoints by a single position on the left, and the endpoint of a second edge  $f$  on the right.

Any function of the form  $F(\sigma) = \sum_{I \subseteq [n]} f_\sigma(I)$  can be decomposed in the form

$$F(\sigma) = \sum_{I \subseteq [n] \setminus \{e, f\}} (f_\sigma(I) + f_\sigma(I \cup \{e\}) + f_\sigma(I \cup \{f\}) + f_\sigma(I \cup \{e, f\})).$$

Call  $\tau = L(\sigma)$ . It can be verified that, for the function  $\bar{A}(\sigma)$ ,

$$\begin{aligned} f_\sigma(I) &= f_\tau(I), & f_\sigma(I \cup \{e\}) &= f_\tau(I \cup \{e\}), \\ f_\sigma(I \cup \{f\}) &= f_\tau(I \cup \{e, f\}), & f_\sigma(I \cup \{e, f\}) &= f_\tau(I \cup \{f\}), \end{aligned}$$

so that the sum of the four terms is invariant for any given  $I \subseteq [n] \setminus \{e, f\}$ .

### 1.4.3 Cycles of length 1 and primitivity

We have stated in Section 1.4.1 that a certain graphical construction leads to the definition of a ‘‘cycle invariant’’. In this section we discuss how cycles of length 1 have an especially simple behaviour.

Establishing this simplifying feature is helpful in our proof of the main classification theorem. It goes in the direction of understanding as many as possible relevant combinatorial features of these classes, and allows us to rule out a large part of the massive numerics associated to this problem.

**Definition 1.10** (descent and special descent). *For a permutation  $\sigma$  in the dynamics  $\mathcal{S}_n$ , we say that the edge  $(i, \sigma(i))$  is a descent if  $\sigma(i+1) = \sigma(i) - 1$ , and it is a special descent if  $\sigma(1) = \sigma(i) - 1$  and  $\sigma(i+1) = n$ . For  $\sigma$  in the dynamic  $\mathcal{S}_n^{\text{ex}}$ , we say that  $(i, \sigma(i))$  is a special descent also if  $\sigma^{-1}(i-1) = 1$  and  $\sigma^{-1}(n) = \sigma(i) + 1$ .*

Note that the descents of a permutation (special or not) are associated to cycles of length 1 (see figure 7 left). In particular, the number of descents is preserved by the dynamics. Say that  $\sigma$  is *primitive* if it has no descents. Hence in a given class  $C$  either all permutations are primitive (in this case we say that  $C$  is a *primitive class*), or none is. We define  $\text{prim}(\sigma)$ , the *primitive of  $\sigma$* , as the configuration obtained by removing descent- and special-descent-edges from  $\sigma$  (see figure 7 for an example in the  $\mathcal{S}$  dynamics). We have

**Proposition 1.11.**  $\sigma \sim \tau$  iff  $\text{prim}(\sigma) \sim \text{prim}(\tau)$  and  $|\sigma| = |\tau|$ .

In other words, within a class we can ‘move the descents freely’. In particular, this gives

**Corollary 1.12.** *The map  $\text{prim}(\cdot)$  is a homomorphism for the dynamics.*

I.e., if  $\sigma \sim \tau$ , then  $\text{prim}(\sigma) \sim \text{prim}(\tau)$ . In fact, much more is true (various other properties are discussed in Appendix B).

## 1.5 Exceptional classes

As we have outlined, a simple preliminary analysis allows to restrict to ‘irreducible’ and ‘primitive’ classes. Then, as anticipated, the invariants described above allow to characterise all primitive classes for the dynamics on irreducible configurations, *with two exceptions*. These two exceptional classes, for the  $\mathcal{S}_n$  dynamics, are called  $\text{Id}_n$  and  $\text{Id}'_n$ . In the  $\mathcal{S}_n^{\text{ex}}$  dynamics, only  $\text{Id}_n$  remains exceptional and primitive (in the literature on Rauzy dynamics,  $\text{Id}_n$  is called the ‘*hyperelliptic class*’, because the Riemann surface associated to  $\text{Id}_n$  is hyperelliptic. Similarly  $\text{Id}'_n$  is often referred to as the ‘*hyperelliptic class with a marked point*’).

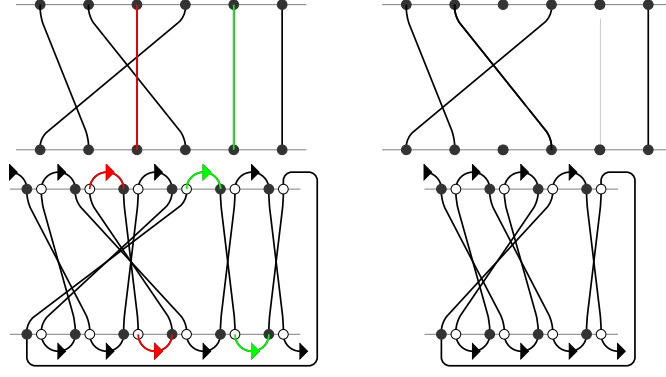
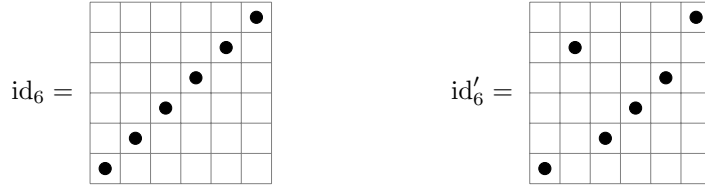


Figure 7: Top left: A non-primitive permutation  $\sigma \in \mathcal{S}_6$  with a descent in red and the special descent in green. Its cycle invariant is  $(\{1, 1\}, r = 3)$  as can be seen explicitly in the cycle construction shown on the bottom left of the figure. Top right: the permutation  $\text{prim}(\sigma)$ , the primitive of  $\sigma$ . Its cycle invariant is  $(\emptyset, r = 3)$ , as can be seen on the bottom right of the figure.

The most compact definition of  $\text{Id}_n$  and  $\text{Id}'_n$  is as being the classes containing  $\text{id}_n$  and  $\text{id}'_n$ , respectively, where  $\text{id}_n$  is the identity of size  $n$ , and, for  $n \geq 3$ ,  $\text{id}'_n$  is the permutation  $\sigma$  of size  $n$  such that  $\sigma(1) = 1$ ,  $\sigma(2) = n - 1$ ,  $\sigma(n) = n$  and  $\sigma(i) = i - 1$  elsewhere, for example



The cycle and sign invariants of these classes depend from their size mod 4, and are described in Table 1. The classes  $\text{Id}_n$  and  $\text{Id}'_n$  are atypical w.r.t. other classes, in various respects:

- They have ‘small’ cardinality. More precisely, at size  $n$ ,  $|\text{Id}_n| = 2^{n-1} - 1$  and  $|\text{Id}'_n| = (2^{n-2} + n - 2)$  (compare this to the fact that all other classes have size  $\geq \exp(cn \ln n)$ , with  $c \geq \frac{2}{3}$ , i.e. at least size  $\sim n!^{2/3}$ ).
- Contrarily to all other classes, the Cayley Graph associated to the dynamics can be described in a compact way, in terms of one or more complete binary trees of a certain height, in the case of  $\text{Id}'_n$  complemented by ‘few’ other nodes and transitions (a linear number).

	$n$ even		$n$ odd					
$(\lambda, r)$ of $\text{Id}_n$	$(\emptyset, n - 1)$		$(\{\frac{n-1}{2}\}, \frac{n-1}{2})$					
$(\lambda, r)$ of $\text{Id}'_n$	$(\{\frac{n-2}{2}, \frac{n-2}{2}\}, 1)$		$(\{n - 2\}, 1)$					
$n \pmod 8$	0	1	2	3	4	5	6	7
$s$ of $\text{Id}_n$	+	0	-	-	-	0	+	+
$s$ of $\text{Id}'_n$	+	+	0	-	-	-	0	+

Table 1: Cycle, rank and sign invariants of the exceptional classes. The sign  $s \in \{-1, 0, +1\}$  is shortened into  $\{-, 0, +\}$ .

$n$	Id	Id'	non-exceptional classes					
4	$\emptyset 3-$							
5	$2 2$	$3 1-$						
6	$\emptyset 5+$	$22 1$	$\emptyset 5-$					
7	$3 3+$	$5 1+$	$2 4$	$4 2$	$3 3-$	$5 1-$		
8	$\emptyset 7+$	$33 1+$	$22 3$	$32 2$	$42 1$	$33 1-$	$\emptyset 7+$	$\emptyset 7-$

Table 2: List of invariants  $(\lambda, r, s)$  for  $n \leq 8$ , for which the corresponding class in the  $\mathcal{S}_n$  dynamics exists. We shorten  $s$  to  $\{-, +\}$  if valued  $\{-1, +1\}$ , and omit it if valued 0.

- The configurations of these classes have a simple structure, labeled by a certain array of integers, and related to the position of the configuration in the Cayley graph. This structure makes easy to verify, in linear time, if a configuration is in  $\text{Id}_n$ , in  $\text{Id}'_n$ , or in none of the above, and thus allows to restrict the quest for a classification to non-special classes.

These results are illustrated at length in Appendix C.

## 1.6 The classification theorems

For the case of the  $\mathcal{S}$  dynamics, we have a classification involving the cycle structure  $\lambda(\sigma)$ , the rank  $r(\sigma)$  and sign  $s(\sigma)$  described in Section 1.4

**Theorem 1.13.** *Two permutations  $\sigma$  and  $\sigma'$  are in the same class iff they have the same number of descents, and  $\text{prim}(\sigma)$ ,  $\text{prim}(\sigma')$ , are in the same class.*

*A permutation  $\sigma$  is primitive iff  $\lambda(\sigma)$  has no parts of size 1 (note that the rank may be 1). Besides the exceptional classes Id and Id', which have cycle and sign invariants described in Table 1, the number of primitive classes with cycle invariant  $(\lambda, r)$  (no  $\lambda_i = 1$ ) depends on the number of even elements in the list  $\{\lambda_i\} \cup \{r\}$ , and is, for  $n \geq 9$ ,*

**zero**, if there is an odd number of even elements;

**one**, if there is a positive even number of even elements; the class then has sign 0.

**two**, if there are no even elements at all. The two classes then have non-zero opposite sign invariant.

*For  $n \leq 8$  the number of primitive classes with given cycle invariant may be smaller than the one given above, and the list in Table 2 gives a complete account.*

*As a consequence, two primitive permutations  $\sigma$  and  $\sigma'$ , not of Id or Id' type, are in the same class iff they have the same cycle and sign invariant.*

For the case of the  $\mathcal{S}^{\text{ex}}$  dynamics, we have only two invariants left, as defined in Section 1.4: the cycle structure  $\lambda'(\sigma)$  and the sign  $s(\sigma)$ . Recall that  $\lambda'(\sigma) = \lambda(\sigma) \cup \{r(\sigma)\}$ , when the

$n$	Id	non-exceptional classes	
4	$3-$		
5	$22$		
6	$5+$	$5-$	
7	$33+$	$24$	$33-$

Table 3: List of invariants  $(\lambda', s)$  for  $n \leq 7$ , for which the corresponding class in the  $\mathcal{S}_n^{\text{ex}}$  dynamics exists. We shorten  $s$  to  $\{-, +\}$  if valued  $\{-1, +1\}$ , and omit it if valued 0.

same configuration is considered under the  $\mathcal{S}$  dynamics. Note however that a permutation that is primitive and of rank 1 in  $\mathcal{S}$ , is not primitive in  $\mathcal{S}^{\text{ex}}$ . In particular, the class  $\text{Id}'_n$ , which has rank 1 for all  $n$ , is non-primitive in  $\mathcal{S}^{\text{ex}}$ . We have

**Theorem 1.14.** *Two permutations  $\sigma$  and  $\sigma'$  are in the same class iff they have the same number of descents, and  $\text{prim}(\sigma)$ ,  $\text{prim}(\sigma')$ , are in the same class.*

*A permutation  $\sigma$  is primitive iff  $\lambda'(\sigma)$  has no parts of size 1. Besides class  $\text{Id}$ , which has invariant as in the previous theorem (the rank is just added to  $\lambda'$ ), the number of primitive classes with cycle invariant  $\lambda'$  (no  $\lambda'_i = 1$ ) depends on the number of even elements in the list  $\{\lambda'_i\}$ , and is, for  $n \geq 8$ ,*

**zero**, *if there is an odd number of even elements;*

**one**, *if there is a positive even number of even elements;*

**two**, *if there are no even elements at all. The two classes have non-zero opposite sign invariant.*

*For  $n \leq 7$  the number of primitive classes with given cycle invariant may be smaller than the one given above, and the list in Table 3 gives a complete account.*

*As a consequence, two primitive permutations  $\sigma$  and  $\sigma'$ , not of  $\text{Id}$  type, are in the same class iff they have the same cycle and sign invariant.*

We will first obtain Theorem 1.13 and then Theorem 1.14 as an almost-straightforward corollary. Curiously enough, historically, the first and fundamental article [KZ03] proved Theorem 1.14, and it was only a few years later that the proof technique was adapted from the  $\mathcal{S}^{\text{ex}}$  case to  $\mathcal{S}$ , and the article [Boi12] proved Theorem 1.13.

On the contrary, within our techniques, it is both (a bit) easier to prove Theorem 1.13 than Theorem 1.14, if we had to do both of them from scratch, and is considerably easier to prove Theorem 1.14 as corollary of 1.13, while we are not aware of a simple derivation of Theorem 1.13 from Theorem 1.14.

## 1.7 Surgery operators

The hardest part in our proof of Theorem 1.13, concerning the dynamics  $\mathcal{S}_n$ , is the proof by induction that all the classes with a given admissible set of invariants are non-empty and connected. Classes of different rank (in the three cases  $r = 1$ ,  $r = 2$  and  $r > 2$ ) are treated differently, so we do this with 3 operators, that we call  $q_1$ ,  $q_2$  and  $T$ , for these three cases, respectively. These operators produce (representants within) classes of given rank at size  $n$  from (representants within) classes at smaller sizes, by performing local manipulations of the configurations, which, in the language of translation surfaces (see section 2.3), correspond in a hidden way to the insertion of a ‘handle’ or of a ‘cylinder’ in a Riemann surface. Thus we call them *surgery operators*. In the next paragraphs we make a preliminary discussion on which combinatorial properties such operators have, in order to provide the appropriate tool in our proof’s scheme.

First of all, for each operator  $X$ , we will require that it is a homomorphism, i.e., that for all pairs of configurations in the same class,  $\sigma \sim \tau$ , we have  $X(\sigma) \sim X(\tau)$ . As a consequence,  $\bar{X}(C)$ , the class obtained by applying  $X$  to any configuration in  $C$ , is well-defined.

Then, we have a simple yet crucial constraint on the action the operators may possibly have, given by the dimension formula, equation (3): for a permutation  $\sigma$  of size  $n$  with cycle invariant  $(\lambda, r)$ , we have  $r + \sum_i \lambda_i = n - 1$ . We know in retrospective, from the statement of Theorem 1.13 (see Section 6.1, Lemma 6.1 for a proof), that the number of even elements in  $\lambda \cup \{r\}$  must be even, so that the cycle invariant shall change consistently under the action of the surgery operator.

For example, suppose that we aim to construct an operator  $X$  such that, for every  $\sigma$  with invariant  $(\lambda, r, s)$ ,  $X(\sigma)$  has invariant  $(\lambda, r + 1, s)$ . This operator would be a viable candidate for constructing an induction. However, the number of even elements in the two

lists  $\{\lambda_i\} \cup \{r\}$  and  $\{\lambda_i\} \cup \{r+1\}$  have different parity, so that we know in advance that such an operator  $X$  cannot exist. The best hope is to identify instead an operator – it will be our operator  $T$  – such that, for every  $\sigma$  with invariant  $(\lambda, r, s)$ ,  $T(\sigma)$  has invariant  $(\lambda, r+2, s)$ . Such an operator increases the size of a configuration by 2 (by the dimension formula), while preserving the forementioned parity constraint.

The classes in the image of  $T$  have rank  $r > 2$ , thus for the cases of rank 1 and rank 2 we need to define two other operators,  $q_1$  and  $q_2$ . For the first one, tentatively, we may hope to have an operator such that, if  $\sigma$  has invariant  $(\lambda, r, s)$  and size  $n$ , then  $q_1(\sigma)$  has invariant  $(\lambda', 1, s)$  and size  $n+1$ <sup>6</sup>. Again, by equation (3) we have that  $1 + \sum \lambda'_i = r + \sum \lambda_i + 1$ . What should we hope as a possible natural choice of  $\lambda'$ ? The answer is deceptively simple, namely  $\lambda' := \lambda \cup \{r\}$ , i.e. we add a new cycle, of length  $r$ , in order to satisfy equation (3).

Finally, it remains the case of  $q_2$ . This operator works on a similar basis as  $q_1$ , with the following difference: if  $\sigma$  has invariant  $(\lambda, r, s)$  and size  $n$ , then  $q_2(\sigma)$  has invariant  $(\lambda'', 2, 0)$  and size  $n+1$  with  $\lambda'' := \lambda \cup \{r-1\}$ . Note that the sign invariant of the image class is set to zero, regardless of the sign in the pre-image. This is consistent with the statement of the theorem: the new rank is 2, so the number of even entries in  $\lambda \cup \{r\}$  becomes positive (while keeping its parity due to our definition of  $q_2$ ).

Which properties of these operators shall we establish?

As we will prove the theorem by induction, we can assume that at size  $n-1$  and  $n-2$  the classes are fully characterized by the triple  $(\lambda, r, s)$  (where  $s = s(\sigma) \in \{-1, 0, 1\}$ ), as described in the statement of the theorem, and then concentrate on size  $n$ .

For the operator  $T$ , we need the following to hold: let  $C$  be some class with invariant  $(\lambda, r, s)$ , with  $r > 2$ , and let  $B$  be the (unique by induction) class with invariant  $(\lambda, r-2, s)$ , then  $\bar{T}(B) = C$ . The mere existence of this operator, once established that it is a homomorphism, would provide the inductive step, from size  $n-2$  to size  $n$ , for every class with rank more than 2. Indeed the operator  $\bar{T}$  is a bijection between classes of invariant  $(\lambda, r, s)$  and classes of invariant  $(\lambda, r+2, s)$ .

For  $q_1$ , we have a slightly more complex requirement. Let  $C$  be a class with invariant  $(\lambda, 1, s)$ . For every  $i$  an integer appearing in  $\lambda$  with positive multiplicity, let  $\lambda(i) = \lambda \setminus \{i\}$ . Define  $\Delta(C, i)$  as the (unique by induction) class with invariant  $(\lambda(i), i, s)$ . Clearly, for all such  $i$ ,  $\bar{q}_1(\Delta(C, i))$  has invariant  $(\lambda, 1, s)$ . Moreover, it turns out that no other classes  $B$  are such that  $\bar{q}_1 B$  has this invariant. Now, establishing that  $q_1$  is a homomorphism is not enough. We need to further establish that  $\bar{q}_1(\Delta(C, i)) = C$  for every  $i$ , ruling out the possibility that, e.g., if  $\sigma \in \Delta(C, i)$  and  $\tau \in \Delta(C, j)$ , then  $q_1(\sigma) \not\sim q_1(\tau)$  despite the fact that they have the same invariants. A crucial simplifying property of the operator  $q_1$  we will introduce is that  $q_1$  is an injective map that is almost surjective, because, when  $q_1^{-1}(\tau)$  is not defined, then  $q_1^{-1}(R^{-1}\tau)$  is.

Finally, it remains the case of  $q_2$ . This operator works on a similar basis as  $q_1$ , but the loss of memory of the sign invariant introduces a further subtlety. Now we need the following. Let  $C$  have invariant  $(\lambda, 2, 0)$ . The set of  $(\lambda', r', s')$  such that it may be  $\bar{q}_2(C') = C$  for some  $C'$  with invariant  $(\lambda', r', s')$  is a bit complicated. First of all, its elements have the form  $(\lambda(i-1), i, s)$  for  $i \in \lambda$  and  $s \in \{0, \pm 1\}$ . Then, if there are no even cycles in  $\lambda(i-1)$ , we have  $s \in \{\pm 1\}$ , otherwise  $s = 0$ . For  $i$  and  $s$  in the set as above (depending on  $\lambda$ ), define  $\mathcal{E}(C, i, s)$  as the class with invariant  $(\lambda(i-1), i, s)$  (by induction, there is at most one class with such invariant). Thus  $\bar{q}_2(\mathcal{E}(C, i, s))$  has invariant  $(\lambda, 2, 0)$ . We ask that  $\bar{q}_2(\mathcal{E}(C, i, s)) = C$  for every such  $i$  and  $s$ . Again, besides the list we have just described, there are no other classes  $B$  such that  $\bar{q}_2 B$  has invariant  $(\lambda, 2, 0)$ . Similarly as was the case for  $q_1$ ,  $q_2$  is injective and almost surjective.

The construction of these operators would produce the core of the induction steps. Some further subtleties are in order, though. In particular, the existence of exceptional classes requires to verify the behaviour of classes  $T(\text{Id}_n)$ ,  $q_1(\text{Id}_n)$ ,  $q_2(\text{id}_n)$  and  $T(\text{Id}'_n)$ ,  $q_1(\text{Id}'_n)$ ,  $q_2(\text{Id}'_n)$ , at all sizes  $n$ , as these could create a proliferation of new classes, even if the properties

<sup>6</sup>We may consider also a larger increase of size, as was for  $T$ , but let us consider the simplest scenario first.

outlined above are determined for non-exceptional classes. For example, in such a case  $\{T^{2k}(\text{Id}_4), T^{2(k-1)}(\text{Id}_8), \dots, T^2(\text{Id}_{4k}), \text{Id}_{4k+4}\}$  could be  $k + 1$  different classes, according to Table 1, all with invariant  $(\emptyset, k + 1, 1)$ . Luckily enough, what really happens (and we manage to prove) is that for each of the three operators  $X \in \{\bar{T}, \bar{q}_1, \bar{q}_2\}$ , and each of the two families of exceptional classes  $C \in \{\text{Id}_n, \text{Id}'_n\}$ , for  $n$  above a finite (small) value, there exists a non-exceptional class  $D$  such that  $X(C) = X(D)$ .

In our proof, it is convenient to establish separately this last fact (this is done in Section 6.2), and the behaviour of the operators on non-exceptional classes (this is done in Sections 5.1 and 5.2).

Table 8, which provides the worked-out procedure of the induction at size 11, may be illuminating.

## 2 Connection with the geometry of translation surfaces

In this section we illustrate how the combinatorial operators and invariants introduced in Section 1 are related to certain operations, called *Rauzy–Veech induction*, acting on interval exchange transformations associated to the Poincaré map of an interval on a translation surface. This correspondance implies that the classification of equivalence classes w.r.t. the combinatorial operators is equivalent to the classification of strata of translation surfaces with a given set of conical singularities.

A first part reviews the geometrical background (and explains all the terms used in the paragraph above), while a second part defines the geometrical version of the invariants (illustrated in Section 1.4) that turned out to provide a complete set in the classification theorem. Finally a last part describes the geometrical interpretation of our combinatorial surgery operators (illustrated in Section 1.7).

Note that this section introduce the minimal amount of terminology required to make sense of the invariants and the surgery operators in the geometrical context. The interested reader may find a more extensive account in the three surveys [Zor06], [Yoc07] and [FM14], which develop respectively the theory of (quasi-)flat surfaces, of interval exchange transformations and of Teichmüller spaces (the three texts have a large amount of overlap between them).

### 2.1 Strata of translation surfaces

A *translation surface* is a connected compact oriented surface  $M$  of genus  $g$ , equipped with a Riemannian metric which is flat except for a discrete set  $S$  of conical singularities, and has trivial  $\text{SO}(2)$ -holonomy. In this context, trivial  $\text{SO}(2)$ -holonomy means that the parallel transport of a tangent vector along any closed curve (avoiding the singularities) brings the vector back to itself (instead of having it rotated). A condition for this to happen is that the angle of each singularity is a multiple of  $2\pi$ . Indeed, for ‘small’ closed curves, which encircle one conical singularity of angle  $\alpha$  while staying far from all the others, the parallel transport of a vector would rotate the vector by the angle  $\alpha$ , which is defined modulo  $2\pi$ .

Additionally, the trivial holonomy allows us to choose a vertical direction. Choose one (non-singular) point on the surface, and one vector  $x$  in the tangent space at that point. Then, one can define a vector field via the parallel transport of  $x$ . The resulting parallel vector field is defined only outside of the singularities, but it can be extended to the singularities in a multivalued way: in a singularity of angle  $2\pi(d_i + 1)$  it would take  $d_i + 1$  distinct values.

Equivalently, a translation surface with the choice of a vertical direction can be described as a triplet  $(M, U, S)$ , where  $M$  is a topological connected surface,  $S = \{s_1, \dots, s_k\}$  is the discrete subset of singularities of  $M$ , and  $U = \{U_i, z_i\}$  is an atlas on  $M \setminus S$  such that every transition function is a translation:

$$\forall i, j \quad z_i \circ z_j^{-1} : \begin{array}{ccc} z_j(U_i \cap U_j) & \rightarrow & z_i(U_i \cap U_j) \\ z & \mapsto & z + c \end{array}$$



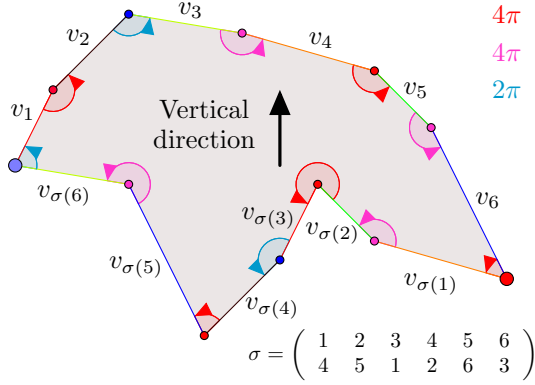


Figure 8: From the datum of  $n$  vectors  $v_1, \dots, v_n$  in  $\mathbb{C}$  and a permutation  $\sigma \in \mathfrak{S}_n$ , we construct a  $2n$ -gon. Then every pair of parallel sides of the polygon are identified by translation. The conical singularities of the associated translation surface are represented directly on the figure, by small angles, and the stratum  $H(d_1^{m_1}, \dots, d_k^{m_k})$  to which the surface belongs can be evinced from this representation: the vertices of the polygon are partitioned into equivalence classes (due to the identification of the sides of the polygon by translation) represented by the coloured arcs in the figure. Each class is associated to a singularity, and the angle of each singularity is the sum of the angles around the vertices in its equivalence class. We can also directly compute the angle of a singularity, divided by  $2\pi$ , by counting the number of arcs of the given colour on any of the two broken lines  $P_{\pm}$  of the polygon (the two arcs around the vertices  $0$  and  $\sum_{i=1}^n v_i$ , where  $P_+$  and  $P_-$  meet, are not counted). In this example there are three equivalence classes, denoted in blue, red and magenta. The angle of the blue, red and magenta classes are  $2\pi$ ,  $4\pi$  and  $4\pi$ , respectively. Indeed, there are 1 blue, 2 red and 2 magenta arcs both on the top and on the bottom broken lines.

and for each  $s_i \in S$  there exists a neighborhood that is isometric to a cone of angle  $2\pi(d_i+1)$ . Since  $z_i = z_j + c$  for all pairs of intersecting  $U_i$  and  $U_j$ , we can define on each chart a holomorphic complex 1-form  $\omega_{z_i} = dz_i$ , and thus the abelian differential  $\omega$  on  $M \setminus S$ . This abelian differential  $\omega$  extends to the points  $s_i \in S$ , where it has zeroes of degree  $d_i$ .

Conversely, given a non-zero abelian differential  $\omega$  on a compact connected Riemann surface  $M$ , with a finite set of zeroes  $S = \{s_1, \dots, s_k\}$ , of degree  $d_1, \dots, d_k$ , we define a *translation atlas* as follows. Let  $(U, \zeta)$  be a chart containing  $p \in M \setminus S$  such that  $\omega_{\zeta} = \Phi(\zeta)d\zeta$ . From this, one can obtain a chart  $(U, \xi)$  of adapted local coordinates at  $p$  with  $\omega_{\xi} = d\xi$  on  $U$  by defining  $\xi = \int_p^z \Phi(w)dw$ . Likewise, we can show that a neighbourhood of the zero  $s_i$  is isometric to an Euclidean cone of angle  $2\pi(d_i+1)$ , by finding local coordinates  $\eta$  for which  $\omega_{\eta} = \eta^{d_i}d\eta$ .

A geometric construction of a translation surface can be done as follows. Choose  $n$  distinct vectors  $v_1, \dots, v_n$  of  $\mathbb{C}$  and a permutation  $\sigma \in \mathfrak{S}_n$  and construct the two broken lines (i.e., polygonal chains)  $P_+$  and  $P_-$  in  $\mathbb{C}$ , with vertices

$$P_+ = (0, v_1, v_1 + v_2, \dots, v_1 + \dots + v_n)$$

and

$$P_- = (0, v_{\sigma(n)}, v_{\sigma(n)} + v_{\sigma(n-1)}, \dots, v_{\sigma(n)} + \dots + v_{\sigma(1)}).$$

Occasionally, we will use  $u_1, u_2, \dots, u_n$  as synonym of  $v_{\sigma(n)}, v_{\sigma(n-1)}, \dots, v_{\sigma(1)}$ .

If the vectors  $v_i$  satisfy certain inequalities (see Definition 2.1 below),  $P_+$  and  $P_-$  intersect only at their endpoints, so the concatenation of  $P_+$  and the reverse of  $P_-$  defines a polygon

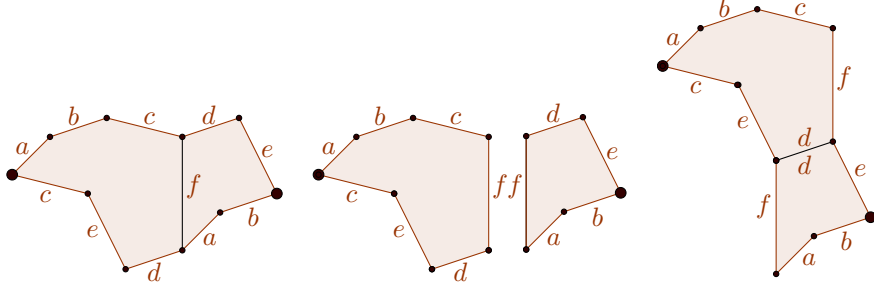


Figure 9: A cut and paste move.

embedded in the plane, with  $2n$  sides, which are naturally paired: if  $\sigma(i) = j$ , the  $j$ -th side of  $P_+$  has the same direction and orientation as the  $(n+1-i)$ -th side of  $P_-$ . These pairs of sides can thus be identified, so that the resulting surface has no border. By this procedure, illustrated in figure 8, we obtain a translation surface.

It is known that any translation surface can be represented in such a way, and under the canonical choice of the vertical direction for the vector field, the corresponding abelian differential is the canonical  $dz$  of the complex plane. As explained on figure 8, the set of conical singularities can be directly read on the polygon.

For  $g \geq 2$ , the moduli space of abelian differentials  $H_g$  is the space of pairs  $(M, \omega)$ , where  $M$  a compact connected Riemann surface of genus  $g$  and  $\omega$  is a non-zero abelian differential, with the following identification: the points  $(M, \omega)$  and  $(M', \omega')$  are equivalent if there is an analytic isomorphism  $f : M \rightarrow M'$  such that  $f^*\omega' = \omega$ .  $H_g$  is a complex orbifold of dimension  $4g - 3$ .

Let  $d_1 \leq \dots \leq d_k$  and  $m_1, \dots, m_k$  be sequences of nonnegative integers. We denote by  $H(d_1^{m_1}, \dots, d_k^{m_k})$  the subspace of  $H_g$  such that for all points  $(M, \omega)$  the abelian differential  $\omega$  has  $m_i$  zeroes of degrees  $d_i$ , for  $i = 1, \dots, k$ . It was shown by Masur and Veech that the stratum  $H(d_1^{m_1}, \dots, d_k^{m_k})$  is a complex orbifold of dimension  $n = 2g - 1 + \sum_i m_i$ . By the Gauss–Bonnet formula, if  $M$  has genus  $g$  then the degrees of the conical singularities must verify

$$\sum_{i=1}^k m_i d_i = 2g - 2. \quad (6)$$

In fact,  $H_g$  can be partitioned in terms of the strata  $H(d_1^{m_1}, \dots, d_k^{m_k})$  for  $d_i$ 's and  $m_i$ 's such that (6) is satisfied.

In term of polygons, two translation surfaces  $S_1$  and  $S_2$  with the same area are in the same stratum  $H(d_1^{m_1}, \dots, d_k^{m_k})$  if and only if there exists a sequence of cut and paste moves from  $S_1$  to  $S_2$  (see figure 9). The ‘if’ part is obvious, while the ‘only if’ part is a result of [Mas82].

Let  $M$  be a translation surface with a vertical direction, and let  $I$  be a horizontal open segment on  $M$ . The *first return map*  $T$  (or *Poincaré map*) of the translation flow<sup>7</sup> from  $I$  is an *interval exchange transformation* (IET). An IET is a one-to-one map  $\phi$  from  $I \setminus \{x_1, \dots, x_k\}$  to  $I \setminus \{x'_1, \dots, x'_k\}$  that is piecewise of the form  $\phi(z) = z + c_i$ , i.e., there exists some minimal set of points  $\{x_1, \dots, x_k\} \subset I$ , and  $\{x'_1, \dots, x'_k\} \subset I' \equiv \phi(I)$ , such that, if we subdivide  $I \setminus \{x_1, \dots, x_k\}$  into  $k+1$  maximal open subintervals  $\{I_1, \dots, I_{k+1}\}$ , of lengths  $\lambda_1, \dots, \lambda_{k+1}$ , and  $I' \setminus \{x'_1, \dots, x'_k\}$  into subintervals  $\{I'_1, \dots, I'_{k+1}\}$  of the same lengths, the map  $\phi$  is identified by the datum of  $\tau \in \mathfrak{S}_{k+1}$ , and of  $(\lambda_1, \dots, \lambda_{k+1}) \in (\mathbb{R}_+)^{k+1}$ , with a convention on the labelings as shown in the example of Figure 10 (i.e., the intervals of  $I' \setminus \{x'_1, \dots, x'_k\}$ , in their natural order from left to right, have lengths  $\lambda_{\tau(k+1)}, \lambda_{\tau(k)}, \dots, \lambda_{\tau(1)}$ ).

<sup>7</sup>I.e., the flow associated to the vertical foliation with singularities at the conical points defined by taking the integral curve of the parallel vector field i.e. defined by  $\phi_t(x) = x + it$

Consequently, also a first return map  $T$  is parametrised by the same combinatorial datum, of the permutation  $\tau \in \mathfrak{S}_{k+1}$ , and a “vector of lengths”  $\lambda = (\lambda_1, \dots, \lambda_{k+1})$  (see figure 11). Moreover, the permutation  $\tau$  is irreducible (i.e., it has no non-trivial blocks) since the vertical foliation is uniquely ergodic (see [Vee82] and [Mas82] for a proof of the unique ergodicity).

The construction of a polygon with identified sides for a given datum of  $(\tau, \lambda)$ , with some useful geometric properties, involves the notion of *suspension*:

**Definition 2.1** (Suspension). *Let  $\sigma$  be an irreducible permutation of size  $n$  and  $\lambda$  a vector of lengths. We say that the vectors  $(v_i)_{i=1, \dots, n} \in \mathbb{C}^n$  are a suspension data of  $(\sigma, \lambda)$  if*

- $\forall i, \Re(v_i) = \lambda_i$ .
- $\forall i < n, \sum_{j=1}^i \Im(v_j) > 0$  and  $\sum_{j=1}^i \Im(v_j) < 0$ .

(Recall,  $u_j = v_{\sigma(n+1-j)}$ ). Given a suspension datum  $(v_i)_i$  of  $(\sigma, \lambda)$  we can build the translation surface  $S = (\sigma, (v_i)_i)$  and choose the interval  $]0, \sum_{i=1}^n \lambda_i[$  on the real line so that the interval exchange map  $T$  on  $I$  is encoded exactly by  $(\sigma, \lambda)$ . (See figures 12 and 13). In this case we say that  $S$  is a suspension of  $(\sigma, \lambda)$ . Veech proved that almost any translation surface could be obtained as a suspension.

Let  $(M, \omega) \in H(d_1^{m_1}, \dots, d_k^{m_k})$ , and introduce the shortcut  $n = 2g - 1 + \sum_i m_i$  for the dimension of the stratum. In analogy with the previous section, we state that the Rauzy class of  $(M, \omega)$  is the subset of  $\mathfrak{S}_n$  containing all the permutations which are the combinatorial datum of some interval exchange map  $T$  over an interval  $I$  on  $(M, \omega)$ .

If  $(\sigma, (v_i)_i)$  is a polygon representation of  $S = (M, \omega)$ , then the Rauzy class of  $S$  contains  $\sigma$ , since  $S$  can be obtained as a suspension of  $(\sigma, \lambda)$  by Veech theorem, and is thus the class  $C(\sigma)$ , in the notations of the previous section.

More generally, on  $H(d_1^{m_1}, \dots, d_k^{m_k})$  we have a notion of connectivity due to the orbifold structure of this space. Veech proved the two following things :

- Two points  $(M, \omega)$  and  $(M', \omega')$  of the stratum  $H(d_1^{m_1}, \dots, d_k^{m_k})$  are in the same connected component if and only if they are in the same extended Rauzy class.
- Two permutations  $\tau, \tau' \in \mathfrak{S}_n$  are in the same extended Rauzy class if and only if they are connected with respect to the extended Rauzy dynamics  $\mathcal{S}_n^{\text{ex}}$ .

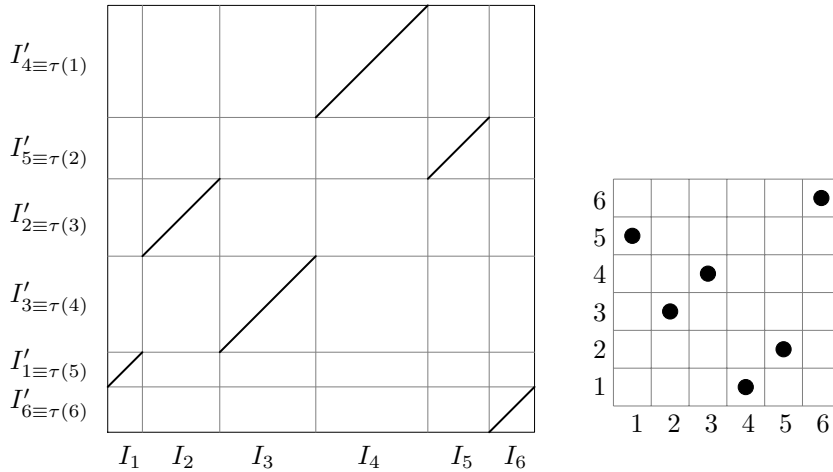


Figure 10: Left: an IET  $\phi$ . Right: the associated permutation  $\tau = \tau(\phi)$ . We have a bullet at coordinate  $(i, j)$  if  $\tau(i) = j$ . Note that there is a reflexion along the horizontal axis in the correspondence between  $\tau$  and the obvious diagram interpretation of the graphics of  $\phi$ , i.e.  $\tau$  describes the graphics of  $-\phi(x)$ .

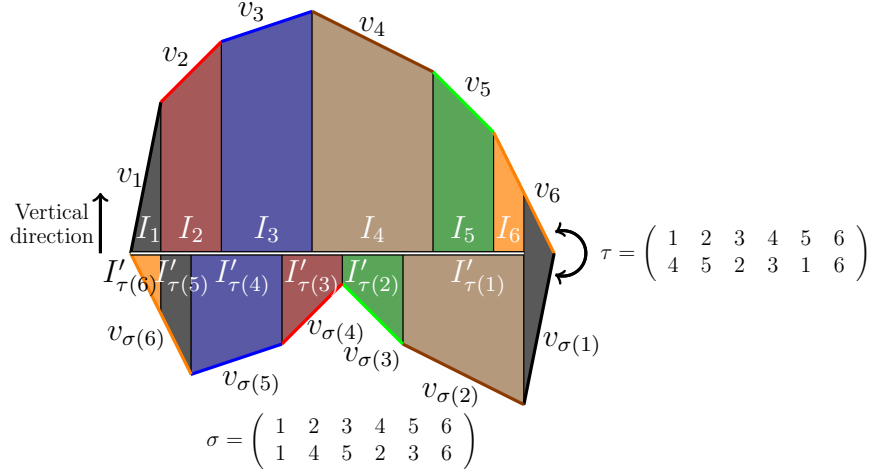


Figure 11: Let  $\sigma$  and  $(v_i)_{1 \leq i \leq n}$  define a translation surface and choose a horizontal open interval  $I$ . The interval exchange map  $T$  is obtained by following the vertical flow from almost each point of  $I$ , until it returns for the first time to  $I$ . The image by  $T$  of a point of  $I$  is not defined if its vertical flow meets a singularity before reaching  $I$ , and these are the points  $x_i$  mentioned in the text. In the figure, the top sub-intervals  $(I_i)$  of  $I$  are numbered from left to right, and the bottom ones  $(I'_{\tau(j)})$  are numbered with  $j$  increasing from right to left.

Thus, if  $(M, \omega)$  and  $(M', \omega') \in H(d_1^{m_1}, \dots, d_k^{m_k})$  are suspensions of  $(\tau, \lambda)$  and  $(\tau', \lambda')$ , respectively, we have  $(M, \omega) \sim (M', \omega')$  iff  $\tau \sim \tau'$  (the two  $\sim$  symbols are different, the first one is the connectivity within the orbifold, the second one is the connectivity on the Cayley graph of the Rauzy extended dynamics), and consequently the extended Rauzy classes completely determine the connected components of the strata of  $H_g$ .

Let us now interpret the combinatorial definition of the extended Rauzy classes, given in Section 1.2, in terms of the *Rauzy-Veech induction*. Let  $M$  be a translation surface with a vertical direction,  $I$  an open interval and  $T = (\tau, \lambda)$  the associated interval exchange map. We label the top and bottom sub-intervals induced by  $T$  as in Figure 11 above. The Rauzy-Veech induction concerns the study of the possible configurational changes in the structure of the IET, when the surface  $(M, \omega)$  is kept fixed, while the interval  $I$  is modified. A *right step* of the Rauzy-Veech induction consists in shortening the interval  $I$ , from its right-end, by removing the shortest sub-interval among  $I_n$  and  $I'_{\tau(1)}$ . If we call  $J$  the new

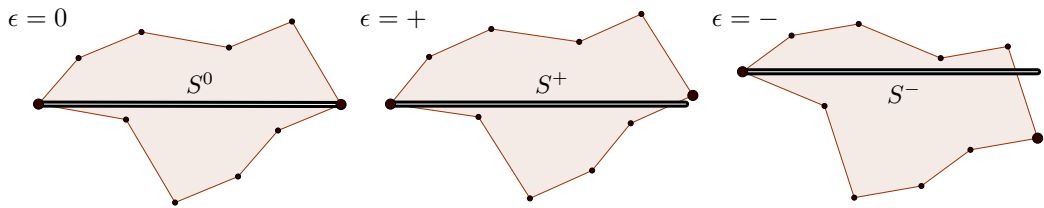


Figure 12: Let  $(\sigma, \lambda)$  describe an IET. The three figures describe three suspensions of  $(\sigma, \lambda)$ ,  $(v_i^\epsilon)_{1 \leq i \leq n}$  for  $\epsilon = 0, +, -$ . The second condition in the definition of a suspension means that for the translation surface  $S^\epsilon = (\sigma, (v_i^\epsilon)_i)$  the top and bottom broken lines remain always above and below the real line, except possibly for their last segment. In the figure, the endpoint of the broken lines  $P_+$  and  $P_-$  are on, above or below the real axis, for  $\epsilon = 0, +$  and  $-$ , respectively.

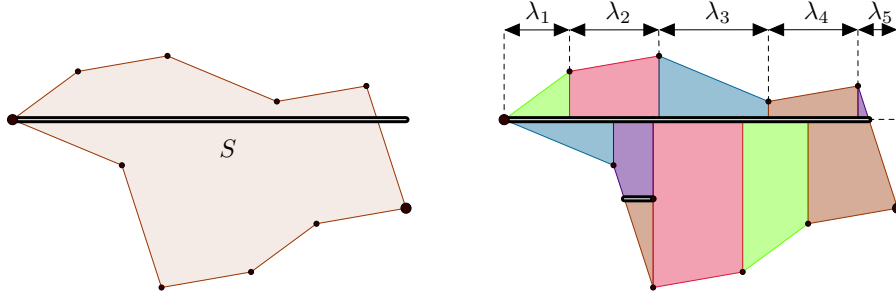


Figure 13: As illustrated by Figure 12, and here on the left picture, in the construction of the translation surface  $S = (\sigma, (v_i)_i)$  from the suspension  $(v_i)_i$  of  $(\sigma, \lambda)$ , the interval  $I$  can be in part outside the polygon. In this case, the construction of the interval exchange map involves a small subtlety, detailed on the right picture. We cut the portion of  $I$  outside the polygon, and translate it according to the identification of opposite sides. When this is done, the interval exchange map has a clear behaviour also on the right-most interval  $I_n$ .

(total) interval, we have

$$\begin{cases} J = I \setminus I'_{\tau(1)} & \text{if } |I_n| > |I'_{\tau(1)}| \\ J = I \setminus I_n & \text{if } |I_n| < |I'_{\tau(1)}| \end{cases}$$

The case  $|I_n| = |I'_{\tau(1)}|$  never occurs if the  $\lambda_i$ 's are generic in  $(\mathbb{R}_+)^n$  (and thus they do not satisfy any linear relation with coefficients in  $\mathbb{Q}$ ), so we omit any discussion of this possibility. Conforming to the customary language, in the first case of the analysis above we say that  $T$  is of *right type 0*, and in the second case we say that  $T$  is of *right type 1*. We also shorten right type with R-type.

Let us call  $R_{\text{RV-ind}}$  the operation that sends the ‘old’ IET  $T$  to the ‘new’ one,  $T_1 = (\tau_1, \lambda_1) = R_{\text{RV-ind}}(T)$ . We use this verbose notation in order to make a distinction with operators  $L$  and  $R$  defined in Section 1.2, whose role here is as follows: if  $T$  is of R-type 0, then  $\tau_1 = R(\tau)$ , while if  $T$  is of R-type 1, then  $\tau_1 = L(\tau)$  (see figure 14).

Likewise, a *left step* of the Rauzy–Veech induction consists in shortening the interval  $I$  from the left-end. We have

$$\begin{cases} J = I \setminus I'_{\tau(n)} & \text{if } |I_1| > |I'_{\tau(n)}| \\ J = I \setminus I_1 & \text{if } |I_1| < |I'_{\tau(n)}| \end{cases}$$

and we say that  $T$  is of *left type 0* in the first case and of *left type 1* in the second case. Let us call  $T_2 = (\tau_2, \lambda_2) = L_{\text{RV-ind}}(T)$  the resulting new IET. Then, the map  $L_{\text{RV-ind}}$  has the property that  $\tau_2 = R'(\tau)$  or  $L'(\tau)$  depending on the left-type of  $T$ , still with  $L'$  and  $R'$  defined as in Section 1.2.

The extended Rauzy dynamic  $\mathcal{S}_n^{\text{ex}}$  acts on a permutation  $\sigma$ , while the Rauzy–Veech induction acts on IET  $(\sigma, \lambda)$ . As we have seen, the two operations are strictly related. Finally, we can define a third version of the operation, an induction based on cut and paste operations (which we also call the Rauzy–Veech induction), that acts on a suspension  $(\sigma, (v_i)_i)$ .

Given a suspension  $(\sigma, (v_i)_i)$  of  $(\sigma, \lambda)$ , a right step of the Rauzy–Veech induction for suspensions shortens the interval  $I$  into an interval  $J$  as it would for (the right step of) the Rauzy–Veech induction for IETs, then identifies a triangle within the polygon, namely, the one with vertices  $p = \sum_{i=1}^n v_i$ ,  $p - v_n$  and  $p - v_{\sigma(1)}$ , and pastes it back on the polygon, accordingly to the identification of the sides of the polygon and of the triangle, either on top of the broken line  $P_+$ , or below the broken line  $P_-$  in case of a Rauzy induction of right type 1 or 0, respectively. (see Figure 15).

Likewise, a left step cuts the left-end of the interval, and replaces a triangle on the far left, with vertices  $0, v_1$  and  $v_{\sigma(n)}$ , in a way that depends on the type of the left step of the Rauzy induction.

The relation of this version of the induction with the previous ones is based on the following fact. If  $(\sigma, (v_i)_i)$  is a suspension of  $(\sigma, \lambda)$ ,  $(\sigma_1, (v_i^1)_i)$  is the surface obtained by the Rauzy–Veech induction for suspensions, and  $(\sigma_1, \lambda_1)$  is the IET obtained by Rauzy–Veech induction for IETs. Then,  $(\sigma_1, (v_i^1)_i)$  is a suspension of  $(\sigma_1, \lambda_1)$ .

As we have mentioned above, in [Vee82] Veech showed that the extended Rauzy classes were generated by the four operators  $L, R, L', R'$  that we have introduced, and, more generally, that for every finite word  $w$  in the alphabet  $\{L_{\text{RV-ind}}, R_{\text{RV-ind}}\}$ , and every word  $\omega$  of the same length in the alphabet  $\{0, 1\}$ , there exists an IET  $T$  such that the induction performed according to the word  $w$  visits IET's  $T_i$  of type  $\omega_i$  (namely, of left-type or right-type  $\omega_i$ , according to  $w_i$ ), and this crucial result is at the basis of our combinatorial study of the classes determined by the action of  $L, R, L'$  and  $R'$  on permutations. In other words, if we call  $\Pi_1$  the projection from a suspension  $S$  to the associated IET  $T = (\tau, \lambda)$ , and  $\Pi_2$  the projection from  $T$  to the associated permutation  $\tau$ , we have the commuting diagram

$$\begin{array}{ccc}
\text{Rauzy–Veech induction} & S = (\tau, (v_i)_i) \xrightarrow{\sim \text{ w.r.t. } L_{\text{RV-ind}}; R_{\text{RV-ind}}} S' = (\tau', (v'_i)_i) & \\
\text{for suspensions:} & \downarrow \Pi_1 & \downarrow \Pi_1 \\
\text{Rauzy–Veech induction} & T = (\tau, \lambda) \xrightarrow{\sim \text{ w.r.t. } L_{\text{RV-ind}}; R_{\text{RV-ind}}} T' = (\tau', \lambda') & (7) \\
\text{for IETs:} & \downarrow \Pi_2 & \downarrow \Pi_2 \\
\text{Combinatorial} & \tau \xrightarrow{\sim \text{ w.r.t. } L, R; L', R'} \tau' & \\
\text{operators:} & & 
\end{array}$$

The (standard) Rauzy classes defined in Section 1.2 also have a geometric interpretation. Given a stratum  $H(d_1^{m_1}, \dots, d_k^{m_k})$ , we denote by  $H(d_1^{m_1}, \dots, \bar{d}_i^{m_i}, \dots, d_k^{m_k})$  the space with a

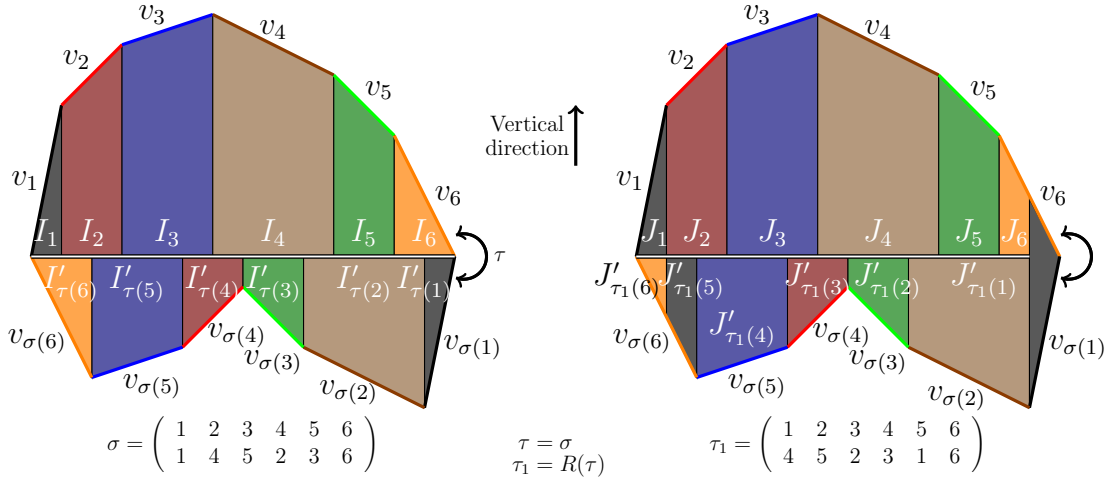


Figure 14: We apply the right step of the Rauzy–Veech induction on the surface shown on the left. In this case  $T = (\tau, \lambda)$  is of right type 0, since  $|I_6| > |I'_{\tau(1)}|$ , thus  $J = I \setminus I'_{\tau(1)}$ . The new interval exchange map  $T_1 = (\tau_1, \lambda_1)$  on  $J$  verifies  $\tau_1 = R(\tau)$ , namely, in our example,

$$\tau = \begin{array}{|c|c|c|c|c|c|} \hline \bullet & & & & & \\ \hline & \bullet & & & & \\ \hline & & \bullet & & & \\ \hline & & & \bullet & & \\ \hline & & & & \bullet & \\ \hline & & & & & \bullet \\ \hline \end{array} \quad \text{and} \quad \tau_1 = R(\tau) = \begin{array}{|c|c|c|c|c|c|} \hline & & & & & \bullet \\ \hline & \bullet & & & & \\ \hline & & \bullet & & & \\ \hline & & & \bullet & & \\ \hline & & & & \bullet & \\ \hline & & & & & \bullet \\ \hline \end{array} .$$

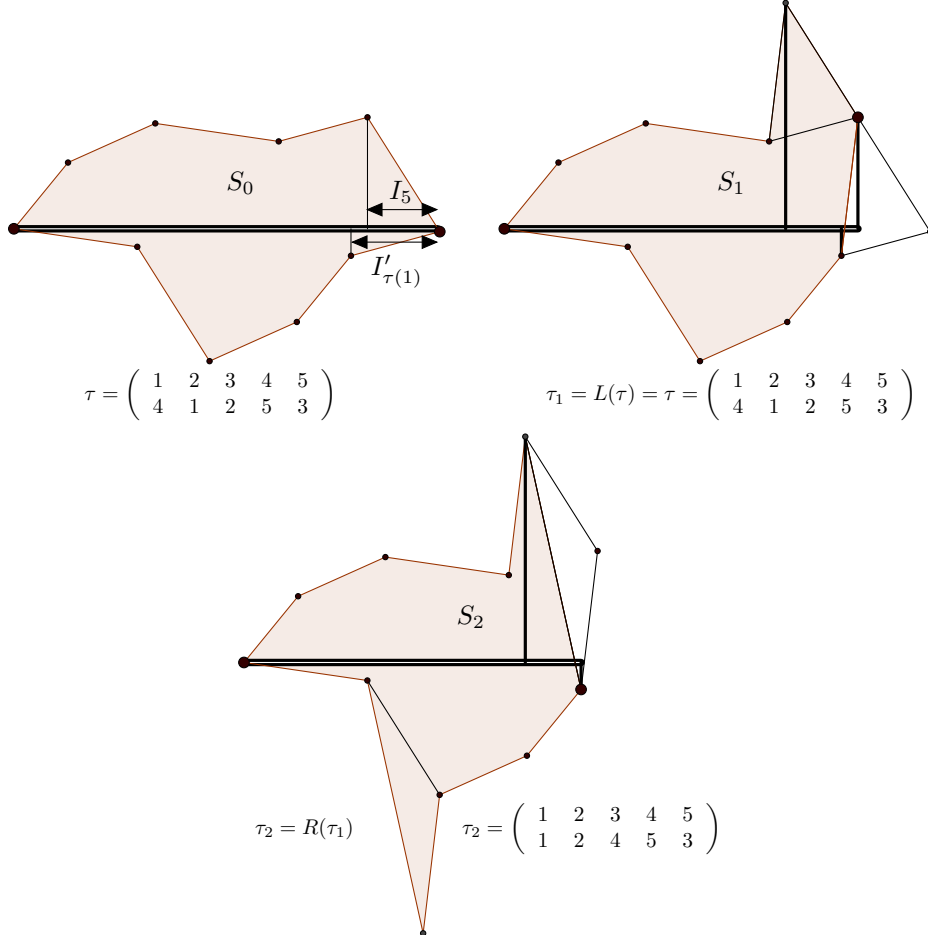


Figure 15: We apply two times the right version of the Rauzy–Veech induction on the left figure. In the first case  $T = (\tau, \lambda)$  is of right type 1, since  $|I_5| < |I'_{\tau(1)}|$ , thus  $J = I \setminus I_5$ . The new interval exchange map  $T_1 = (\tau_1, \lambda_1)$  on  $J$  verifies  $\tau_1 = L(\tau)$ . We cut the triangle on the right part of  $S_0$  and paste it on the top broken line, since we are in type 1. In this way we obtain the suspension  $S_1$  of  $(\tau_1, \lambda_1)$ . Then, with a second right-step of the Rauzy–Veech induction for suspensions, we obtain the suspension  $S_3$  from  $S_2$ . In this case the step is of type 0, thus  $\tau_2 = R(\tau_1)$ .

marked singularity of degree  $d_i$ . A point  $(M, \omega)$  is in  $H(d_1^{m_1}, \dots, \bar{d}_i^{m_i}, \dots, d_k^{m_k})$  if, for  $(M, \omega)$  represented by a polygon as in Figure 8, the angle of the singularity of the equivalence class containing the vertex 0 is  $2\pi(d_i + 1)$ . Thus  $H(d_1^{m_1}, \dots, d_k^{m_k})$  is partitioned into  $k$  parts, one for every possible value for the angle of the marked singularity. For example, in the figure 8 the angle around the singularity passing through  $(0, 0)$  is  $2\pi$ , so the corresponding translation surface  $(M, \omega)$  in the figure is in  $H(\bar{0}^1, 1^2)$ .

Finally the *Rauzy–Veech induction* is also defined and it corresponds to the induction where only right steps are allowed. It should be clear from figure 15 that the degree of the singularity around the vertex 0 does not change after a right move of the Rauzy–Veech induction for suspensions, since the cut and paste at the level of the triangle can never change the colour class of the left-most vertex, thus the colour class of the left-most vertex is an invariant of the (non-extended) Rauzy dynamics, and this corresponds to the marking.

In analogy to the forementioned result of Veech, Boissy proved in [Boi12] that the standard Rauzy classes are in one-to-one correspondence with the connected components of the

strata of the moduli space of abelian differentials with a marked singularity, so that we have a commuting diagram analogous to the one in (7), justifying the study of the combinatorial dynamics  $\mathcal{S}$ .

To conclude this section, let us describe some more recent works closely connected to the classification of the connected components of the strata of the moduli space of abelian differentials of Kontsevich and Zorich and of Boissy [KZ03, Boi12].

In [Lan08], Lanneau classified the connected components of the strata of the moduli space of *quadratic differentials*. Then, Lanneau together with Boissy [BL09] have formulated a combinatorial definition of extended Rauzy classes for quadratic differentials. These are defined as IETs on half-translation surfaces and are once again in one-to-one correspondence with the connected components of the strata of quadratic differentials. In this context the combinatorial datum is no longer a permutation but a linear involution (i.e. a matching with a one marked point between two given arcs), and are related, to a certain extent, to the dynamics  $\mathcal{M}$  of Section 1.2.

More recently, Boissy studied the *labelled Rauzy classes* in [Boi13], an object that we will also consider in forthcoming work, because this notion will lead us to a second and independent proof of the classification of the Rauzy classes, and it will emerge as a general method to classify Rauzy-type dynamics in more general circumstances. Boissy also classified the connected components of the strata of the moduli space of *meromorphic differentials* in [Boi15]. Delecroix studied the cardinality of Rauzy classes in [Del13], and Zorich provided representatives of every Rauzy class in the form of Jenkins–Strebel differentials [Zor08]. Finally, in [Fic16] Fickenscher has presented a combinatorial proof, independent of the one presented here, of the Kontsevich–Zorich–Boissy classification of Rauzy classes.

## 2.2 Geometric interpretation of the invariants

In this section we define the geometric version of two invariants of the strata, and show that they correspond to our combinatorial definitions of the *cycle-* and the *sign-*, or *arf-invariant* presented in Section 1.4. We start by working at the level of the connected components of a stratum  $H(d_1^{m_1}, \dots, \bar{d}_i^{m_i}, \dots, d_k^{m_k})$  of abelian differentials with a marked singularity.

The first invariant that we introduce consists of an integer partition with one marked part, and can be represented by the list

$$\underbrace{(d_1 + 1, \dots, d_1 + 1, \dots, d_i + 1, \dots, d_i + 1, \dots, d_k + 1, \dots, d_k + 1)}_{m_1 \text{ times}}; d_i + 1$$

Each entry  $d_i + 1$  is associated to a conical singularity, and corresponds to its angle, divided by  $2\pi$ . As said above, in the standard (non-extended) dynamics there is a singularity passing through the vertex  $(0, 0)$  of the polygon representation, and its degree does not change in the dynamics (because the Rauzy–Veech induction is acting on the other end-point of the interval i.e. only the right step of the induction is allowed for the standard dynamics), and this accounts for the fact that one entry, the one after the semicolon, is singled out. This invariant corresponds to the cycle invariant  $(\lambda, r)$  of any permutation of the associated Rauzy class, as is apparent from what we said above. More precisely, let  $(M, \omega) \in H(d_1^{m_1}, \dots, \bar{d}_i^{m_i}, \dots, d_k^{m_k})$ , let  $(\sigma, (v_i)_{1 \leq i \leq n})$  be a suspension data of  $(M, \omega)$  and let  $C$  be the (standard) Rauzy class associated to the connected component containing  $(M, \omega)$ . As we said before,  $\sigma \in C$ , since the translation surface is a suspension of  $(\sigma, \mu)$  for some  $\mu \in (\mathbb{R}_+)^n$ .

The results now follows from Figure 16, which indicates the correspondance between the angles around the vertices in the polygon and the counting of top (or bottom) arcs of the cycle invariant in the permutation.

The second invariant is more subtle, and corresponds to the parity of the spin structure of the surface, that we now describe. Let  $\gamma : S^1 \rightarrow M$  be a smooth closed curve on  $M$ , avoiding the conical singularities. Using as a reference our fixed parallel vector field (i.e., the vertical direction), we can define the *Gauss map*  $G$  from  $\gamma$  to  $[0, 2\pi[\simeq S^1$  as follows: to



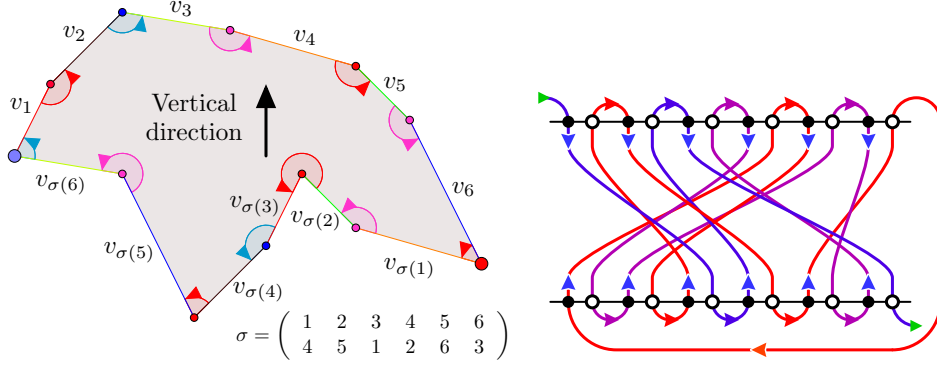


Figure 16: On the left, the polygon construction associated to the permutation  $\sigma = (4, 5, 1, 2, 6, 3)$ , and a certain set of  $v_i$ 's. The arcs around the singularities are represented, with colours denoting their classes. On the right, the cycle invariant construction associated to the same permutation. One can see that the arcs (from left to right) of the top broken line of the polygon correspond to the top arcs (from left to right) of the cycle invariant construction, while the arcs (now from right to left) of the bottom broken line of the polygon correspond to the bottom arcs (still from left to right) of the cycle invariant construction. As a result, the angle of a singularity divided by  $2\pi$  corresponds to the length of a cycle.

every point of the curve,  $\gamma(x)$ , we associate the angle  $\theta(x) \in S^1$  corresponding to the angle between the tangent vector  $\gamma'(x)$  and the vector field in  $x$ . The index  $\text{ind}(\gamma)$ , called the *degree* of the Gauss map, is the integer counting (with sign) the number of times the curve  $G \cdot \gamma$  is wrapped around  $S^1$ .

This allows us to define:

**Definition 2.2** (Parity of the spin structure). *Let  $(\alpha_i, \beta_i)_{1 \leq i \leq g}$  be a collection of smooth closed curves avoiding the singularities, and representing a symplectic basis for the homology  $H_1(M, \mathbb{Z})$ . The parity of the spin structure of  $M$  is the quantity*

$$\Phi(M) = (-1)^{\sum_{i=1}^g (\text{ind}(\alpha_i) + 1)(\text{ind}(\beta_i) + 1)} \quad (8)$$

It follows from [Ati71] that this is an invariant of the connected components of the stratum, and from [Joh80] that it is well-defined and independent of the choice of symplectic basis. More precisely, Johnson in [Joh80] shows that the quantity is the *Arf invariant* of a certain quadratic form  $\Phi : H_1(M, \mathbb{Z}_2) \rightarrow \mathbb{Z}_2$ . We will describe this second point of view in a few paragraphs, and we now proceed to construct  $\Phi$  concretely in the special case of translation surfaces.

Let  $c$  be a cycle of  $H_1(M, \mathbb{Z}_2)$ , and let  $\gamma$  be a smooth simple closed curve avoiding the singularities, and representing  $c$ . We define the function  $\Phi : H_1(S, \mathbb{Z}_2) \rightarrow \mathbb{Z}_2$  as

$$\Phi(c) = \text{ind}(\gamma) + 1 \pmod{2}.$$

This function is only well-defined when all the zeroes of  $\omega$  have even degree (i.e.  $(M, \omega) \in H(2d_1^{m_1}, \dots, 2\bar{d}_i^{m_i}, \dots, 2d_k^{m_k})$ ), otherwise two curves representing the same cycle  $c$  might have opposite index.

Suppose we are in the even-degree case. For  $c$  and  $c'$  distinct cycles, and  $\gamma$  and  $\gamma'$  representing  $c$  and  $c'$  respectively, and in generic mutual position (i.e., they may cross, but only in generic way), we define the bilinear *intersection form*  $\Omega(c, c')$  as the number of intersections between  $\gamma$  and  $\gamma'$ , mod 2.

The following theorem (obtained as a corollary of a theorem of [Joh80]) certifies that our function is a quadratic form:

**Theorem 2.3.** *The function  $\Phi$  is well-defined on  $H_1(M, \mathbb{Z}_2)$ . It is a quadratic form associated to the bilinear intersection form  $\Omega$  in the following sense:*

$$\forall c, c' \quad \Phi(c + c') = \Phi(c) + \Phi(c') + \Omega(c, c').$$

For our quadratic form  $\Phi : H_1(S, \mathbb{Z}_2) \rightarrow \mathbb{Z}_2$  the Arf invariant is defined as

$$\text{arf}(\Phi) = \frac{1}{\sqrt{|H_1(S, \mathbb{Z}_2)|}} \sum_{x \in H_1(S, \mathbb{Z}_2)} (-1)^{\Phi(x)} = 2^{-g} \sum_{x \in H_1(M, \mathbb{Z}_2)} (-1)^{\Phi(x)}. \quad (9)$$

Let  $(a_i, b_i)_{1 \leq i \leq g}$  be a symplectic basis of  $H_1(S, \mathbb{Z}_2)$ , then it can be shown that

$$\text{arf}(\Phi) = (-1)^{\sum_{i=1}^g \Phi(a_i)\Phi(b_i)}. \quad (10)$$

Let  $(\alpha_i, \beta_i)_{1 \leq i \leq g}$  be a family of smooth closed curves (avoiding the singularities) representing the family of cycles  $(a_i, b_i)_{1 \leq i \leq g}$ . Since we defined our quadratic form by  $\Phi(c) = \text{ind}(\gamma) + 1 \pmod 2$  for any cycle  $c$  and curve  $\gamma$  representing  $c$ , by comparing (8) and (10) we have

$$\text{arf}(\Phi) = \Phi(S),$$

i.e., the parity of the spin structure is the Arf invariant of  $\Phi$ .

Let us now describe how to obtain our definition of the Arf invariant, given in section 4.1, starting from the formula in (9).

Let  $(M, \omega)$  be a translation surface defined as the suspension  $(\sigma, (v_i)_i)$  of an IET  $T$ . Say that  $\sigma(i) = j$ . For  $x \in [0, 1]$  sufficiently small, there exists a curve  $\gamma_{n+1-j}$  from the point  $p_i^- = v_{\sigma(n)} + v_{\sigma(n-1)} + \dots + x v_{\sigma(i)}$  on  $P_-$  to the point  $p_j^+ = v_1 + v_2 + \dots + x v_j$  on  $P_+$ , such that the Gauss map  $G$  discussed above remains within the interval  $[-\pi/2, \pi/2]$ . Indeed, this fact is true for all  $x$ , whenever  $j < n$ , but only for  $x$  small enough for  $j = n$  and when the suspension has  $\epsilon \neq 0$  w.r.t. the notations of Figure 12. This can be seen from the existence of a positive  $\delta$  such that a strip of width  $\delta$  around the interval  $I$  leaves the points  $p_i^-$  and the points  $p_i^+$  on opposite half-planes. Figure 17 provides an example of this construction.

Because of the identification of the sides of the polygon, the  $\gamma_i$ 's are closed curves. As  $G \cdot \gamma_i(x) \in [-\pi/2, \pi/2]$ , it is easily seen that they all have index zero. Let  $(c_i)_i$  be the family of cycles represented by the curves  $(\gamma_i)_i$ , then it can be shown that

**Lemma 2.4.** *The family of cycles  $\{c_1, \dots, c_n\}$  is a generating family of  $H_1(M, \mathbb{Z}_2)$ .*

For a permutation  $\pi$ , define the symmetric matrix  $K(\pi)$  to be zero on the diagonal, and elsewhere

$$(K(\pi))_{ij} = \begin{cases} 1 & \text{if } (\pi(i) - \pi(j))(i - j) < 0 \\ 0 & \text{if } (\pi(i) - \pi(j))(i - j) > 0 \end{cases}$$

Then, for all  $c_i$  and  $c_j$  ( $i \neq j$ ),  $\Omega(c_i, c_j) = K(\pi)_{i,j}$  (see figure 17 for this correspondence). Defining  $\sigma$  as the (right-)reverse of  $\tau$ , i.e.  $\sigma = \tau\omega$  where  $\omega = (n, n-1, \dots, 1)$  is the longest permutation, we also have  $\Omega(c_i, c_j) = 1 - K(\sigma)_{i,j}$ . From the fact, proven above, that  $\text{ind}(\gamma_j) = 0$ , we get  $\Phi(c_j) = \text{ind}(\gamma_j) + 1 \pmod 2 = 1$ .

For a set  $I \subseteq \{1, \dots, n\}$  we define  $\Phi(I) = \Phi(\sum_{i \in I} c_i)$  and  $\chi'_I(\pi) = \sum_{\{i,j\} \subset I} K(\pi)_{ij}$  as the number of pairs  $i < j$  of edge labels, both in  $I$ , which are crossing in  $\pi$ . In Section 1.4.2 we already have defined the analogous quantity  $\chi_I(\pi) = \sum_{(i,j) \subset I} (1 - K(\pi)_{ij})$ , as the number of pairs  $i < j$  in  $I$  which do not cross in  $\pi$ . Then we have

**Proposition 2.5.** *If the surface  $S$  is in the Rauzy class  $C(\sigma)$ , for all  $I \subset \{1, \dots, n\}$  we have*

$$\Phi(I) = |I| + \chi'(I)(\sigma\omega) = |I| + \chi(I)(\sigma). \quad (11)$$

*Proof.* Call again  $\tau = \sigma\omega$ . We have, by iterated application of Theorem 2.3,

$$\Phi(I) := \Phi\left(\sum_{i \in I} c_i\right) = \sum_{i \in I} \Phi(c_i) + \sum_{(i,j) \subset I} K(\tau)_{ij}. \quad (12)$$

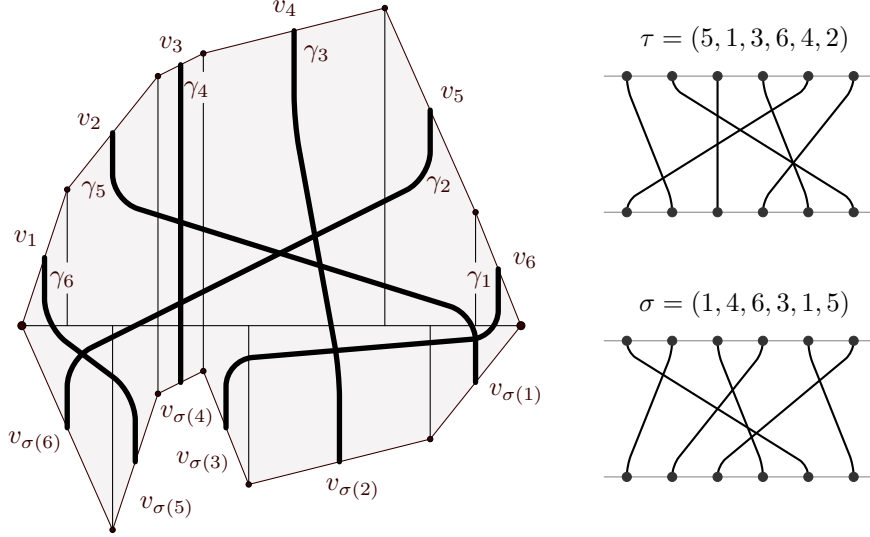


Figure 17: On the left, the polygon construction associated to the permutation  $\sigma = (1, 4, 6, 3, 1, 5)$  with a collection of simple smooth closed curves  $(\gamma_i)_{1 \leq i \leq n}$ . On the right, the permutation  $\tau = (5, 1, 3, 6, 4, 2)$  represents the collection of curves  $(\gamma_i)_{1 \leq i \leq n}$ : two closed curves  $\gamma_i$  and  $\gamma_j$  intersect if and only if the edges  $(i, \tau(i))$  and  $(j, \tau(j))$  of  $\tau$  intersect, since the set of curves  $(\gamma_i)_{1 \leq i \leq n}$  and the permutation  $\tau$  have the same topology. The permutation  $\sigma$  is the reverse of  $\tau$ , i.e. it is obtained from  $\tau$  by multiplying with the longest permutation  $\omega = (n, n-1, \dots, 1)$ , thus two closed curves  $\gamma_i$  and  $\gamma_j$  intersect if and only if the edges  $(n-i+1, \sigma(n-i+1))$  and  $(n-j+1, \sigma(n-j+1))$  of  $\sigma$  do *not* intersect.

Recall that, on one side,  $\Phi(c_i) = 1$  for all  $i$ , and, on the other side,  $\sum_{(i,j) \subseteq I} K(\tau)_{ij}$  is the definition of  $\chi'(I)(\tau)$ . Thus

$$\Phi(I) = |I| + \chi'(I)(\tau). \quad (13)$$

Similarly for  $\sigma$ , as  $K(\tau)_{ij} = 1 - K(\sigma)_{ij}$  and  $\sum_{(i,j) \subseteq I} (1 - K(\sigma)_{ij})$  corresponds to the definition of  $\chi(I)(\sigma)$ ,

$$\Phi(I) = |I| + \chi(I)(\sigma). \quad (14)$$

□

As a result, we can rewrite the definition (5) of  $\bar{A}(\sigma)$  as

$$\bar{A}(\sigma) := \sum_{I \subseteq \{1, \dots, n\}} (-1)^{|I| + \chi(I)} = \sum_{I \subseteq \{1, \dots, n\}} (-1)^{\Phi(I)} \quad (15)$$

which, identifying sets  $I$  with cycles  $\sum_{i \in I} c_i$ , is our definition (10) of the Arf invariant, up to an overall factor that we shall now discuss. Let us start by observing:

**Lemma 2.6.** *Let  $(M, \omega) \in H(d_1^{m_1}, \dots, \bar{d}_i^{m_i}, \dots, d_k^{m_k})$  be a translation surface of genus  $g$  represented by a permutation  $\sigma$  of size  $n$ . Finally, let  $k' = \sum_{j=1}^l m_j$  be the total number of singularities, then*

$$n = 2g + k' - 1. \quad (16)$$

*Proof.* This follows from the Gauss–Bonnet and the dimension formulas

$$\sum_{j=1}^k m_j d_j = 2g - 2; \quad r + \sum_{j=1}^k m_j \lambda_j = n - 1; \quad (17)$$

with  $r = \bar{d}_i + 1$  and  $\lambda_j = d_j + 1$  for the non-marked singularities  $z_j$ , since

$$n - 1 = r + \sum_{j=1}^k m_j d_j + 1 = 2g - 2 + \sum_{j=1}^l m_j = 2g - 2 + k'$$

□

Note that the integer  $n \equiv 2g + k' - 1$  on the two sides of (16) is exactly the dimension of the complex orbifold  $H(d_1^{m_1}, \dots, \bar{d}_i^{m_i}, \dots, d_k^{m_k})$ . We have

**Proposition 2.7.**

$$\bar{A}(\sigma) = 2^{k'-1+g} \text{arf}(\Phi).$$

*Proof.* We already know that  $\{c_i, \dots, c_n\}$  is a generating set. Since the basis of  $H_1(S, \mathbb{Z}_2)$  has size  $2g$ , and  $n = 2g + k' - 1$ , whenever  $k' > 1$  this family is linearly dependent on  $\mathbb{Z}_2$ , thus there exists an index  $j$  and a set  $I$  not containing  $j$  such that  $c_j = \sum_{i \in I} c_i$ . Call  $X = \{1, \dots, \hat{j}, \dots, n\}$ . Denoting by  $\Delta$  the symmetric difference of two sets, we can rearrange the summands in  $\bar{A}(\sigma)$  as

$$\begin{aligned} \bar{A}(\sigma) &= \sum_{J \subseteq X} (-1)^{\Phi(J)} + \sum_{J \subseteq X} (-1)^{\Phi(J \cup \{j\})} \\ &= \sum_{J \subseteq X} (-1)^{\Phi(J)} + \sum_{J \subseteq X} (-1)^{\Phi(J \Delta I)} \\ &= 2 \sum_{J \subseteq X} (-1)^{\Phi(J)}, \end{aligned}$$

where in the last passage we use the fact that, as  $J$  ranges over subsets of  $X$  and  $I \subseteq X$ , then also  $J' = J \Delta I$  ranges over subsets of  $X$ .

Hence by induction, performing  $k' - 1$  steps, and up to relabeling the indices of the cycles so that the remaining family  $(c_1, \dots, c_{2g})$  forms a basis,

$$\bar{A}(\sigma) = 2^{k'-1} \sum_{J \subseteq \{1, \dots, 2g\}} (-1)^{\Phi(J)} = 2^{k'-1+g} 2^{-g} \sum_{x \in H_1(M, \mathbb{Z}_2)} (-1)^{\Phi(x)} = 2^{k'-1+g} \text{arf}(\Phi).$$

□

Recall that in Proposition 1.9 we claimed that  $s(\sigma) = 2^{-\frac{n+k'-1}{2}} \bar{A}(\sigma)$  (this fact is proven later on), thus, when  $\Phi$  is defined, that is, for  $(M, \omega) \in H(2d_1^{m_1}, \dots, 2\bar{d}_i^{m_i}, 2d_k^{m_k})$ , this quantity is equal to  $\text{arf}(\Phi)$ , since  $\frac{n+k'-1}{2} = \frac{2g-2+2k'}{2} = k' - 1 + g$  by Lemma 2.6.

When  $(M, \omega) \notin H(2d_1^{m_1}, \dots, 2\bar{d}_i^{m_i}, 2d_k^{m_k})$ , i.e. when  $\omega$  has some zeroes of odd degree, the function  $\Phi$  is not defined. Nonetheless the function  $s(\sigma)$  remains well-defined, and its value is 0 in this case (see the following Lemma 6.1 for a proof).

In summary, we have

$$\begin{aligned} s(\sigma) \in \{\pm 1\} &\iff s(\sigma) = \text{arf}(\Phi) \text{ and } (M, \omega) \in H(2d_1^{m_1}, \dots, 2\bar{d}_i^{m_i}, 2d_k^{m_k}); \\ s(\sigma) \in \{0\} &\iff \text{An even number of conical singularities with angle multiple of } 4\pi. \end{aligned}$$

## 2.3 Surgery operators

In this section we describe two families of ‘geometric surgery operations’ which can be performed on translation surfaces, and more notably on suspensions. Some special cases of these will correspond to the combinatorial surgery operators, introduced in Section 1.7, and crucially used in the main body of the paper.

For this purpose it will be useful to introduce a convention on the visualisation of conical singularities. We have seen that the degree  $d_i$  of a zero  $z_i$  can be computed directly on the translation surface, either by adding the angles of the polygon which are associated to the singularity (then dividing by  $2\pi$ , and subtracting 1) or also, more conveniently, just by counting the number of top (or bottom) arcs around the vertices of the singularity, minus 1 (cf. figure 8 and figure 18). In order to visualise a singularity, say at  $z_i$ , it is useful to consider a small neighbourhood, say of radius  $\epsilon \ll |v_i|$ . Such a neighbourhood is isometric

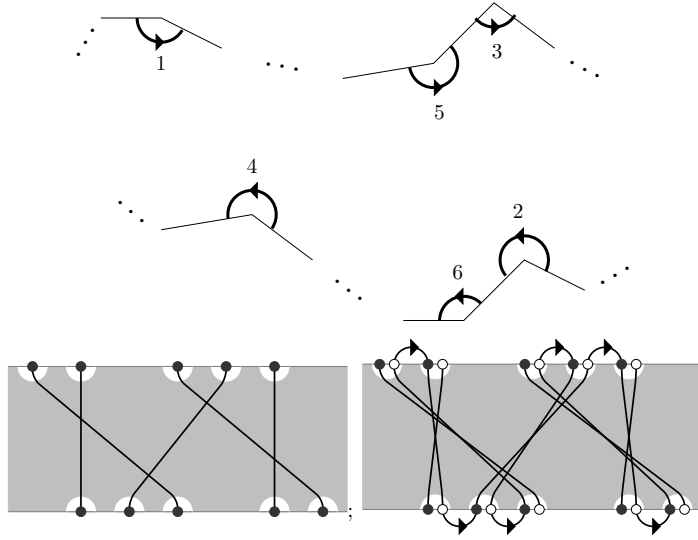


Figure 18: Top: a translation surface with a conical singularity of angle  $6\pi$ . Bottom: the associated permutation.

to a cone of angle  $2\pi(d_i + 1)$ , i.e. the glueing of  $2(d_i + 1)$  half-disks of radius  $\epsilon$ . If, in a picture, we take care of drawing some trajectories of the vertical foliation, we can trade half-disks for angular sectors of circle with smaller angles  $\alpha_j$ , so that, in total, we can squeeze the  $2\pi(d_i + 1)$  cone into an ordinary disk (by choosing  $\alpha_j$ 's such that  $\sum_{j=1}^{2(d_i+1)} \alpha_j = 2\pi$ ), and still provide a picture in which the foliation is reconstructed unambiguously. Such a representation is illustrated in figure 19.

We now introduce a family of suspensions, with certain special properties guaranteeing that the behaviour of the geometric surgery operations is more simple than what is the case on a generic suspension: (recall,  $u_j$  are synonyms for  $v_{\tau(n+1-j)}$ )

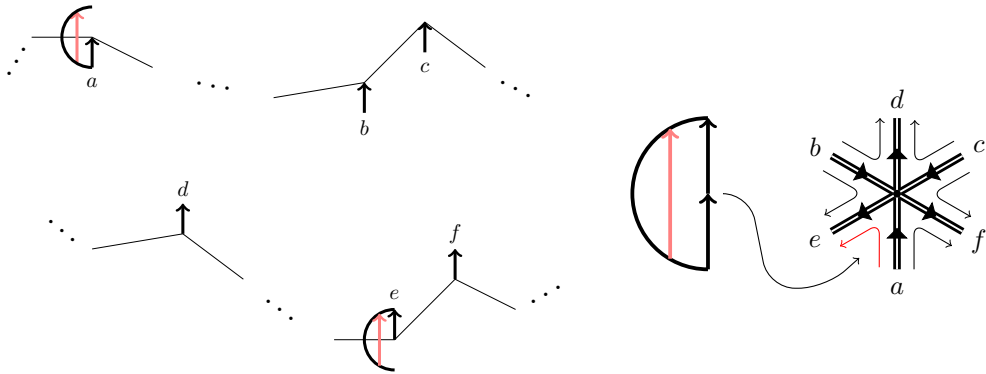


Figure 19: On the left picture, the black arrows represent the leaves of the foliation on the critical point  $z_i$ . Since  $z_i$  has conical angle  $6\pi$ , there are 6 half-disks (of radius  $\epsilon$ ) forming together the neighbourhood of  $z_i$ . One such half-disc, adjacent to the leaves  $a$  and  $e$ , is represented. On the right picture, we have a representation of the leaves of the vertical foliation in the neighbourhood of the singularity  $z_i$ . Each angular sector in the picture is of angle  $\pi/3$ , although it corresponds to a half-disc of radius  $\epsilon$ . The red trajectory, associated to a leaf passing in a neighbourhood of the singularity, helps in visualising the glueing procedure.

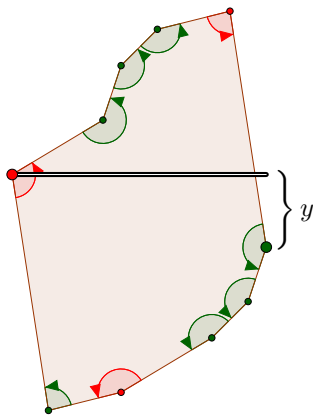


Figure 20: A regular suspension for  $\tau = (23145)$ . This permutation has rank 1, and one cycle of length 3, i.e. the marked singularity has degree zero (red angles) and there is a single further singularity, of degree two (green angles).

**Definition 2.8** (Regular suspension). *We say that a suspension  $S = (\tau; v_1, \dots, v_n)$  is regular, and of shift  $y$  if*

- $-\frac{\pi}{2} < \arg(u_1) < 0 < \arg(u_2) < \arg(u_3) < \dots < \arg(u_n) < \frac{\pi}{2}$ ,
- $\Im(v_1 + v_2 + \dots + v_n) = \Im(u_1 + u_2 + \dots + u_n) = -y$ , with  $y \geq 0$ ,
- $\tau(n) = n$ .

An example is given in Figure 20. In particular, a regular suspension, with reference to the notation of Figure 12, has  $\epsilon \in \{0, -\}$ .

### 2.3.1 Adding a cylinder

The first family of geometric surgery operators consists in *breaking up a zero* (of the abelian differential  $\omega$ ), as discussed, e.g., in [KZ03, sect. 4.2] and [EMZ03]. Geometrically, this consists in adding a cylinder on one given singularity of the translation surface.

Let  $S$  be a translation surface, represented as a polygon with identified sides, and let  $z_i$  be a zero of degree  $d_i$ . A *saddle connection* from  $z_i$  to  $z_i$  is a geodesic (i.e., in our case, a straight line segment which may wrap along the identified sides of the polygon) connecting a vertex of the equivalence class of  $z_i$  on the top broken line to a vertex of the equivalence class of  $z_i$  on the bottom broken line. So, for a zero of degree  $\ell = d + 1$ , there are  $\ell^2$  families of saddle connections, one per top/bottom choice of angle, with segments in the same family differing for the choice of the winding.

In order to break up a zero  $z_i$ , we choose one such saddle connection, in one such family, and “add a cylinder”. This operator may be denoted as  $\mathcal{Q}_{i,h,k,s}(v)$ , with  $i$  an index associated to the singularity,  $h, k \in \{1, \dots, d_i + 1\}$  associated to the choice of top/bottom angle,  $s$  associated to the choice of saddle connection within the family, and  $v$  a two-dimensional vector with positive scalar product with the versor of the saddle connection.

This construction is especially simple if, for the given polygon  $S$  and triple  $(i, h, k)$  as above, there exists one saddle connection  $s_0$  in the family which consists just in a straight segment, and doesn’t go through the sides of the polygon (if it exists, it is unique). I.e., if the segment in the plane between the two angles  $h$  and  $k$  of the polygon is contained within the polygon. In this case adding a cylinder corresponds, in the polygon representation, to adding a parallelogram, with one pair of opposite sides associated to the saddle connection, and the other pair associated to a vector  $v$ , which is thus inserted (at the appropriate position) in the list of  $v_j$ ’s describing the polygon  $S = (\tau; v_1, \dots, v_n)$ . This also adds one edge to

the permutation  $\tau$ , or, in other words, it adds the same vector  $v$  both at a position in the list  $(v_j)_j$  and in the list  $(u_j)_j$ . The procedure in this simplified situation is described in Figure 21. In this situation we denote the corresponding operator as  $\mathcal{Q}_{i,h,k}(v)$ , i.e. we omit the index  $s = s_0$  for the choice of saddle connection.

When, instead, we choose a saddle connection with a non-trivial winding, in the polygon representation we shall add the vector  $v$  at several places along the list of  $v_j$ 's. The other copies are associated to the introduction of false singularities (i.e. zeroes of  $\omega$  of degree zero, i.e., in the permutation, edges associated to descents). This does not change the topology of the surface, but gives non-primitive representants, or forces to study further manipulations which allow to remove false singularities. We will not discuss this analysis here.

Let us describe in more detail why the construction depicted above is legitimate, now at the level of the translation surface as a whole (and not of the polygon representation). The saddle connection on the surface is a closed curve, since its endpoints are identified in the polygonal construction. Neglecting the identification, it consists of some vector  $w$ , if the trajectory is followed from vertex  $h$  to  $k$ , in the local flat metric. We cut the surface along this curve, obtaining a new surface  $S'$  with two boundary components homeomorphic to circles. Finally, we construct a cylinder by taking a parallelogram with sides  $(+v, +w, -v, -w)$ , gluing its two  $\pm w$  sides to the two boundaries of  $S'$ , and its two  $\pm v$  sides among themselves. This gives the desired surface  $S_{\text{new}} = \mathcal{Q}_{i,h,k,s}(v)S$ .

This operation breaks up the singularity  $z_i$  of degree  $d_i$  into two singularities  $z$  and  $z'$  of degrees  $d$  and  $d'$  such that  $d + d' = d_i$ . The value of  $d$  and  $d'$  depends on which pair of vertices (in the equivalence class of  $z_i$ ) are connected by the geodesic. In particular, for each  $h$  there exists exactly one value  $k$  such that the pair  $(d, d')$  is attained, and similarly for  $k$  (see figure 21).

This operation is especially clear in the neighbourhood of  $z_i$ : the introduction of the cylinder separates the singularity into two new singularities, each one with its own neighbourhood represented by a concatenation of half-planes (cf. Figure 22).

In order to avoid the complicancy on the polygon representation deriving by the presence of winding geodesics (and the resulting introduction of false singularities), we will remark the crucial property:

**Proposition 2.9.** *If  $S$  is a regular suspension of shift  $y$  for a permutation  $\tau$  of rank  $r$ ,  $\bar{r}$  is the singularity associated to the rank,  $r_0$  is the top angle at the beginning of the rank cycle, and  $k < r$  is the  $k$ -th bottom angle of the rank cycle, there exists one saddle connection in the family  $(r_0, k)$  which is contained within the polygon, and, for all  $v$  with argument in a non-empty range and  $\Im(v) < y$ ,  $\mathcal{Q}_{\bar{r},r_0,k}(v)S$  is a regular suspension of shift  $y - \Im(v)$ .*

*The range for  $\arg(v)$  is as follows. If the new edge of the permutation is added to the list  $(u_j)_j$  at  $j$ , we shall have*

$$\theta_- < \arg(v) < \theta_+ \quad \theta_- = \begin{cases} \arg(u_j) & j > 1 \\ 0 & j = 1 \end{cases} \quad \theta_+ = \begin{cases} \arg(u_{j+1}) & j < n \\ \frac{\pi}{2} & j = n \end{cases} \quad (18)$$

This construction is illustrated in Figure 23.

The two surgery operators  $q_1$  and  $q_2$  correspond to  $\mathcal{Q}_{\bar{r},r_0,k}(v)$  as in Proposition 2.9, for  $k$  being such that the degree  $d_i$  of the marked singularity is divided into  $d$  and  $d_i - d$ , with the degree of the new marked singularity being  $d = 0$  or  $1$ , for  $q_1$  and  $q_2$ , respectively.

We note in passing that the construction described so far, of breaking up a zero, can be made local, i.e. can be realised in a way such that the flat metric does not change outside of some neighbourhood of  $z_i$  (see [KZ03, sect. 4.2] for details). This, however, and at difference with Proposition 2.9, yet again comes at the price of introducing false singularities in the polygon (and permutation) representation.

### 2.3.2 Adding a handle

Our second family of geometric surgery operations  $\mathcal{T}$  corresponds to adding a handle, and will be related to the operator  $T$ . Let us start by describing this operation on the translation

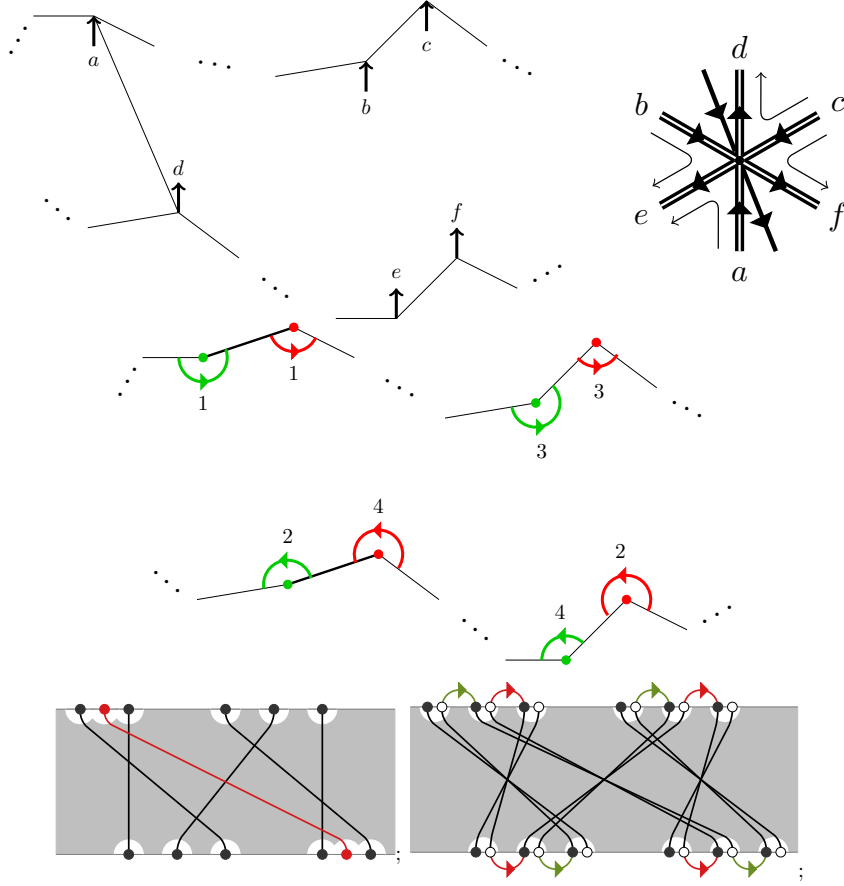


Figure 21: Top left: a saddle connection between two vertices of the conical singularity of angle  $6\pi$  on the translation surface. Top right: the same geodesic in a neighbourhood of  $z_i$ . Middle: we cut the surface along the geodesic and glue the two boundary of a cylinder to the two newly formed boundaries of the surface. Adding the cylinder breaks up the singularity of angle  $6\pi$  into two singularities of angle  $4\pi$  (in green and red respectively). Bottom: the projection on the permutation of this procedure consists in adding an edge (in red in the figure) in between two arcs belonging to the same cycle (cf figure 18 for the drawing of the cycle invariant).

surface. Let  $z_i$  be a singularity. We choose a direction  $\theta \in [0, 2(d_i + 1)\pi]$  and a length  $\rho$ , and consider the arc of geodesic  $\gamma$  starting from  $z_i$  with direction  $\theta$  and length  $\rho$ . Assume that this arc does not contain any singularity except for its starting point. We call  $w$  the corresponding vector. We cut the surface  $S$  along the vector  $w$ , and call  $S'$  the resulting surface. Choose a vector  $v$  with positive scalar product with the versor of  $w$  (i.e., with an angle within  $[0, \pi]$  w.r.t. the local metric at the starting point), and construct a cylinder, by folding a parallelogram  $(+v, +w, -v, -w)$  analogously to how was the case for  $\mathcal{Q}$ , i.e. gluing its two  $\pm w$  sides to the two boundaries of  $S'$ , and its two  $\pm v$  sides among themselves. This gives the desired surface  $S_{\text{new}} = \mathcal{T}_{i,w}(v)S$ . This procedure is illustrated, in a somewhat simplified picture, in Figure 24.

Let us describe this now at the level of the polygon representation. Say that the direction  $\theta$  is within the angle  $x$  on the top boundary of the polygon, and call  $P$  the endpoint of  $w$ . Similarly to the case of  $\mathcal{Q}$ , if  $P$  is on the boundary of the polygon, and the vector  $w$  is completely contained within the polygon (i.e., it goes from  $x$  to  $P$  without passing through the identified sides), then the construction is especially simple also at the level of the polygon:



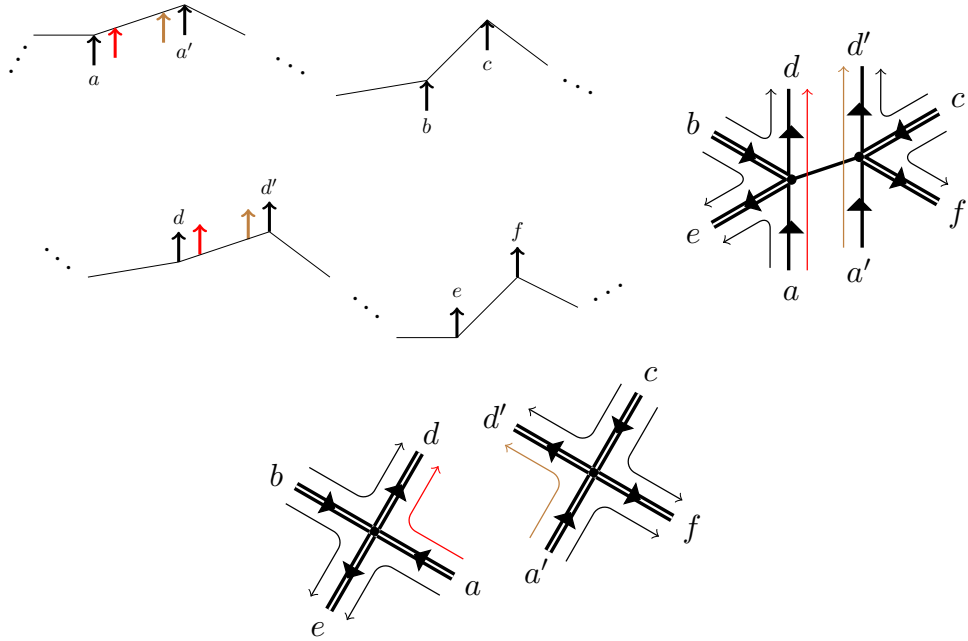


Figure 22: Top right: adding the cylinder breaks up the singularity of angle  $6\pi$  in two, as is shown globally on the polygon, on the left, and in a neighbourhood of the saddle connection, on the right. Bottom: after this operation, we see that there are two singularities in this case each of total angle  $4\pi$  (neighbourhoods centered around each of them are shown). In red and brown, two leaves of a foliation parallel to the saddle connection, passing next to the singularities, help in visualising the local modification. In this case, in order to simplify the drawing, we have a description of the local neighbourhoods which corresponds to the case in which the saddle connection is itself vertical.

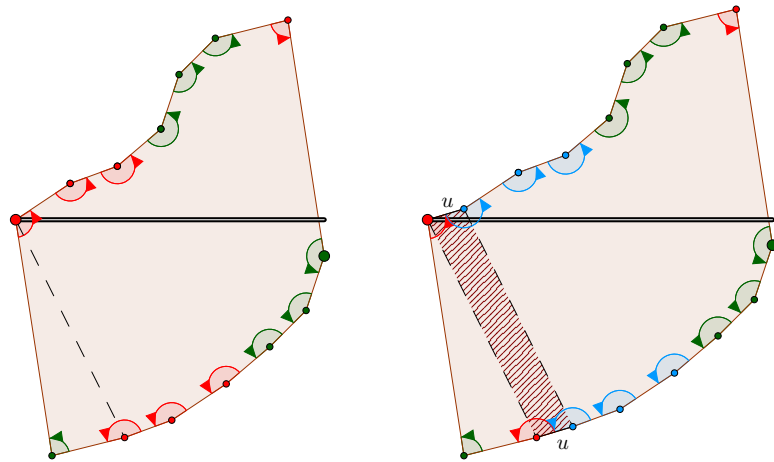


Figure 23: Left: a regular suspension for  $\tau = (413256)$ . This permutation has rank 3 (red angles), thus the marked singularity is of degree 2, and one cycle of length 3 (green), i.e. a singularity of degree 2. Right: the result of applying the operator  $\mathcal{Q}$ , which breaks the marked singularity into a marked singularity of degree zero and a new singularity of degree 2.

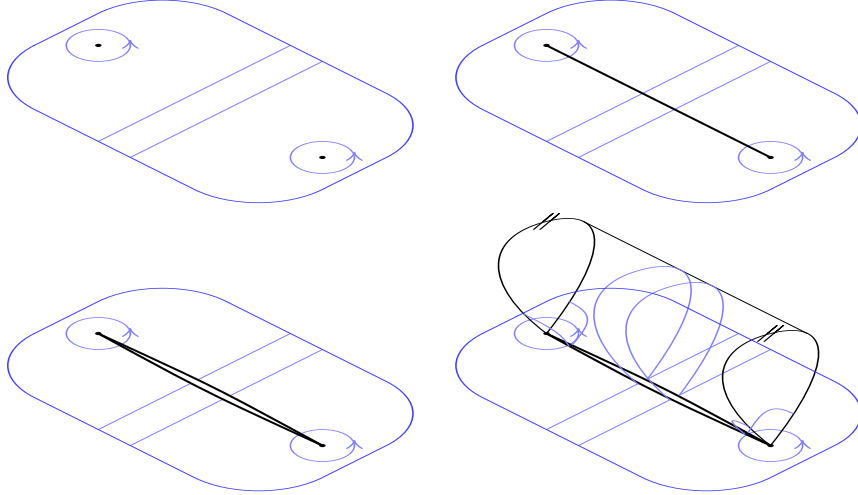


Figure 24: Top left: two singularities on a portion of a translation surface. In this case, in order to simplify the drawing, they are both false-singularities. A small circle around each of them, and a couple of typical leaves of the vertical foliation, are shown. Top right: a saddle connection between the two singularities is added. Bottom left: the surface is cut along this line. Bottom right: a handle is added along these boundaries. Note how both the circles around the singularities and the leaves are modified. In particular, now we have a unique singularity, in this case of angle  $6\pi$ , as the arcs on the cylinder are connected in such a way to concatenate the two circles.

it does not require the introduction of false singularities, and consists in the introduction of a parallelogram. More precisely, if  $P$  is on the bottom side  $u_j$  of the polygon, the operation consists of two parts: first, it cuts the side  $u_j$  into two consecutive and collinear sides  $u'_j$  and  $u''_j$ , thus adding (temporarily) a false singularity of angle  $2\pi$  on  $P$ , and then it inserts a cylinder following  $w$ , which is now a saddle connection between two angles of the polygon (just as in  $\mathcal{Q}$ , but with the two angles associated to distinct singularities).

By this operation we have added a handle to the surface  $S$  on the singularity  $z_i$ . If the degree of  $z_i$  on  $S$  is  $d_i$ , then its degree on  $S_{\text{new}}$  is  $d_i + 2$ , as explained in figure 25. Seen in a neighbourhood of the singularity, this operation corresponds to adding four angular sectors between two consecutive angular sectors (see figure 26), and, in particular, the false singularity that was temporarily added is now merged to the original singularity  $z_i$ .

If the point  $P$  is not on a side of the polygon, we can proceed by a slight generalisation of the first part of the operation: choose a bottom side  $u_j$ , call  $P'$  and  $P''$  its endpoints, and suppose that the triangle  $(P, P', P'')$  can be added/removed on the top/bottom copies of the edge (i.e.,  $u_j$  on the bottom and  $v_{\tau^{-1}(n+1-j)}$  on top), so to obtain an equivalent representation of the polygon, with the introduction of a unique false singularity (this happens when the segments  $(P, P')$  and  $(P, P'')$  on the plane do not cross the boundary of the polygon). If we do so, we are in the same situation as before, i.e. we have decomposed  $u_j = u'_j + u''_j$ , with  $u'_j = (P', P)$  and  $u''_j = (P, P'')$ , the only difference being the fact that  $u'_j$  and  $u''_j$  are not collinear.

In order to describe the procedure at the level of the polygon, and with a generic point  $P$  as above (not necessarily on the boundary), we need to supplement the choice of  $x$  and  $j$  to the notation, so we will write  $S_{\text{new}} = \mathcal{T}_{x,j,w}(v)S$ .

Similarly as was the case with adding a cylinder, if we follow this procedure on a regular suspension, and the point  $P$  is chosen appropriately, we can have a regular suspension as

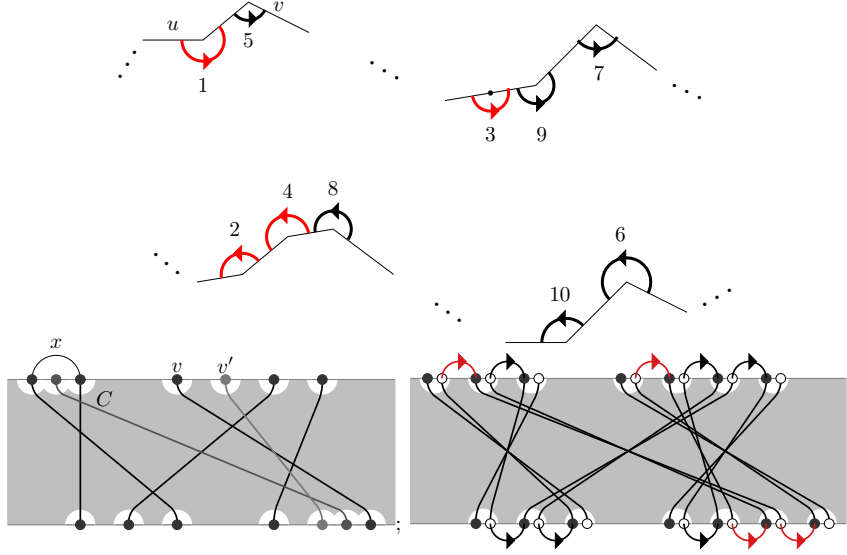


Figure 25: Top : In A portion of a translation surface  $S'$  corresponding to an operator  $\mathcal{T}$  acting on the example surface  $S$  of Figure 18. For what concerns the construction of small circles around the singularities, while in  $S$  we have an arc from  $u$  to  $v$ , here instead the arcs labeled with indices from 1 to 5 ultimately connect  $u$  to  $v$ , while also encircling the newly introduced false singularity, and the rest remains unchanged. The four arcs in red (two on the top broken line, and two on the bottom) are added to the same cycle, and thus increase by 2 the degree of the corresponding singularity, in this example passing from angle  $6\pi$  to angle  $10\pi$ . Bottom: the procedure at the level of permutations. Let us describe the surgery procedure in details, comparing the language of permutations with the geometric counterpart:

outcome, as illustrated in the following:

**Proposition 2.10.** *Given a side  $u_j = (P', P'')$  on the bottom side of a regular suspension, excluded the leftmost one, define  $\theta_{\pm}$  as in (18). Consider the triangle  $\Delta$  with one side  $u_j$ , and the other two sides with slopes  $\theta_{\pm}$ . For each  $P$  in the interior of  $\Delta$ , if we add the triangle  $(P, P', P'')$  to the polygon, below  $u_j$ , and remove the corresponding copy of the triangle below  $v_{\tau^{-1}(n+1-j)}$ , we obtain a new suspension which is regular, has the same shift parameter, and has a false singularity in  $P$ .*

**Proposition 2.11.** *Let  $S$  be a regular suspension of shift  $y$ , for a permutation  $\tau$  of rank  $r$ ,  $\bar{r}$  is the singularity associated to the rank,  $r_0$  is the top angle at the beginning of the rank cycle,  $1 \leq j \leq n-1$  is the index of a vector on the bottom side, excluded the left-most one.*

*Let notations be as in Proposition 2.10, with  $S'$  being the outcome polygon, and  $w$  be the saddle connection connecting  $r_0$  to  $P$ , by passing through no sides of the polygon  $S'$ . Let  $v$  be a vector with  $\arg(u'_j) < \arg(v) < \arg(u''_j)$ , and  $\Im(v) < y$ . Then the suspension  $\mathcal{T}_{r_0, j, w}(v)S$  is regular with shift  $y - \Im(v)$ .*

This construction is illustrated in Figure 27.

Our  $T$  operator is a special case of this operation, corresponding to  $j$  being the rightmost vector of the polygon, on the bottom side. We can define, more generally, operators  $\{T_j\}_{1 \leq j \leq n-1}$ , of which  $T \equiv T_1$  is the special case above. For what concerns the invariants, all of these  $T_j$  behave in the same way: the degree of the marked singularity increases by 2, and all the rest of the invariant stays put.

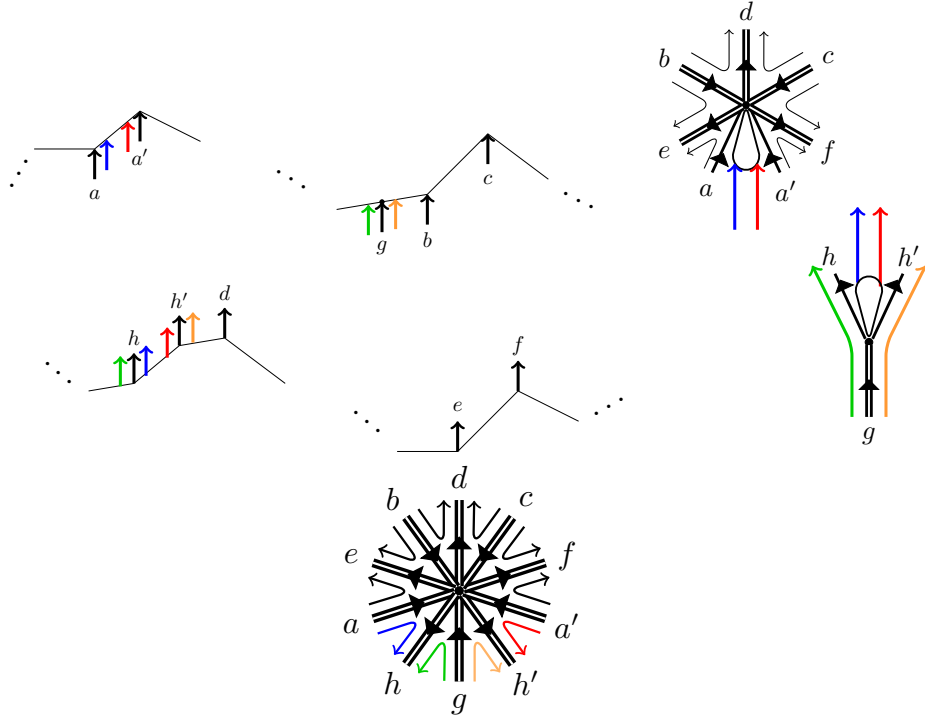


Figure 26: Adding the point  $P$  on the boundary  $v$  of the polygon divides this side in two, thus  $P$  becomes a false singularity of angle  $2\pi$  (i.e. a zero of degree 0). The two half-disks are denoted here by the presence of a green and an orange leaf in the vertical foliation. Adding the cylinder glues together the two singularities, resulting in this case in a  $10\pi$  singularity, whose neighbourhood, obtained by the insertion of the parallelogram with blue and red leaves on the two singularities (see top-right), is isomorphic to the neighbourhood illustrated at the bottom of the image.

### 2.3.3 Regular suspensions in a given Rauzy class

Our classification theorem, based on the analysis of surgery operators  $q_{1,2}$  and  $T$ , and the results of the present section, in particular Propositions 2.9 and 2.11, allow to describe large families of regular suspensions (with no false singularities) which are certified to be within one given (primitive) Rauzy class.

For a class  $C$ , let us call  $\mathcal{R}(C)$  the set of such regular suspensions. Thus we have  $\mathcal{R}(C) = \{S\}$ , with  $S = (\tau; v_1, \dots, v_n)$  satisfying certain properties, which we now explicitate. We describe explicitly  $\mathcal{R}(\text{Id}_n)$  and  $\mathcal{R}(\text{Id}'_n)$ , and, for  $C$  a non-exceptional primitive class with invariant  $(r, \lambda, s)$ , we describe  $\mathcal{R}(C) \equiv \mathcal{R}(r, \lambda, s)$  recursively in terms of the invariant.

We say that  $(v_1, \dots, v_n)$  is a *regular vector* if it satisfies the first two conditions of Definition 2.8. We can then anticipate a corollary of the results presented in this section and in the body of the paper:

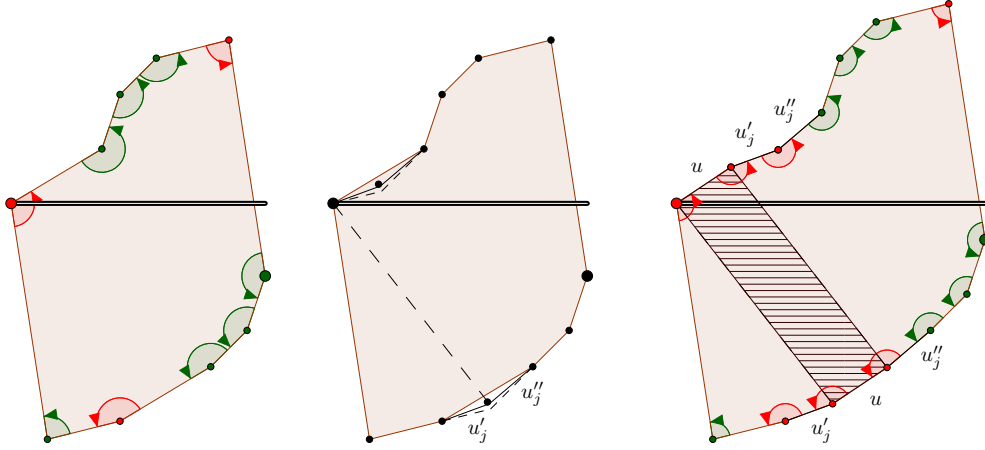


Figure 27: Left: a regular suspension  $S$  for  $\tau = (23145)$  (the same as in figure 20). Middle: the construction of  $S'$  described by Proposition 2.10. Right: the operation  $\mathcal{T}_{r_0, j, w}(v)S$  described by Proposition 2.11 (this suspension is as in the left part of figure 23). The resulting permutation,  $\tau = (413256)$ , has the same cycle structure as the starting one, except for the rank, which has increased by 2.

**Corollary 2.12.** *The surfaces in the sets  $\mathcal{R}(C)$  below are all regular suspensions:*

$$\mathcal{R}(\text{Id}_n) = \left\{ \left( \begin{array}{|c|} \hline \text{X} \\ \hline \end{array}; v_1, \dots, v_n \right) \text{ with } (v_1, \dots, v_n) \text{ regular} \right\} \quad (19)$$

$$\mathcal{R}(\text{Id}'_n) = \left\{ \left( \begin{array}{|c|} \hline \text{X} \\ \hline \end{array}; v_1, \dots, v_n \right) \text{ with } (v_1, \dots, v_n) \text{ regular} \right\} \quad (20)$$

$$\mathcal{R}(1, \lambda, s) = \bigcup_{\ell \mid \exists \lambda_i = \ell} \{ \mathcal{Q}_{\bar{r}, r_0, 1}(v)S \}_{S \in \mathcal{R}(\ell, \lambda \setminus \ell, s); v \text{ as in Prop. 2.9}} \quad (21)$$

$$\mathcal{R}(2, \lambda, 0) = \bigcup_{\substack{\ell \mid \exists \lambda_i = \ell \\ s=0, \pm 1}} \{ \mathcal{Q}_{\bar{r}, r_0, 2}(v)S \}_{S \in \mathcal{R}(\ell+1, \lambda \setminus \ell, s); v \text{ as in Prop. 2.9}} \quad (22)$$

$$\mathcal{R}(r, \lambda, s) = \bigcup_{j=1}^{n-1} \{ \mathcal{T}_{r_0, j, w}(v)S \}_{S \in \mathcal{R}(r-2, \lambda, s); w \text{ and } v \text{ as in Props. 2.10 and 2.11}} \quad r \geq 3 \quad (23)$$

where, in (22), the set of invariants which contribute to the set-union is as follows: if  $\lambda \setminus \ell$  has a positive number of even cycles, then  $s = 0$ , otherwise,  $s = \pm 1$ .

(The domains in the sums are explained in detail in the following Corollaries 5.13 and 5.15).

This result is complementary to the work present in an article of Zorich [Zor08], in which he constructs representatives of every connected component of every strata, consisting of Jenkins–Strebel differentials. One advantage of our approach is the fact that the representatives given in Corollary 2.12 are a large number (the smallest asymptotics for a non-exceptional class, corresponding to the iterated application of  $\mathcal{T} \circ \mathcal{Q}_2$ , is of the order of  $n!$ ). A second advantage is that each representative has a simple interpretation in terms of nested insertions of handles and cylinders.

## 2.4 A summary of terminology

We end this section by collecting a list of notions which appear both in our approach and in the geometric construction (but, sometimes, under different names). First, we recall in words some notational shortcuts for the strata which were used in [KZ03] and [Boi12]:

- They call  $H^{\text{hyp}}(2g - 2)$  and  $H^{\text{hyp}}(g - 1, g - 1)$  the *hyperelliptic classes*, which, by Lemma 2.6, correspond to  $\text{Id}_n$  with  $n = 2g$  and  $\text{Id}_n$  with  $n = 2g + 1$ , respectively.
- They call  $H^{\text{even}}(2d_1^{m_1}, \dots, 2d_k^{m_k})$  and  $H^{\text{odd}}(2d_1^{m_1}, \dots, 2d_k^{m_k})$  the two connected components of the stratum  $H(2d_1^{m_1}, \dots, 2d_k^{m_k})$  with Arf invariant  $+1$  and  $-1$  respectively.
- We shall call  $H^{\text{even}}(2d_1^{m_1}, \dots, 2\bar{d}_i^{m_i}, \dots, 2d_k^{m_k})$  and  $H^{\text{odd}}(2d_1^{m_1}, \dots, 2\bar{d}_i^{m_i}, \dots, 2d_k^{m_k})$  the two connected components of the marked stratum  $H(2d_1^{m_1}, \dots, 2\bar{d}_i^{m_i}, \dots, 2d_k^{m_k})$  with Arf invariant  $1$  and  $-1$  respectively (in analogy with their notation).
- Finally, we use symbols  $H(d_1^{m_1}, \dots, d_k^{m_k})$  (respectively  $H(d_1^{m_1}, \dots, \bar{d}_i^{m_i}, \dots, d_k^{m_k})$ ) only when a positive number of the  $d_i$ 's are odd. In this case, these symbols denote a stratum (respectively, a marked stratum) with some zeroes of odd degree, so that the Arf invariant is not defined, and the stratum is connected.

Then, Table 4 gives a list of correspondences between the terminology adopted in [KZ03] and [Boi12], related to the geometric notions associated to the strata, and the one, issued from the combinatorial approach, used in this article

### 3 Some basic facts

#### 3.1 Properties of the cycle invariant

In this section we come back to the cycle invariant introduced in Section 1.4.1. In particular, we shall prove Propositions 1.7 and 1.8, concerning the fact that  $(\lambda, r)$  is invariant in the  $\mathcal{S}$  dynamics, and  $\lambda$  is invariant in the  $\mathcal{S}^{\text{ex}}$  dynamics. These facts are especially evident in the diagrammatic representation, which we illustrate in Figure 28.

The idea is that the operators of the dynamics, i.e. the permutations  $\gamma_{L,n}(i)$  and  $\gamma_{R,n}(i)$  defined in (2), perform local modifications on portions of paths, without changing their lengths. For all cycles (or the rank path) except for at most two of them, this is completely evident: each arc of the cycles is deformed by (say) the permutation  $\gamma_{L,n}(i)$  in a way which can be retracted without changing the topology of the connections, this in turns certifying that the length of the involved cycle does not change. (We recall that the length is defined as the number of top or bottom arcs). Furthermore, it also preserves the path-lengths of these cycles.

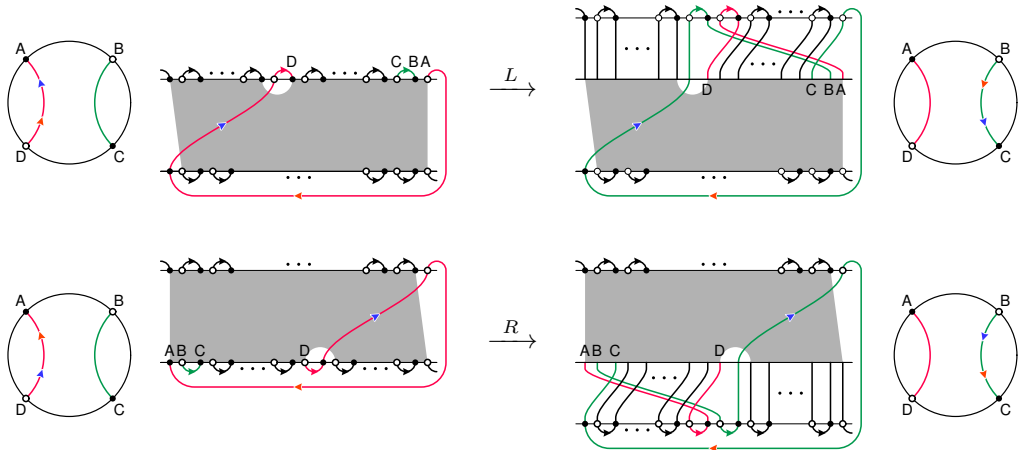


Figure 28: Invariance of  $\lambda(\sigma) \cup \{r\}$  in  $\mathcal{S}_n$ , and of  $\lambda'(\sigma)$  in  $\mathcal{S}_n^{\text{ex}}$ , illustrated for the operators  $L$  (top) and  $R$  (bottom). For  $\mathcal{S}_n^{\text{ex}}$ , the cases of operators  $L'$  and  $R'$  are deduced analogously.

Geometric and topological objects	Combinatorial objects
Translation surface with vertical direction Riemann surface with abelian differential $(M, \omega)$	Suspension data $(\sigma, (v_i)_i)$
Conical singularity of angle $2\pi(d_i + 1)$ Zero of $\omega$ of degree $d_i$ False singularity (zero of $\omega$ of degree 0)	Cycle of length $\lambda_i = d_i + 1$ descent (cycle of length 1)
Marked conical singularity of angle $2\pi(d + 1)$ Marked zero of $\omega$ of degree $d$	Rank path of length $r = d + 1$
Arf invariant $\text{arf}(\Phi)$	Arf (or sign) invariant $s(\sigma)$
$H^{\text{hyp}}(2g - 2)$ $H^{\text{hyp}}(g - 1, g - 1)$	$\text{Id}_n$ with $n = 2g$ even $\text{Id}_n$ with $n = 2g + 1$ odd
$H^{\text{hyp}}(2g - 2, \bar{1})$ $H^{\text{hyp}}(g - 1, g - 1, \bar{1})$	$\text{Id}'_n$ with $n = 2g + 1$ odd $\text{Id}'_n$ with $n = 2g + 2$ even
Connected component in $\mathcal{S}$ $H^{\text{even}}(2d_1^{m_1}, \dots, 2\bar{d}_i^{m_i}, \dots, 2d_k^{m_k})$	Rauzy class with invariant $(\lambda, r = 2d_i + 1, s = +1)$ $\lambda = ((2d_1 + 1)^{m_1} \dots (2d_i + 1)^{m_i - 1} \dots (2d_k + 1)^{m_k})$
Connected component in $\mathcal{S}$ $H^{\text{odd}}(2d_1^{m_1}, \dots, 2\bar{d}_i^{m_i}, \dots, 2d_k^{m_k})$	as above, with $s = -1$
Connected component in $\mathcal{S}$ $H(d_1^{m_1}, \dots, \bar{d}_i^{m_i}, \dots, d_k^{m_k})$	Rauzy class with invariant $(\lambda, r = d_i + 1, s = 0)$ $\lambda = ((d_1 + 1)^{m_1} \dots (d_i + 1)^{m_i - 1} \dots (d_k + 1)^{m_k})$
Connected component in $\mathcal{S}^{\text{ex}}$ $H^{\text{even}}(2d_1^{m_1}, \dots, 2d_k^{m_k})$	Extended Rauzy class with invariant $(\lambda, s = +1)$ $\lambda = ((2d_1 + 1)^{m_1} \dots (2d_k + 1)^{m_k})$
Connected component in $\mathcal{S}^{\text{ex}}$ $H^{\text{odd}}(2d_1^{m_1}, \dots, 2d_k^{m_k})$	as above, with $s = -1$
Connected component in $\mathcal{S}^{\text{ex}}$ $H(d_1^{m_1}, \dots, d_k^{m_k})$	Extended Rauzy class with invariant $(\lambda, s = 0)$ $\lambda = ((d_1 + 1)^{m_1} \dots (d_k + 1)^{m_k})$
Bubbling a handle	$T$ operator
Adding a cylinder	$q_1$ and $q_2$ operators

Table 4: Correspondence between the terminology adopted in [KZ03] and [Boi12] and the one used in this article.  $\text{Id}'_n$  (i.e the hyperelliptic class with a marked point) was studied in [BL12].

For the paths passing from four special endpoints (marked as  $A, B, C$  and  $D$  in the figure), the invariance of the cycle structure holds through a more subtle mechanism, involving the exchange of two arcs, and, for what concerns path-lengths, by a crucial use of the  $-1$  mark. The way in which the topology of connections among these four points is modified by the permutation  $\gamma_{L,n}(i)$  is hardly explained in words, but is evident from Figure 28. This

proves that the list  $\lambda' = \lambda \cup \{r\}$  is invariant. We shall prove also that, in the  $\mathcal{S}_n$  dynamics, the rank length is also preserved (and thus, by set difference,  $\lambda$  is). This comes from the fact that the two endpoints of the rank path cannot move under the action of  $L$  and  $R$  (while they *would* move under  $L'$  and  $R'$ ). Figure 28 shows that path lengths are preserved also if the paths are coloured (e.g., in the figure, if the lengths of the green and purple paths in  $\sigma$  are  $\ell_1$  and  $\ell_2$ , respectively, they are still  $\ell_1$  and  $\ell_2$  in  $L\sigma$ ). As we perform local modifications on portions of paths adjacent to arcs, these do not affect the rank-path endpoints, and thus do not affect the rank-path ‘colour’. From this we deduce that also the length  $r$  of the rank path is invariant. This completes the proof.

Note that the length of the principal cycle (i.e. the cycle going through the  $-1$  mark) is *not* preserved. Also, is not preserved the boolean value [does the rank-path pass through the  $-1$  mark]. Indeed, in the figure, the purple path goes through the mark in  $\sigma$ , while the green path does, in  $L\sigma$ . Nonetheless, these quantities evolve in a rather predictable way. If we annotate which cycles/paths go through the arcs in the top-right portion of the diagram (namely, at the right of  $\sigma(1)$ ), we can observe that iterated powers of  $L$  make a circular shift on these labels (yet again, represented by the green and purple colours on the arcs), and this immediately reflects on which cycle (or the rank path) goes through the  $-1$  mark. This fact is analysed in more detail in Section 3.3 below.

## 3.2 Standard permutations

As we have seen in the introduction, irreducibility is a property of classes: either all permutations of a class are irreducible or none is. It is a trivial and graphically evident property, as the block structure is clear both from the matrix representation of  $\sigma$ , and from the diagram representation of  $\sigma$ . There is a further, less obvious, characterisation of irreducibility, which leads us to the definition of ‘standard permutations’. Both notions are already present in the literature. For example, standard permutations are introduced by Rauzy [Rau79], they play a crucial role in [KZ03] (and various other papers), and their enumerations are investigated in [Del13].

**Definition 3.1** (standard permutation). *The permutation  $\sigma$  is standard if  $\sigma(1) = 1$ .*

(This definition is slightly different from the common one, where  $\sigma$  is standard if  $\sigma(1) = 1$  and  $\sigma(n) = n$ . As we will see below, in Proposition 3.9, this is a minor problem, because the two notions are easily related.) As mentioned above, we have:

**Lemma 3.2.** *A class  $C \subseteq \mathcal{S}_n$  is irreducible if and only if it contains a standard permutation.*

This lemma is proven towards the end of this subsection. Before doing this, we need to introduce *zig-zag paths* (see also Figure 29).

**Definition 3.3.** *A set of edges  $((i_1, j_1), (i_2, j_2), \dots, (i_\ell, j_\ell))$  is a  $L$  zig-zag path if  $i_1 = 1$ , the indices satisfy the pattern of inequalities*

$$j_{2b} > j_{2b-1}, \quad i_{2b} > n - j_{2b-1} + 1, \quad i_{2b} > i_{2b+1}, \quad n - j_{2b+1} + 1 > i_{2b}, \quad (24)$$

*and either  $i_\ell = n$  or  $j_\ell = 1$ . The analogous structure starting with  $j_1 = n$  is called  $R$  zig-zag path.*

It is easy to see that, if  $\sigma$  has a  $L$  zig-zag path, no set  $[s] \subsetneq [n]$  can have  $\sigma[s] = [n, \dots, n-s+1]$ , as, from the existence of the path, there must exist either a pair  $(u, v) = (i_{2b+1}, j_{2b+1})$  such that  $u \leq s$ ,  $n - s + 1 > v$  and  $v = \sigma(u)$ , or a pair  $(u, v) = (j_{2b}, i_{2b})$  such that  $u \geq n - s + 1$ ,  $s < v$ , and  $v = \sigma^{-1}(u)$  (this is seen in more detail below). A similar argument holds for  $R$  zig-zag paths. Thus zig-zag paths provide a concise certificate for irreducibility.

We now illustrate an algorithm that, for a given  $\sigma \in \mathfrak{S}_n$ , produces in linear time either a certificate of reducibility, by exhibiting the top-left block of the permutation, or a certificate of irreducibility in the form of a canonically-chosen  $L$  zig-zag path, that we shall call the



greedy  $L$  zig-zag path of the permutation. A completely analogous algorithm gives the greedy  $R$  zig-zag path. This algorithm will imply the following:

**Lemma 3.4.** *A permutation  $\sigma$  is irreducible if and only if it has a zig-zag path.*

*Proof.* For  $X = \{x_a\} \subseteq [n]$ , we use  $\sigma(X)$  as a shortcut for  $\{\sigma(x_a)\}$ . Set  $J_1 := \sigma(\{1\})$  and  $i_1 = 1$ . Now, either  $\sigma$  is reducible, and has top-left block of size 1, or  $j_1 := \max(J_1) < n$ . If  $j_1 = 1$ , then  $((i_1, j_1))$  is a  $L$  zig-zag path. If  $j_1 > 1$ , consider the set  $I_1 = \sigma^{-1}(\{n, n-1, \dots, n-j_1+1\})$ . Either the largest element of this set is  $n-j_1+1$ , in which case we certify reducibility of  $\sigma$  with a first block of size  $n-j_1+1$ , or it is some index  $i_2 > n-j_1+1$ . Say  $\sigma(i_2) = j_2 < j_1$ . If  $i_2 = n$ , then  $((i_1, j_1), (i_2, j_2))$  is a  $L$  zig-zag path. If  $i_2 < n$ , consider the set  $J_2 = \sigma\{i_1+1 = 2, \dots, i_2\}$ . Either the smallest element of this set is  $n-i_2+1$ , in which case we certify reducibility of  $\sigma$ , and with top-left block of size  $i_2$ , or it is some index  $j_3$  such that  $n-j_3+1 > i_2$ . Say  $i_3 := \sigma^{-1}(j_3) < i_2$ . Continue in this way. At each round we query the image or pre-image of values in some interval  $(i_a+1, i_a+2, \dots, i_{a+1})$ , or same with  $j$ , so the total amount of queries is bounded by  $2n$ . At the various rounds at which we do not halt we have  $i_{b+2} > i_b$  and  $j_{b+2} < j_b$ . As the indices  $i_a, j_a$  are in the range  $[n]$ , the algorithm must terminate in at most  $\sim n$  rounds, and can only terminate either because we have found a reducible block, or because  $i_{2b} = n$  for some  $b$ , or because  $j_{2b-1} = 1$  for some  $b$ . This proves both the lemma and the statement on the linearity of the algorithm.  $\square$

Figure 30 illustrates an example of the construction of the greedy  $L$  zig-zag path, in matrix representation, and the caption illustrates the run of the algorithm.

Let us analyse a bit more carefully the complexity. One can see that the worst case is for irreducibility, and is attained on the permutation  $\sigma$  such that the vectors  $(i_{a+1}, j_{a+1}) - (i_a, j_a)$  of the greedy  $L$  or  $R$  zig-zag path are  $\dots (3, 1), (-1, -3), (3, 1), (-1, -3)\dots$ , with

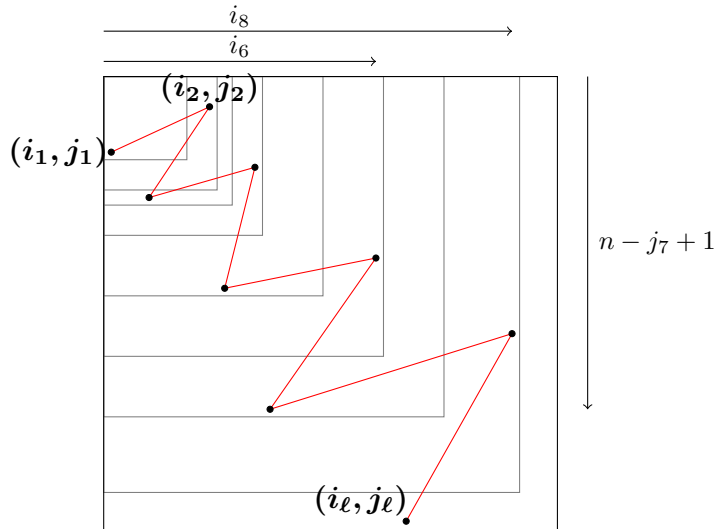


Figure 29: Structure of a zig-zag path, in matrix representation. It is constructed as follows: for each pair  $(i_a, j_a)$ , put a bullet at the corresponding position, and draw the top-left square of side  $\max(i_a, j_a)$ . Draw the segments between bullets  $(i_a, j_a)$  and  $(i_{a+1}, j_{a+1})$  (here in red). The resulting path must connect the top-left boundary of the matrix to the bottom-right boundary. If the bullets are entries of  $\sigma$ , then a top-left  $k \times k$  square cannot be a block of the matrix-representation of  $\sigma$ , because, in light of the inequalities (24), one of the two neighbouring rectangular blocks (the  $k \times (n-k)$  block to the right, or the  $(n-k) \times k$  block below) must contain a bullet of the path, and thus be non-empty.

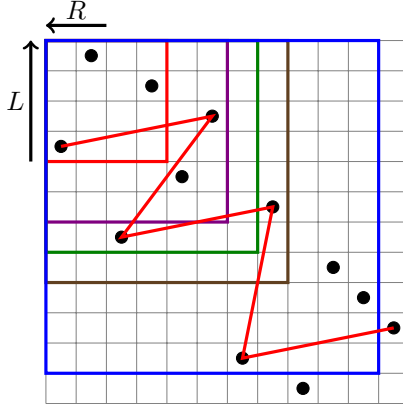


Figure 30: We construct the shortest  $L$  zig-zag path of  $\sigma$  in a greedy way: we take  $(i_1, j_1) = (1, \sigma(1))$ , then draw the square (here in red) and take  $(i_2, j_2)$  the rightmost point above row  $j_1$ . If it were inside the square, the permutation would have been reducible. It is not the case here, so we draw a larger square (here in violet), and take  $(i_3, j_3)$  as the lowest point to the left of column  $i_2$ . We continue this way, up to when the point  $(i_6, j_6)$  is reached. As  $i_6 = n$ , we terminate by certifying the irreducibility of  $\sigma$ .

an exception at the first and last elements (either a  $(3, 1)$  replaced by  $(2, 1)$ , or a  $(-1, -3)$  replaced by  $(-1, -2)$ , depending on parities). In this case the algorithm takes  $n - 1$  rounds, and overall performs all of the  $2n$  queries.

An analogous construction can be done by starting with  $j_1 = n$ . By this, in the reducible case we find the same certifying block, and in the irreducible case we construct the greedy  $R$  zig-zag path.

One can see that at least one among the two greedy paths ( $L$  and  $R$ ) has minimal length among all zig-zag paths, and that the length of the two greedy paths differ by at most 1. We call this value the *level* of  $\sigma$ , and denote it by the symbol  $lv(\sigma)$ .

Of course, an irreducible permutation  $\sigma$  of level 1 is a standard permutation. More is true:

**Lemma 3.5.** *An irreducible permutation  $\sigma$  is at alternation distance at most  $lv(\sigma) - 1$  from a standard permutation.*

*Proof.* Say that the level of  $\sigma$  is  $\ell > 1$ , and is realised by its greedy  $L$  zig-zag path (the argument for  $R$  is symmetric). So we have indices  $j_2 < j_1$  and  $i_1 = 1 < i_2$ .

The action of  $L^{n-j_2}$  moves the bullet  $(i_2, j_2)$  in position  $(i_2, n)$  without affecting any other edge of the path. Indeed, because of the inequalities satisfied by the indices of the greedy  $L$  zig-zag path,  $j_a < j_1$  for all  $a \geq 3$ . Then, the path obtained by dropping the first edge is a  $R$  zig-zag path of level  $\ell - 1$  for the new configuration  $\sigma' = L^{n-j_2}\sigma$ , and the two configurations  $\sigma, \sigma'$  are nearest neighbour for alternation distance. The reasoning in the other case is analogous, with  $R \leftrightarrow L$  and  $i_a \leftrightarrow n - j_a + 1$ .  $\square$

Now Lemma 3.2 follows as an immediate corollary.

### 3.3 Standard families

Here we introduce a property of permutations which is not invariant under the dynamics, nonetheless it is useful in a combinatorial decomposition of the classes, both for classification and enumeration purposes.

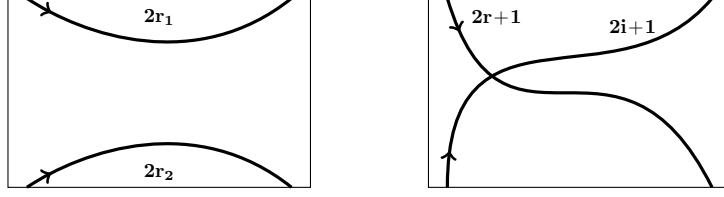


Figure 31: Left: a schematic representation of a permutation of type  $H(r_1, r_2)$ . Right: a representation of a permutation of type  $X(r, i)$ . These configurations have rank  $r_1 + r_2 - 1$  and  $r$ , respectively.

**Definition 3.6.** A permutation  $\sigma$  is of type  $H$  if the rank path goes through the  $-1$  mark, and of type  $X$  otherwise. In the case of a type- $X$  permutation, we call principal cycle the cycle going through the  $-1$  mark.

The choice of the name is done for mnemonic purposes. Imagine to cut the cycle invariant at the  $-1$  mark. Then we have two open paths. In a type- $H$  permutation, these paths have a  $\asymp$  connectivity pattern (which reminds of a  $H$ ), and in a type- $X$  permutation they have a  $\times$  pattern (which reminds of a  $X$ ).

A more refined definition is as follows

**Definition 3.7.** A permutation  $\sigma$  is of type  $H(r_1, r_2)$  if it is of type  $H$ , and the portions of the rank path before and after the  $-1$  mark have path-length  $2r_1$  and  $2r_2$ , respectively (so the rank length is  $r = r_1 + r_2 - 1$ ). It is of type  $X(r, i)$  if it is of type  $X$ , has rank  $r$ , and the principal cycle has path-length  $2i + 1$  (i.e., it contributes a  $i$  entry to the cycle structure  $\lambda$ ).

See Figure 31 for a schematic illustration.

A standard permutation is a notion with a simple definition. More subtle is the associated notion:

**Definition 3.8** (standard family). Let  $\sigma$  be a standard permutation. The collection of  $n - 1$  permutations  $\{\sigma^{(i)} := L^i \sigma\}_{0 \leq i \leq n-2}$  is called the standard family of  $\sigma$ .

The properties established in Section 3.1 ultimately imply the following statement:

**Proposition 3.9** (Properties of the standard family). Let  $\sigma$  be a standard permutation, and  $S = \{\sigma^{(i)}\}_i = \{L^i(\sigma)\}_i$  its standard family. The latter has the following properties:

1. Every  $\tau \in S$  has  $\tau(1) = 1$ ;
2. The  $n - 1$  elements of  $S$  are all distinct;
3. There is a unique  $\tau \in S$  such that  $\tau(n) = n$ ;
4. Let  $m_i$  be the multiplicity of the integer  $i$  in  $\lambda$  (i.e. the number of cycles of length  $i$ ), and  $r$  the rank. There are  $i m_i$  permutations of  $S$  which are of type  $X(r, i)$ , and 1 permutation of type  $H(r - j + 1, j)$ , for each  $1 \leq j \leq r$ .<sup>8</sup>
5. Among the permutations of type  $X(r, i)$  there is at least one  $\tau$  with  $\tau^{-1}(2) < \tau^{-1}(n)$ .

*Proof.* The first three statements are obvious.

The fourth statement is based on the definitions of Section 3.1. Let us analyse the top arcs: the cycle or path going through the  $-1$  mark is also the one going through the rightmost arc, thus, as the family  $L^i(\sigma)$ , for  $1 \leq i \leq n - 1$ , corresponds to a cyclic shift of the ‘colours’ on these arcs, we deduce that each cycle/path goes through the  $-1$  mark a number

<sup>8</sup>Note that, as  $\sum_i i m_i + r = n - 1$  by the dimension formula (3), this list exhausts all the permutations of the family.

of times identical to its length value, contributing to the cycle invariant. I.e., there are  $i m_i$  permutations in  $S$  of type  $X(r, i)$ , and  $r$  permutations of type  $H$ , as claimed. In order to prove that, among the latter, we have exactly one permutation per type  $H(r - j + 1, j)$ , for  $1 \leq j \leq r$ , we need to add some more structure. Let us number the top arcs of the rank path in  $\sigma$  from 1 to  $r$ , following the order by which they are visited by the path, starting from the top-left corner. Then it becomes clear that  $L^i(\sigma)$  has type  $H(r - j + 1, j)$  exactly when the arc  $n - i$  is the  $(r - j + 1)$ -th arc of the rank path (this is also illustrated in Figure 32)

Let us now pass to the fifth statement. As we are in type  $X$ , we have at least one cycle. Let  $a_1, \dots, a_k$  be the arcs associated to a cycle of length  $k$ . For  $j = 1, \dots, k$  we consider the edge  $(\ell_{j,1}, \sigma(\ell_{j,1}))$  incident to the left endpoint of the arc  $a_j$ , and the edge  $(\ell_{j,2}, \sigma(\ell_{j,2}) = \sigma(\ell_{j,1}) + 1)$  incident to the right endpoint. Since we have a cycle (and not the rank path), at least one of these arcs (say  $a_j$ ) must have  $\ell_{j,1} > \ell_{j,2}$ , because the  $\ell_j$ 's form a cyclic sequence of distinct integers, thus must have at least one descent in this list.

This reasoning may not work if we deal with the principal cycle, as we may have only one descent, in correspondence of the  $-1$  mark. There are two possible workarounds to this apparent problem. The first one is that we can start by looking at a configuration  $\tau_0$  of type  $H$  (there must be at least one such configuration in the family, because the rank is at least 1). In this configuration no cycle is the principal cycle, and we can choose one arc per cycle with the required property. The second workaround is the fact that the reasoning doesn't apply only when the principal cycle has only one descent, and in correspondence of the  $-1$  mark, but in fact in this very case we just have  $\tau^{-1}(2) < \tau^{-1}(n)$  with no need of further analysis.

Let us continue the analysis of the generic case, of an arc  $a_j$  with  $\ell_{j,1} > \ell_{j,2}$ . Then  $\sigma' = L^{n-a_j}(\sigma)$  has a principal cycle of length  $k$ , and these two edges, in  $\sigma'$ , become  $(\ell_{j,1}, n)$  and  $(\ell_{j,2}, 2)$  (see figure 33). This allows to establish the fifth property.  $\square$

**Corollary 3.10.** *As a consequence of the property (5), let  $\tau'$  be the permutation resulting*

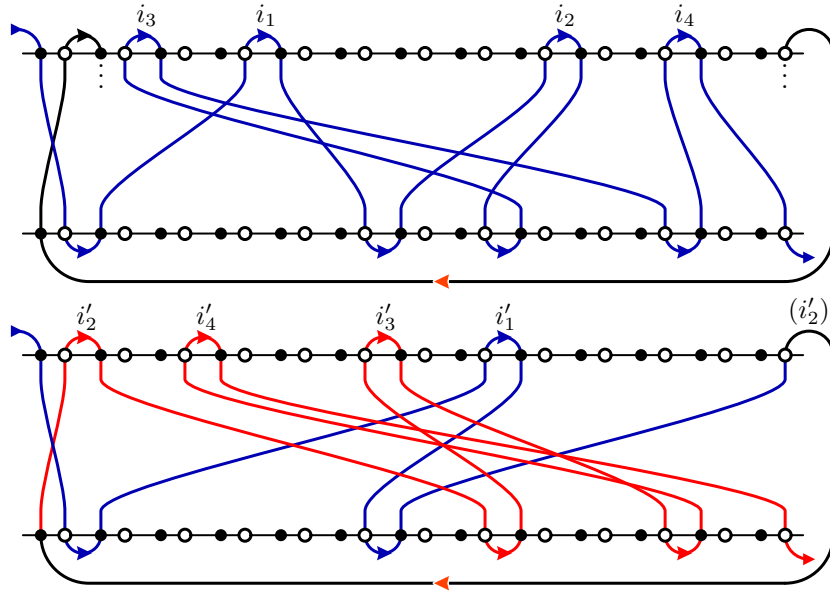


Figure 32: Illustration of the proof of an aspect of the fourth property in Proposition 3.9. Top: portions of a configuration  $\sigma$ , with rank 4, of type  $X(4, *)$ . The top arcs in the rank are at positions  $i_1, \dots, i_4$ , and numbered according to their order along the path. Bottom: the result of applying  $L^{n-i_2}$  to  $\sigma$ . The new configuration is of type  $H(2, 3)$ , as the blue and red paths have path-length 4 and 6, respectively.

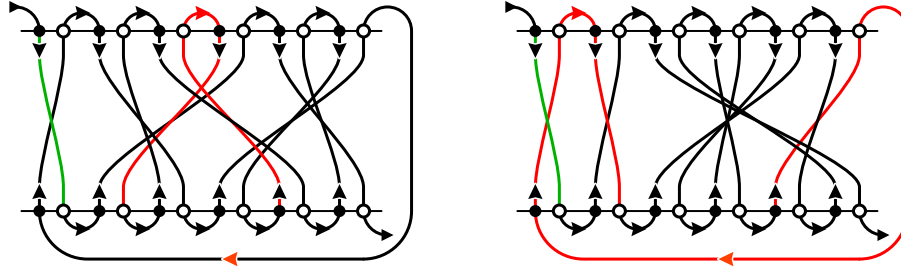


Figure 33: Illustration of the proof of the fifth property in Proposition 3.9. Left: a configuration  $\sigma$ , with cycle invariant  $(3, 1; 1)$ , of type  $X(1, 1)$  (in order to produce a small but generic example, we have taken a non-primitive configuration). The cycle of length 3 is not the principal cycle, thus it must have an arc such that  $\ell_{j,1} > \ell_{j,2}$ . One such arc, and the two incident edges, are denoted in red. Right: the configuration  $\sigma'$  obtained by applying  $L$  the appropriate number of times, so to make this arc go through the  $-1$  mark. At this point, if we remove the left-most edge, the resulting configuration is irreducible.

from removing the edge  $(1, 1)$  from a permutation  $\tau$  as in (5). Then  $\tau'$  is irreducible, and there exists  $\ell$  (namely,  $\ell = \tau^{-1}(2) - 2$ ) such that  $R^\ell(\tau')$  is standard.

This corollary will be of crucial importance in establishing the appropriate conditions of the surgery operators  $q_1$  and  $q_2$ , outlined in Section 1.7. (More precisely it will be a key element of the proof of Theorems 5.17 and 5.18.)

*Proof.* For  $\tau$  as in the proof of the property (5), note that removing the edge  $(1, 1)$  provides an irreducible permutation  $\tau'$ . Moreover it is clear that  $\tau'$  has level  $\ell v(\tau') = 2$ , as in fact  $R^{\ell_{j,2}-2}(\tau')$  is standard.<sup>9</sup>  $\square$

### 3.4 Reduced dynamics and boosted dynamics

Some parts of our proof are just obtained from the inspection of certain given (finite) patterns. How can such a simple ingredient be compatible with a classification of classes of dynamics of arbitrary size? A crucial notion is the definition of ‘reduced’ dynamics and ‘boosted’ dynamics, i.e., the analysis of the behaviour of *patterns* in configurations under the dynamics.<sup>10</sup>

Given a permutation  $\sigma$ , we can partition the set of edges into two colors: black and gray. Say that  $c : [n] \rightarrow \{\text{black}, \text{gray}\}$  describes this colouration. The permutation  $\tau$  corresponding to the restriction of  $\sigma$  to the black edges is called the *reduced permutation* for  $(\sigma, c)$ . Conversely, call  $\hat{c}$  a data structure required to reconstruct  $\sigma$  from the pair  $(\tau, \hat{c})$ . A choice for  $\hat{c}$  is as an unordered list of quadruples,  $(i, k|j, h)$ . Such a quadruple means that there is a gray edge with bottom endpoint being the  $k$ -th gray point at the right of the  $i$ -th black point, and top endpoint being the  $h$ -th gray point at the left of the  $j$ -th black point. These quadruples evolve in a simple way under the action of  $L$  and  $R$  (i.e., they evolve consistently with the base values  $i$  and  $j$ , while  $k$  and  $h$  stay put). As a corollary, if we consider the dynamics on  $\tau$  as an edge-labeled permutation, we can reconstruct the evolution of  $\hat{c}$  from the evolution of  $\tau$ .

Call *pivots* of  $\sigma$  the two edges  $(1, \sigma(1))$  and  $(\sigma^{-1}(n), n)$ , if we work in the  $\mathcal{S}_n$  dynamics. [If we are in  $\mathcal{S}_n^{\text{ex}}$ , we call pivot also  $(n, \sigma(n))$  and  $(\sigma^{-1}(1), 1)$ ]

For a pair  $(\sigma, c)$ , we say that  $\sigma$  is *proper* if no gray edge of  $\sigma$  is a pivot. In this case the dynamics on  $\tau$  extends to what we call the *boosted dynamics* on  $\sigma$ , defined as follows: for every operator  $H$  (i.e.,  $H \in \{L, R\}$  for  $\mathcal{S}_n$  and  $H \in \{L, L', R, R'\}$  for  $\mathcal{S}_n^{\text{ex}}$ ), we define

<sup>9</sup>We have an exponent  $\ell_{j,2} - 2$ , instead of  $\ell_{j,2} - 1$  because we have removed the edge  $(1, 1)$ .

<sup>10</sup>Here ‘pattern’ is said in the sense of Permutation Pattern Theory, and is clarified in the following.

$\alpha_H(\sigma, c)$  as the smallest positive integer such that  $H^{\alpha_H(\sigma, c)}(\sigma)$  is proper, and, for a sequence  $S = H_k \cdots H_2 H_1$  acting on  $\tau$ , the sequence  $B(S)$ , the *boosted sequence* of  $S$ , acting on  $\sigma$  is  $B(S) = H_k^{\alpha_k} \cdots H_2^{\alpha_2} H_1^{\alpha_1}$  for the appropriate set of  $\alpha_j$ 's.

In other words, the boosted dynamics is better visualised as the appropriate notion such that the following diagram makes sense: for  $(\tau, \hat{c})$  an edge-labeled permutation with colouring data, as described above, and calling  $\Phi$  the operator that reconstructs  $(\sigma, c)$  from it, we have

$$\begin{array}{ccc} (\tau, \hat{c}) & \xrightarrow{S} & (\tau', \hat{c}') \\ \downarrow \Phi & & \downarrow \Phi \\ (\sigma, c) & \xrightarrow{B(S)} & (\sigma', c') \end{array}$$

Working in the reduced dynamics gives concise certificates of connectedness: we can prove that  $\sigma \sim \sigma'$  by showing the existence of a triple  $(\tau, \hat{c}, S)$  that allows to reconstruct the full diagram above. The idea is that one can often show the existence of a given pair  $(\tau, S)$  (of finite size), and a family  $\{\hat{c}_n\}_{n \in \mathbb{N}}$ , which allows to prove the connectedness of families  $\{\sigma_n \sim \sigma'_n\}_{n \in \mathbb{N}}$ . This is the method used in section 5.1 for the proof of the main theorem 5.5 on the  $T$  operator.

In a slightly more general form, instead of having a finite sequence  $S$ , we could have three finite sequences  $S_-, S_0$  and  $S_+$  such that the connectedness of  $\sigma_n$  and  $\sigma'_n$  is proven through the sequence  $S_- S_0^n S_+$ . We use this generalised pattern only once, in order to prove explicitly the connectedness of two permutations inside a given class, in a case which is not covered by any of the ‘big theorems’ on the surgery operators (see Section 6.3, Lemma 6.9)

### 3.5 Square constructors for permutations

In this section we define a rather general surgery operation on permutations, which behaves in a simple way under the Rauzy dynamics:

**Definition 3.11** (Square constructor). *Let  $\tau$  be a permutation matrix of size  $k$ , and let  $0 \leq i, j \leq k$ , with  $i + j > 0$ . The pair  $i, j$  describes a way to decompose  $\tau$  into four (possibly empty) rectangular blocks,  $\tau = \begin{pmatrix} A & B \\ C & D \end{pmatrix}$ , so that  $A$  and  $B$  have  $i$  rows, and  $A$  and  $C$  have  $j$  columns. For  $h, \ell \in \{1, \dots, n\}$ , and  $\sigma$  a permutation of size  $n$  with  $\ell = \sigma(h)$ , the square constructors  $C_{\tau, i, j}^{\text{col}-h}$  and  $C_{\tau, i, j}^{\text{row}-\ell}$ , acting on  $\sigma$ , produce the same configuration  $\sigma'$ , of size  $n + k + 1$ , as described in Figure 34.*

**Lemma 3.12** (reduced dynamics for constructors). *Let  $(\tau, i, j)$  as above. Let  $\sigma$  and  $\sigma'$  be two permutations of the same size, with one coloured edge (say, red and the rest is black). Let  $(h, \sigma(h))$  be the only entry of  $\sigma$  marked in red and  $(h', \sigma'(h'))$  be the only entry of  $\sigma'$  marked in red. If  $\sigma \sim \sigma'$  for the dynamic  $\mathcal{S}$ , with colours as above, then  $C_{\tau, i, j}^{\text{col}-h}(\sigma) \sim C_{\tau, i, j}^{\text{col}-h'}(\sigma')$ .*

*Proof.* This is a case of reduced dynamics, where, in  $C_{\tau, i, j}^{\text{col}-h}(\sigma)$ , the entries of  $\tau$  plus the extra entry at the bottom-right corner of block  $A$  are gray. The red point is the point at the top-left of block  $A$ , this reduced permutation is  $(\sigma, h)$  where  $h$  is the index of the red entry. Thus we can define a bijection  $\phi$  between  $C_{\tau, i, j}^{\text{col}-h}(\sigma)$  and  $(\sigma, h)$ . Now suppose  $\sigma$  and  $\sigma'$  are connected by the sequence of operators  $S$ , i.e.  $S(\sigma) = \sigma'$ . Then we need to show that  $B(S)(\phi^{-1}(\sigma, h)) = \phi^{-1}(\sigma', h')$ .

By transitivity of connectedness, it is not necessary to consider arbitrary sequences, it is enough to consider  $\sigma' = L\sigma$  and  $\sigma' = R\sigma$ . The symmetry of the definition of the square constructor allows to consider just one case, and we choose  $L$ .

If the red point is not a pivot, then neither are the gray edges, and  $B(L) = L$ , so  $L(\phi^{-1}(\sigma, h)) = \phi^{-1}(\sigma', h')$  as wanted. Thus we only need to consider the case when the red point is a pivot. In such a case, (i.e. the red point is  $(h, n)$ ), then  $B(L) = L^{i+1}$  and  $B(L)(\phi^{-1}(\sigma, h)) = \phi^{-1}(L(\sigma), h)$  as wanted (see figure 35).  $\square$

**Lemma 3.13** (square transportation). *Let  $(\tau, i, j)$  as above. Then, the action of the constructor at different locations gives equivalent configurations, i.e. for all  $\sigma$  of size  $n$  and all  $h, h' \in [n]$  we have  $C_{\tau, i, j}^{\text{col}-h}(\sigma) \sim C_{\tau, i, j}^{\text{col}-h'}(\sigma)$ .*

*Proof.* We start by proving that the lemma holds for  $(h, h') = (1, \sigma^{-1}(n))$ . This is not hard to see. In fact,  $R^{j+1}C_{\tau, i, j}^{\text{col}-1}(\sigma)$  and  $L^{i+1}C_{\tau, i, j}^{\text{row}-n}(\sigma)$  are the same configuration, namely the one illustrated in Figure 36.

Now consider the reduced dynamics as in Lemma 3.12. Let  $(\sigma, c_L)$  the colouring of  $\sigma$  with the red entry on the  $L$ -pivot, and  $(\sigma, c_R)$  the one with the red entry on the  $R$ -pivot. Let  $\phi$  be the map of the reduced dynamics. We have just proven that  $\phi^{-1}(\sigma, c_L) \sim \phi^{-1}(\sigma, c_R)$ . Let  $E$  be the operator that exchanges  $(\sigma, c_L)$  and  $(\sigma, c_R)$ , i.e.

$$E\left(\begin{array}{|c|} \hline \bullet \\ \hline \end{array}\right) = \begin{array}{|c|} \hline \bullet \\ \hline \end{array}$$

By Lemma 3.2 we know that, in the reduced dynamics, we have a sequence  $S$  in the dynamics such that  $S\sigma = \sigma'$ , and  $\sigma'$  is standard. In this configuration, either the  $L$ -pivot is red, or exactly one configuration in the associated standard family has a red  $R$ -pivot. In the first case,  $E$  can be applied to any configuration in the standard family. This shows that, for  $\sigma$  standard, all configurations  $(\sigma, c_j)$  for the red point on the  $j$ -th column are connected to  $(\sigma, c_L)$ , by a sequence of the form  $L^{-k}EL^k$ , and thus are connected among themselves by a sequence of the form  $L^{-h}EL^{h-k}EL^k$ . Lemma 3.12 allows us to conclude, for  $\sigma'$  a standard permutation, and, by conjugating with the sequence  $S$ , for  $\sigma$  a generic permutation in the class (see Figure 37). □

**Corollary 3.14.** *Let  $(\tau, i, j)$  as above. Let  $\sigma$  and  $\sigma'$  such that  $\sigma \sim \sigma'$  for the dynamic  $\mathcal{S}$ , then, for every  $1 \leq h, h' \leq n$ ,  $C_{\tau, i, j}^{\text{col}-h}(\sigma) \sim C_{\tau, i, j}^{\text{col}-h'}(\sigma')$ .*

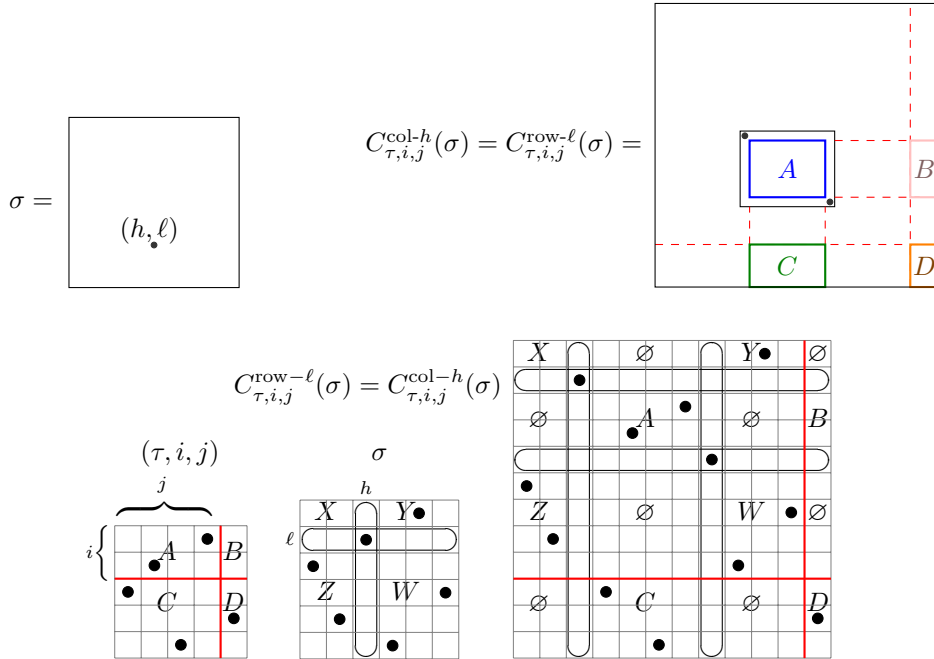


Figure 34: Action of the square constructors on a permutation  $\sigma$ , with  $\tau$  being a matrix with blocks  $A, B, C$  and  $D$ . Top: the general structure. Bottom: an example.

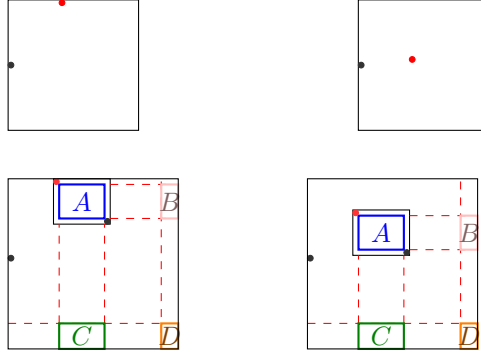


Figure 35: Top left:  $(\sigma, h)$ . Top right:  $(L(\sigma), h)$ . Bottom left:  $C_{\tau, i, j}^{\text{col}-h}(\sigma)$ . Bottom right:  $B(L)(C_{\tau, i, j}^{\text{col}-h}(\sigma))$ .

A further corollary of this lemma is the statement of Proposition 1.11, for which it suffices to take  $A$  a diagonal matrix and  $B, C, D$  empty blocks.

## 4 The sign invariant

### 4.1 Arf functions for permutations

For  $\sigma$  a permutation in  $\mathfrak{S}_n$ , let

$$\chi(\sigma) = \#\{1 \leq i < j \leq n \mid \sigma(i) < \sigma(j)\} \quad (25)$$

i.e.  $\chi(\sigma)$  is the number of pairs of non-crossing edges in the diagram representation of  $\sigma$ .

Let  $E = E(\sigma)$  be the subset of  $n$  edges in  $\mathcal{K}_{n,n}$  described by  $\sigma$ . For any  $I \subseteq E$  of cardinality  $k$ , the permutation  $\sigma|_I \in \mathfrak{S}_k$  is defined in the obvious way, as the one associated to the subgraph of  $\mathcal{K}_{n,n}$  with edge-set  $I$ , with singletons dropped out, and the inherited total ordering of the two vertex-sets.

Define the two functions

$$A(\sigma) := \sum_{I \subseteq E(\sigma)} (-1)^{\chi(\sigma|_I)}; \quad \bar{A}(\sigma) := \sum_{I \subseteq E(\sigma)} (-1)^{|I| + \chi(\sigma|_I)}. \quad (26)$$

When  $\sigma$  is understood, we will just write  $\chi_I$  for  $\chi(\sigma|_I)$ . The quantity  $A$  is accessory in the forthcoming analysis, while the crucial fact for our purpose is that the quantity  $\bar{A}$  is invariant both in the  $\mathcal{S}_n$  and in the  $\mathcal{S}_n^{\text{ex}}$  dynamics. We will prove this in the following subsection.

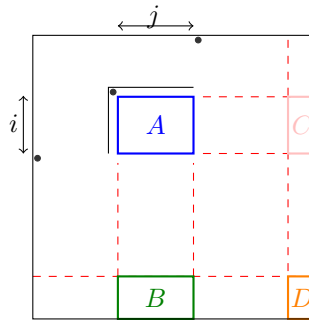


Figure 36: Structure of a configuration  $\sigma'$ , such that  $R^{-j-1}\sigma' = C_{\tau, i, j}^{\text{col}-1}(\sigma)$  and  $L^{-i-1}\sigma' = C_{\tau, i, j}^{\text{row}-n}(\sigma)$ .





Figure 37: The sequence of operations which allow to transport the red mark from one position to another. Here  $\text{Std}$  is the standardising sequence of the (uncoloured) configuration  $\sigma$ .

As a result of a well-known property of Arf functions, rederived in Section 6.1 (Lemma 6.1), the quantity  $\bar{A}(\sigma)$  is either zero or  $\pm$  a power of 2. For now, we content ourselves with the definition

**Definition 4.1.** For  $\sigma$  a permutation, define  $s(\sigma)$ , the sign of  $\sigma$ , as the quantity

$$s(\sigma) := \text{Sign}(\bar{A}(\sigma)) \in \{0, \pm 1\}. \quad (27)$$

However, we will see (in lemma 6.1) that  $s(\sigma) = 2^{-\frac{n+\ell}{2}} \bar{A}(\sigma)$ , where  $\ell$  is the number of cycles (the rank path is not counted).

## 4.2 Calculating with Arf functions

Evaluating the functions  $A$  and  $\bar{A}$  on a generic ‘large’ permutation, starting from the definition, seems a difficult task, as we have to sum an exponentially large number of terms. However, as the name of Arf function suggests, these quantities are combinatorial counterparts of the classical Arf invariant for manifolds (in this case, the translation surfaces where the Rauzy dynamics is defined, see Section 2.2 for more details), and inherits from them the covariance associated to the change of basis in the corresponding quadratic form, and its useful consequences. We will exploit this to some extent, in a simple and combinatorial way, that we now explicate.

The point is that we will *not* try to evaluate Arf functions of large configurations starting from scratch. We will rather compare the Arf functions of two (or more) configurations, which differ by a finite number of edges, and establish linear relations among their Arf functions. Yet another tool is proving that the Arf function of a given configuration is zero, by showing that it contains some finite *pattern* that implies this property.

In order to have the appropriate terminology for expressing this strategy, let us define the following:

**Definition 4.2.** Call  $V_{\pm}$  the two vertex-sets of  $\mathcal{K}_{n,n}$ . For  $\sigma$  a permutation with edge set  $E$ , and  $E' \subseteq E$  of cardinality  $m$ , call  $V_{\pm}''$  the subset of  $V_{\pm}$  not containing the endpoints of  $E'$ . A pair of partitions  $P_+ = (P_{+,1}, \dots, P_{+,h}) \in \mathcal{P}(V_+'' )$  and  $P_- = (P_{-,1}, \dots, P_{-,k}) \in \mathcal{P}(V_-'' )$  are said to be compatible with  $E'$  if each block contains indices which are consecutive in  $[n]$ .

Define the  $m \times (hk)$  matrix valued in  $\text{GF}_2$

$$Q_{e,ij} := \begin{cases} 1 & \text{edge } e \in E' \text{ does not cross the segment connecting } P_{-,i} \text{ to } P_{+,j}, \\ 0 & \text{otherwise.} \end{cases} \quad (28)$$

For  $v \in \text{GF}_2^d$ , let  $|v|$  be the number of entries equal to 1. Similarly, identify  $v$  with the corresponding subset of  $[d]$ . Given such a construction, introduce the following functions on  $(\text{GF}_2)^{hk}$

$$A_{\sigma, E', P}(v) := \sum_{u \in (\text{GF}_2)^{E'}} (-1)^{\chi_u + (u, Qv)}; \quad \bar{A}_{\sigma, E', P}(v) := \sum_{u \in (\text{GF}_2)^{E'}} (-1)^{|u| + \chi_u + (u, Qv)}. \quad (29)$$

The construction is illustrated in Figure 38.

Let us comment on the reasons for introducing such a definition. The quantities  $A_{\sigma, E', P}(v)$  allows to sum together many contributions to the function  $A$ , which behave all in the same way once the subset restricted to  $E'$  is specified. In a way similar to the philosophy behind

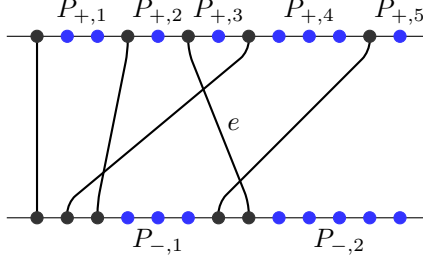


Figure 38: A subset of edges in a permutation, as in Definition 4.2. The represented edge set is  $E'$ , the blue vertices at the bottom constitute the set  $V''$ , while those at the top are  $V'_+$ . The two partitions denoted by the symbols  $P_{\pm,i}$  are the coarsest partitions which are compatible with  $E'$ . We cannot show the full matrix  $Q$  for such a big example, but we can give one row, for the edge which has the label  $e$  in the drawing. The row  $Q_e$  reads  $(Q_e)_{11,12,\dots,15,21,\dots,25} = (1, 1, 0, 0, 0, 0, 0, 1, 1, 1)$ .

the reduced dynamics of Section 3.4, our goal is to have  $E'$  of fixed size, while  $E \setminus E'$  is arbitrary and of unbounded size, so that the verification of our properties, as it is confined to the matrix  $Q$ , involves a finite data structure.

Indeed, let us split in the natural way the sum over subsets  $I$  that defines  $A$  and  $\bar{A}$ , namely

$$\sum_{I \subseteq E} f(I) = \sum_{I' \subseteq E'} \sum_{I'' \subseteq E \setminus E'} f(I' \cup I'')$$

For  $I$  and  $J$  two disjoint sets of edges, call  $\chi_{I,J}$  the number of pairs  $(i, j) \in I \times J$  which do not cross. Then clearly

$$\chi_{I \cup J} = \chi_I + \chi_J + \chi_{I,J}$$

Now let  $u(I') \in \{0, 1\}^{E'}$  be the vector with entries  $u_e = 1$  if  $e \in I'$  and 0 otherwise. Let  $m(I'') = \{m_{ij}(I'')\}$  be the  $k \times h$  matrix describing the number of edges connecting the intervals  $P_{-,i}$  to  $P_{+,j}$  in  $\sigma$ , and  $v(I'') = \{v_{ij}(I'')\}$ ,  $v_{ij} \in \{0, 1\}$ , as the parities of the  $m_{ij}$ 's. Call  $I''_{ij}$  the restriction of  $I''$  to edges connecting  $P_{-,i}$  and  $P_{+,j}$ . Clearly,  $\chi_{I', I''} = \sum_{ij} \chi_{I', I''_{ij}} = \sum_{e, ij} u_e Q_{e, ij} m_{ij}$ , which has the same parity as the analogous expression with  $v$ 's instead of  $m$ 's. Now, while the  $m$ 's are in  $\mathbb{N}$ , the vector  $v$  is in a linear space of finite cardinality, which is crucial for allowing a finite analysis of our expressions.

As a consequence,

$$A(\sigma) = \sum_{I \subseteq E(\sigma) \setminus E'(\sigma)} (-1)^{\chi_I} A_{\sigma, E', P}(v(I)); \quad (30)$$

$$\bar{A}(\sigma) = \sum_{I \subseteq E(\sigma) \setminus E'(\sigma)} (-1)^{|I| + \chi_I} \bar{A}_{\sigma, E', P}(v(I)). \quad (31)$$

Then we have two criteria for establishing relations among Arf functions

**Proposition 4.3.** *Let  $\sigma$ ,  $E'$  and  $P$  as above. If for all  $v \in (\mathbb{GF}_2)^{hk}$  we have  $A_{\sigma, E', P}(v) = 0$ , then  $A(\sigma) = 0$ . The same holds for  $\bar{A}$ .*

**Proposition 4.4.** *Let  $\sigma$  and  $\tau$  be permutations (possibly of different size), with edge sets  $E \cup E'_\sigma$  and  $E \cup E'_\tau$  respectively. Let  $P = (P_-, P_+)$  be a pair of partitions of size  $|E|$  compatible with both  $E'_\sigma$  and  $E'_\tau$ . If there exists  $K \in \mathbb{Q}$  such that for all  $v \in (\mathbb{GF}_2)^{hk}$  we have  $A_{\sigma, E', P}(v) = K A_{\tau, E', P}(v)$ , then  $A(\sigma) = K A(\tau)$ . The same holds with one or both of*

the  $A$ 's replaced by  $\bar{A}$ . Analogous statements hold for linear combinations of Arf functions associated to more than two configurations.<sup>11</sup>

The proof of these propositions is an immediate consequence of equations (30) and (31).

For this purpose of our main classification theorems, we need four facts which are specialisations of the propositions above. One of them establish the invariance of function  $\bar{A}$  under the dynamics, the other three relate the Arf functions on configurations obtained from the ‘‘surgery operators’’ sketched in Section 1.7 and discussed in Section 5, and a few further, simpler manipulations.

**Proposition 4.5** (Invariance of the sign).

$$\bar{A}\left(\tau = \begin{array}{c} P_{+,1} \quad P_{+,2} \\ \diagdown \quad \diagup \\ e_1 \quad e_2 \\ \diagup \quad \diagdown \\ P_{-,1} \quad P_{-,2} \end{array}\right) = \bar{A}\left(\sigma = \begin{array}{c} P_{+,1} \quad P_{+,2} \\ \diagdown \quad \diagup \\ e_1 \quad e_2 \\ \diagup \quad \diagdown \\ P_{-,1} \quad P_{-,2} \end{array}\right) \quad (32)$$

*Proof.* We have in this case

$$Q_\tau = \begin{pmatrix} 0 & 1 & 0 & 1 \\ 1 & 1 & 0 & 0 \end{pmatrix}; \quad Q_\sigma = \begin{pmatrix} 0 & 1 & 0 & 1 \\ 1 & 0 & 0 & 1 \end{pmatrix}; \quad (33)$$

Checking that the conditions of Proposition 4.4 are met, with  $K = 1$ , is a straightforward calculation. The resulting function of  $v$  for  $\tau$  is

$$\begin{aligned} \bar{A}_{\tau, \{e_1, e_2\}, P}(v) &= \sum_{u \in (\mathbb{GF}_2)^2} (-1)^{|u| + \chi_u + (u, Qv)} \\ &= (-1)^{0+0+0} + (-1)^{1+0+(0 \ 1 \ 0 \ 1) \cdot v} + (-1)^{1+0+(1 \ 1 \ 0 \ 0) \cdot v} \\ &\quad + (-1)^{0+1+((0 \ 1 \ 0 \ 1)+(1 \ 1 \ 0 \ 0)) \cdot v} \\ &= 1 - (-1)^{(0 \ 1 \ 0 \ 1) \cdot v} - (-1)^{(1 \ 1 \ 0 \ 0) \cdot v} - (-1)^{(1 \ 0 \ 0 \ 1) \cdot v} \end{aligned}$$

and likewise the resulting function of  $v$  for  $\sigma$  is

$$\begin{aligned} \bar{A}_{\sigma, \{e_1, e_2\}, P}(v) &= \sum_{u \in (\mathbb{GF}_2)^2} (-1)^{|u| + \chi_u + (u, Qv)} \\ &= (-1)^{0+0+0} + (-1)^{1+0+(0 \ 1 \ 0 \ 1) \cdot v} + (-1)^{1+0+(1 \ 0 \ 0 \ 1) \cdot v} \\ &\quad + (-1)^{0+1+((0 \ 1 \ 0 \ 1)+(1 \ 0 \ 0 \ 1)) \cdot v} \\ &= 1 - (-1)^{(0 \ 1 \ 0 \ 1) \cdot v} - (-1)^{(1 \ 0 \ 0 \ 1) \cdot v} - (-1)^{(1 \ 1 \ 0 \ 0) \cdot v} \end{aligned}$$

thus we have

$$\bar{A}_{\tau, \{e_1, e_2\}, P}(v) = \bar{A}_{\sigma, \{e_1, e_2\}, P}(v) \quad \text{for all } v \in \{0, 1\}^4. \quad (34)$$

This proposition implies the invariance of  $\bar{A}$  under the operation  $L$ , as  $\tau = L\sigma$ . The invariance under  $R$ ,  $L'$  and  $R'$  is deduced from the symmetry of the definition of  $A$  and  $\bar{A}$  under the dihedral group on permutation diagrams.

It is convenient to introduce the notation  $\vec{A}(\sigma) = \begin{pmatrix} \bar{A}(\sigma) \\ A(\sigma) \end{pmatrix}$ . We have

<sup>11</sup>We refer here to the obvious generalisation, of the form, for  $\sigma_j$  having edge-set  $E \cup E'_{\sigma_j}$ ,  $P = (P_-, P_+)$  a pair of partitions of size  $|E|$  compatible with all  $E'_{\sigma_j}$ 's, if there exist  $K_j \in \mathbb{Q}$  s.t. for all  $v \in (\mathbb{GF}_2)^{hk}$  we have  $\sum_j K_j A_{\sigma_j, E'_{\sigma_j}, P}(v) = 0$ , then  $\sum_j K_j A(\sigma_j) = 0$ , and similarly with some of the  $A$ 's replaced by  $\bar{A}$ 's.

**Proposition 4.6.**

$$\vec{A}\left(\begin{array}{|c|c|c|} \hline \text{[Diagram: rectangle with two vertical lines]} \\ \hline \end{array}\right) = \begin{pmatrix} 1 & -1 \\ 1 & 1 \end{pmatrix} \vec{A}\left(\begin{array}{|c|} \hline \text{[Diagram: rectangle]} \\ \hline \end{array}\right); \quad (35)$$

$$\vec{A}\left(\begin{array}{|c|} \hline \text{[Diagram: rectangle with a diagonal line from bottom-left to top-right]} \\ \hline \end{array}\right) = \begin{pmatrix} 0 & 0 \\ 0 & 2 \end{pmatrix} \vec{A}\left(\begin{array}{|c|} \hline \text{[Diagram: rectangle]} \\ \hline \end{array}\right); \quad (36)$$

$$\vec{A}\left(\begin{array}{|c|c|} \hline \text{[Diagram: rectangle with two vertical lines and a crossing]} \\ \hline \end{array}\right) = 2\vec{A}\left(\begin{array}{|c|} \hline \text{[Diagram: rectangle with a crossing]} \\ \hline \end{array}\right); \quad (37)$$

$$\vec{A}\left(\begin{array}{|c|c|} \hline \text{[Diagram: rectangle with two vertical lines and a crossing]} \\ \hline \end{array}\right) = \vec{A}\left(\begin{array}{|c|} \hline \text{[Diagram: rectangle with a crossing]} \\ \hline \end{array}\right). \quad (38)$$

These relations are all straightforward applications of Proposition 4.4, with matrices  $Q$  of rather small dimension. Equation (38), involving a larger matrix  $Q$ , may be derived with a shortcut: on the LHS, the sum over  $u \in (\mathbb{GF}_2)^3$  contains the four terms contributing to the RHS, where the left-most edge is absent, and four other terms, which cancel pairwise for obvious reasons, even with no need for analysing the matrices  $Q$  in detail.  $\square$

Equation (35) implies

**Corollary 4.7.**

$$\begin{aligned} \vec{A}(\text{id}_n) &= \begin{pmatrix} 1 & -1 \\ 1 & 1 \end{pmatrix}^{n+1} \begin{pmatrix} 1 \\ 0 \end{pmatrix} = 2^{\frac{n+1}{2}} \begin{pmatrix} \cos \frac{(n+1)\pi}{4} \\ \sin \frac{(n+1)\pi}{4} \end{pmatrix} \\ &= (-1)^{\lfloor \frac{n+1}{4} \rfloor} \begin{cases} \begin{pmatrix} 2^{\frac{n+1}{2}} \\ 0 \end{pmatrix} & n \equiv -1 \pmod{4}; \\ \begin{pmatrix} 2^{\frac{n}{2}} \\ 2^{\frac{n}{2}} \end{pmatrix} & n \equiv 0 \pmod{4}; \\ \begin{pmatrix} 0 \\ 2^{\frac{n+1}{2}} \end{pmatrix} & n \equiv 1 \pmod{4}; \\ \begin{pmatrix} -2^{\frac{n}{2}} \\ 2^{\frac{n}{2}} \end{pmatrix} & n \equiv 2 \pmod{4}; \end{cases} \end{aligned} \quad (39)$$

In particular,  $\vec{A}(\text{id}_4) = -4 < 0$  and  $\vec{A}(\text{id}_6) = 8 > 0$ , this fact is used in section 6.2.

Equations (37) and (38) imply

**Corollary 4.8.**

$$\vec{A}\left(\sigma = \begin{array}{|c|} \hline \text{[Diagram: rectangle with a diagonal line and a crossing]} \\ \hline \end{array}\right) = 2\vec{A}\left(\tau = \begin{array}{|c|} \hline \text{[Diagram: rectangle with a diagonal line and a crossing]} \\ \hline \end{array}\right) \quad (40)$$

This corollary states that, for the operator  $T$  defined in Section 5.1,  $\vec{A}(T\tau) = 2\vec{A}(\tau)$ .

Equations (35) and (36) imply

**Corollary 4.9.**

$$\vec{A}\left(\sigma = \begin{array}{|c|c|} \hline \text{[Diagram: rectangle with two vertical lines and a diagonal line]} \\ \hline \end{array}\right) = 2\vec{A}\left(\tau = \begin{array}{|c|} \hline \text{[Diagram: rectangle with a diagonal line]} \\ \hline \end{array}\right). \quad (41)$$

This corollary states that, for the operator  $q_1$  defined in Section 5.2,  $\vec{A}(q_1\tau) = 2\vec{A}(\tau)$ , because in fact  $q_1\sigma = R\tau$ .

More generally, we have

**Proposition 4.10.**

$$\vec{A}\left(\sigma = \begin{array}{|c|} \hline \text{Diagram 1} \\ \hline \end{array}\right) = \begin{pmatrix} 2 & 0 \\ 0 & 0 \end{pmatrix} \vec{A}\left(\tau = \begin{array}{|c|} \hline \text{Diagram 2} \\ \hline \end{array}\right). \quad (42)$$

that gives, using twice equation (35) in Proposition 4.6,

**Corollary 4.11.**

$$\vec{A}\left(\begin{array}{|c|} \hline \text{Diagram 3} \\ \hline \end{array}\right) = 0. \quad (43)$$

This corollary states that, for the operator  $q_2$  defined in Section 5.2,  $\vec{A}(q_2\tau) = 0$ .

The proof of Proposition 4.10 is done again by applying Proposition 4.4. We have in this case

$$Q_\sigma = \begin{pmatrix} 0 & 0 & 1 & 1 \\ 1 & 0 & 0 & 1 \\ 1 & 0 & 1 & 0 \end{pmatrix}, \quad Q_\tau = \begin{pmatrix} 1 & 0 & 0 & 1 \\ 1 & 0 & 1 & 0 \end{pmatrix}, \quad (44)$$

and in particular  $Q_\sigma = \begin{pmatrix} 1 & 1 \\ 0 & 1 \end{pmatrix} Q_\tau$ . Checking that the conditions of Proposition 4.4 are met, with  $K = 2$  and 0 in the two cases, is a straightforward calculation. The resulting function  $\vec{A}$  of  $v$ , as calculated for the RHS, is

$$1 + (-1)^{1+(1\ 0\ 0\ 1)\cdot v} + (-1)^{1+(1\ 0\ 1\ 0)\cdot v} + (-1)^{3+(0\ 0\ 1\ 1)\cdot v} \quad (45)$$

while for the LHS we have

$$\begin{aligned} & 1 + (-1)^{1+(0\ 0\ 1\ 1)\cdot v} + (-1)^{1+(1\ 0\ 0\ 1)\cdot v} + (-1)^{1+(1\ 0\ 1\ 0)\cdot v} \\ & + (-1)^{3+(1\ 0\ 1\ 0)\cdot v} + (-1)^{3+(1\ 0\ 0\ 1)\cdot v} + (-1)^{3+(0\ 0\ 1\ 1)\cdot v} + (-1)^6 \end{aligned} \quad (46)$$

which, after some simplifications, reduces to twice the expression in (45).

The calculation for function  $A$  is analogous. For example, for the LHS we have

$$\begin{aligned} & 1 + (-1)^{(0\ 0\ 1\ 1)\cdot v} + (-1)^{(1\ 0\ 0\ 1)\cdot v} + (-1)^{(1\ 0\ 1\ 0)\cdot v} \\ & + (-1)^{1+(1\ 0\ 1\ 0)\cdot v} + (-1)^{1+(1\ 0\ 0\ 1)\cdot v} + (-1)^{1+(0\ 0\ 1\ 1)\cdot v} + (-1)^3, \end{aligned} \quad (47)$$

an expression which is identically zero.  $\square$

## 5 Surgery operators

In this section we introduce and study the ‘surgery operators’ which have been outlined in Section 1.7, and whose geometric interpretation has been described in Section 2.3. These operators have a crucial role in the proof of the classification theorem. In particular, we introduce the notion:

**Definition 5.1** (Pullback function). *Let  $f : X_n \rightarrow X_{n+1}$  be a function,  $\sim$  be an equivalence relation on  $X_n$ , with classes  $Y_n$ , and compatible with  $f$ , and let  $\tilde{f}$  be the function which leads to the commuting diagram*

$$\begin{array}{ccc} X_n & \xrightarrow{f} & X_{n+1} \\ \downarrow \cdot/\sim & & \downarrow \cdot/\sim \\ Y_n & \xrightarrow{\tilde{f}} & Y_{n+1} \end{array} \quad (48)$$

Call  $Y(x)$  the function which associates to each  $x \in X_n$  its class in  $Y_n$ . We say that  $f$  is a pullback function if, for all  $x' \in X_{n+1}$ , and for all  $y \in Y_n$  such that  $\tilde{f}(y) = Y(x')$ , there exists a  $x \in X_n$  such that  $Y(x) = y$  and  $f(x) = x'$ .

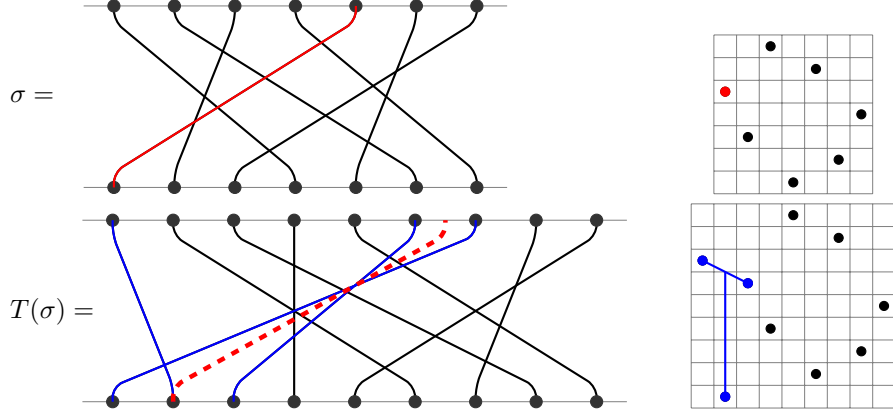


Figure 39: An example of the  $T$  operator

In other words, each diagram on the left can be completed to the diagram on the right:

$$\begin{array}{ccc}
 \forall & \begin{array}{c} x' \\ \downarrow \cdot/\sim \\ y \xrightarrow{\bar{f}} y' \end{array} & \exists x \text{ s.t. } \begin{array}{c} x \xrightarrow{f} x' \\ \downarrow \cdot/\sim \quad \downarrow \cdot/\sim \\ y \xrightarrow{\bar{f}} y' \end{array} \quad (49)
 \end{array}$$

Our operators  $\bar{T}$ ,  $\bar{q}_1$  and  $\bar{q}_2$  are functions on the sets of (non-empty) classes of a give size, and with rank in a certain range. In Theorems 5.5, 5.17 and 5.18 we will establish that they are pullback functions w.r.t. the equivalence relation given by the invariant.

## 5.1 Operator $T$

We define a first operator, in terms of the ‘square constructors’ defined in Section 3.5.

**Definition 5.2.** We define the  $T$  operator  $T : \mathfrak{S}_n \rightarrow \mathfrak{S}_{n+2}$  as  $T = C_{\tau,0,1}^{\text{col}-1}$  with  $\tau = (\bullet \uparrow)$ .

Figure 39 illustrates this with an example.

**Remark 5.3.** From Corollary 3.14, we know that if  $\sigma \sim \sigma'$ , then  $T(\sigma) \sim T(\sigma')$ .

As a consequence, we can define  $\bar{T}$  as the map from classes at size  $n$  to classes at size  $n + 2$ , such that  $\bar{T}(C) = C'$  if there exists  $\sigma \in C$  with  $T(\sigma) \in C'$ .

**Lemma 5.4.** Let  $C$  be a class with invariant  $(\lambda, r, s)$ . Then  $\bar{T}(C)$  has invariant  $(\lambda, r + 2, s)$ .

*Proof.* In light of Corollary 4.8, we know that the sign invariant does not change. For what concerns the cycle invariant, Figure 40 illustrates our claim, which holds more generally also for the constructor  $C_{\tau,0,1}^{\text{col}-\ell}$ , with arbitrary  $\ell$ .  $\square$

Finally, as outlined in Section 1.7, we need to establish the following crucial property:

**Theorem 5.5** (Pullback of  $T$ ). For every non-exceptional class  $C$  at size  $n + 2$  with invariant  $(\lambda, r, s)$ , and  $r > 2$ , there exists an irreducible  $\sigma$  at size  $n$  such that  $T(\sigma) \in C$ . Or equivalently,  $\bar{T}$  is surjective onto the set of (primitive irreducible) non-exceptional classes with rank larger than 2, and more specifically it is a pullback function.

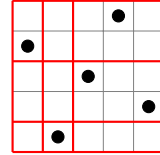
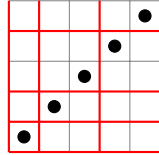
The proof of this theorem takes the largest part of this subsection. Before starting this proof, we need to set some notation for dealing with reduced permutations, as explained in Section 3.4, which are of arbitrary size, but with a finite number of ‘black’ edges (and an arbitrarily large number of ‘gray’ ones).

In the in-line notation for permutations – i.e., the string  $(\sigma(1), \dots, \sigma(n))$  – we will use the notation  $*$  for a sublist of arbitrary length, possibly zero, and the symbol  $n$  to denote the maximal element, while indices such as  $h, k, \dots$  will be used for generic elements. For example, the permutation  $\sigma = (1, 4, 2, 5, 6, 8, 9, 3, 7)$  is one of those of the form  $(1, *, k, k + 1, *, n, *)$ , because it starts with 1, the consecutive 5 and 6 are candidate for  $k$  and  $k + 1$ , and  $n = 9$  comes after them. Note that, when wild characters like  $k$  are used, a permutation can be of a given form in more than one way (e.g., this would have been the case for  $\sigma = (1, 4, 2, 5, 6, 7, 9, 3, 8)$ , as both 5 and 6 are possible choices for  $k$ ). In some specially tailored expressions this never happens. This would have been the case, for example, for the pattern  $(1, *, 2, k, k + 1, *, n, *)$  as the explicit 2 forces  $k$  to admit at most one realisation.

**Notation.** We want to represent graphically permutations in reduced dynamics, explicating only the pattern  $\tau$  of black edges, and, of the auxiliary structure  $\hat{c}$ , which pairs of consecutive black-edge endpoints have no gray endpoints in between them. In a matrix diagram, we use red lines between consecutive rows and columns<sup>12</sup> to denote the certified absence of gray points (in absence of a red line, there may or may not be gray points in between).

Such a data structure, when “not too big”, is also conveniently encoded by an in-line expression of the form mentioned above. For example, the in-line patterns  $(1, 2, *, 3, k, *, (k + 1), *)$  and  $(k, 1, (k - 1), *, n, *, 2)$  are represented graphically as

$$(1, 2, *, 3, k, *, (k + 1), *) : \quad (k, 1, (k - 1), *, n, *, 2) : \quad (50)$$



$$(51)$$

We will use extensively this graphical convention in the following proof of Theorem 5.5.

In particular, in this section, all our patterns are of the form  $(1, 2, \dots)$ , so we have two red lines at the bottom, and two at the left. This implies that we know the position of the  $L$ -pivot, which is the  $\sigma(1) = 1$  entry. If (and only if) we do not have a red line on top, we do not know the position of the  $R$ -pivot. Nonetheless, up to an operator  $L^a$  for some  $a$ , we can move all the gray entries above the top-most black entry, and in turns trade the horizontal red line at position 2 for a red line on top. For example,

<sup>12</sup>And/or before the first/after the last row and column.

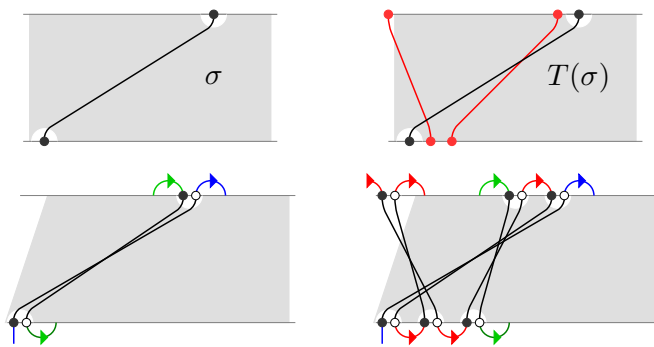
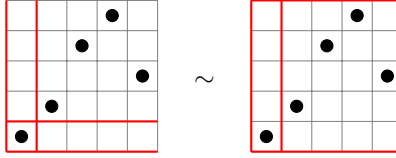
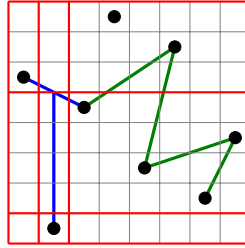


Figure 40: Left: the permutation  $\sigma$ . Right: the permutation  $T\sigma$ . It is clear that the only change in the cycle invariant is the addition of two to the rank length. On the bottom, the edges are drawn ‘doubled’, as in the diagram construction of the cycle invariant.



From this moment on, in the reduced dynamics we will always have a red line on the left and top side of the diagram, and a full control on the position of both pivots. I.e., in the reduced dynamics the pivots are always both ‘black’.

Our aim is to prove that, for a collection of patterns covering all possible cases of the theorem (of standard non-exceptional primitive irreducible configurations of rank at least 3), in the reduced dynamics we can reach a pattern that certifies the presence of a  $T$ -structure, which, when removed, leaves with an irreducible configuration. The presence of a  $T$ -structure is easily verified (in our drawings, we use blue construction lines to evidenciate it). Irreducibility after  $T^{-1}$  is certified by a zig-zag path (that we represent in green), which reaches red lines at its endpoints (for certifying the absence of an irreducible block constituted exclusively of gray entries). For primitivity, in principle there is nothing to check, as the number of descents is preserved both by the dynamics, and by removing the  $T$ . Nonetheless, for reasons explained below, we will keep track explicitly of possible descents involving black edges. A typical “winning outcome” of the dynamics, with the associated construction lines, is as follows:



We call such a pattern a  $T$ -structure certificate.

The irreducibility of the outcome is not for granted. It is not uncommon that shorter and simpler candidate sequences have to be rejected for lack of this property. An example which is instructive in retrospective is the pattern associated to case 4.1 in Table 5. Naïvely, one could have guessed that a good choice of sequence is  $\bar{R}\bar{L}^3$ , just as for case 2. This indeed produces a  $T$ -structure, however the pattern resulting after removing the structure is not irreducible (we have a block of size 4, followed by one of size 2). This forced us to search for the longer sequence appearing in the table.

Patterns are stable by inclusion. If we add points to a pattern  $\tau$  in correspondence of crossing of non-red lines, producing a larger pattern  $\tau'$ , and  $\tau$  could reach a certificate as above, also  $\tau'$  can, this because the relevant features of both the  $T$ -structure and the zig-zag path are related to red lines, which do not interfere with the insertion.

The relation in the other direction is slightly more involved: if  $\tau'$  can reach a certificate, and a point  $p$  in  $\tau'$  is neither used in the  $T$ -structure certificate, nor used as a pivot in the sequence, then  $\tau = \tau' \setminus p$  can reach a certificate.

We will use this relation mostly in the second form. In some cases, when we get a pattern  $\tau'$  from our case analysis, instead of producing a related certificate, we will make the ansatz that a certificate exists also under a certain reduction, and produce the associated (generally smaller) certificate. These reductions will also allow to merge together a number of branches in the case analysis.

Now we can state the following

**Proposition 5.6.** *Table 5 lists triples  $(\tau, \tau', S)$  such that  $S\tau = \tau'$ . (The “names” for the triples are for future reference).*



Gray bullets denote arbitrary blocks, possibly empty, while gray bullets with a black bullet inside denote arbitrary non-empty blocks.

All  $\tau'$  are  $T$ -structure certificates, with the exception of pattern 7, which has a zig-zag path if and only if at least one of the two gray bullets is a non-empty block.

All sequences  $S$  have alternation length at most 6, all zig-zag paths in the certificates have length at most 5.

Curiously, as a corollary (not useful at our purposes), we get that patterns 3.1 and 4.1 are connected, as well as 5.1, 5.2 and 6.1, fact that was not obvious *a priori*.

We are now ready for proving our theorem.

*Proof of Theorem 5.5.* Our aim is to prove that, for each irreducible primitive non-exceptional class  $C$  of rank at least 3, there exists a configuration  $\sigma'$  in the image of the operator  $T$ , such that its preimage is also primitive and irreducible.

The proof will go as follows: we describe how to break the problem into a finite number of cases, amenable to reduced dynamics, and in fact each of a form considered in Proposition 5.6. To this end it is convenient to assume that, to start with, we have some reference configuration  $\sigma$  which is standard (in the sense of Section 3.2). In particular, its in-line expression starts with  $(1, 2, \dots)$ . This is legitimate because, from the results of Section 3.2 (see Lemma 3.2), we know that each irreducible class has at least one standard family. As a matter of fact (and for what we know from Appendix C) the only exceptional configuration of this form of rank at least 3 is  $\text{id}_n$ . Our case analysis is tree-like, and we will see that this case emerge from *a single branch* of our tree, though this was not granted in advance. As it was obvious that it had to come from at least one branch, the relevant feature is that the tree is finite, and in particular that there is a finite number of branches leading to  $\text{id}_n$  configurations (instead, e.g., of one branch per value of  $n$ ), which would have made the reasoning more cumbersome, if not impractical.

Figure 41 summarises the main steps of the case decomposition, which we also describe in words in the following paragraphs.

As we said, by Lemma 3.2, we can suppose that  $\sigma$  is a standard permutation with  $\sigma(2) = 2$ , i.e., in in-line notation, with the pattern  $\sigma = (1, 2, *)$ . We now investigate the possible preimages of 3.

1. If 3 is at the end i.e.  $\sigma = (1, 2, *, 3)$ , then  $\sigma$  has rank 1 and the theorem does not apply.
2. Otherwise  $\sigma = 1, 2, *, 3, k, *$  for some  $k > 3$ .
  - 2.1. If  $k = n$  i.e.  $\sigma = (1, 2, *, 3, n, *)$ , we are in case ‘A’ of Figure 41, which is solved by the homonymous case in Proposition 5.6.
  - 2.2. Otherwise  $k < n$  and we can investigate the possible positions of the image of  $k + 1$ .
    - 2.2.1. If  $\sigma = (1, 2, *, (k + 1), *, 3, k, *)$ , we are in case ‘B’, which yet again is solved by the homonymous case in Proposition 5.6.
    - 2.2.2. If  $\sigma = (1, 2, *, 3, k, *, (k + 1))$  then  $\sigma$  has rank 2 and the theorem does not apply.
    - 2.2.3. Otherwise  $\sigma = (1, 2, *, 3, k, *, (k + 1), *, h, *)$  for one or more  $h$ :
      - 2.2.3.1. If there exists such a  $h$  with  $3 < h < k$ , we are in case ‘C’.
      - 2.2.3.2. Otherwise, we shall analyse with care the case  $\sigma = (1, 2, *, 3, k, *, (k + 1), *, h, *)$  with all entries after  $k + 1$  being larger than  $k + 1$ .

We have reached a case that requires a better control on the extra data structure  $\hat{c}$  of the reduced dynamics. At all intersections of non-red lines, we may or may not have a non-empty block of points. We will take some order on these points, and continue a case analysis

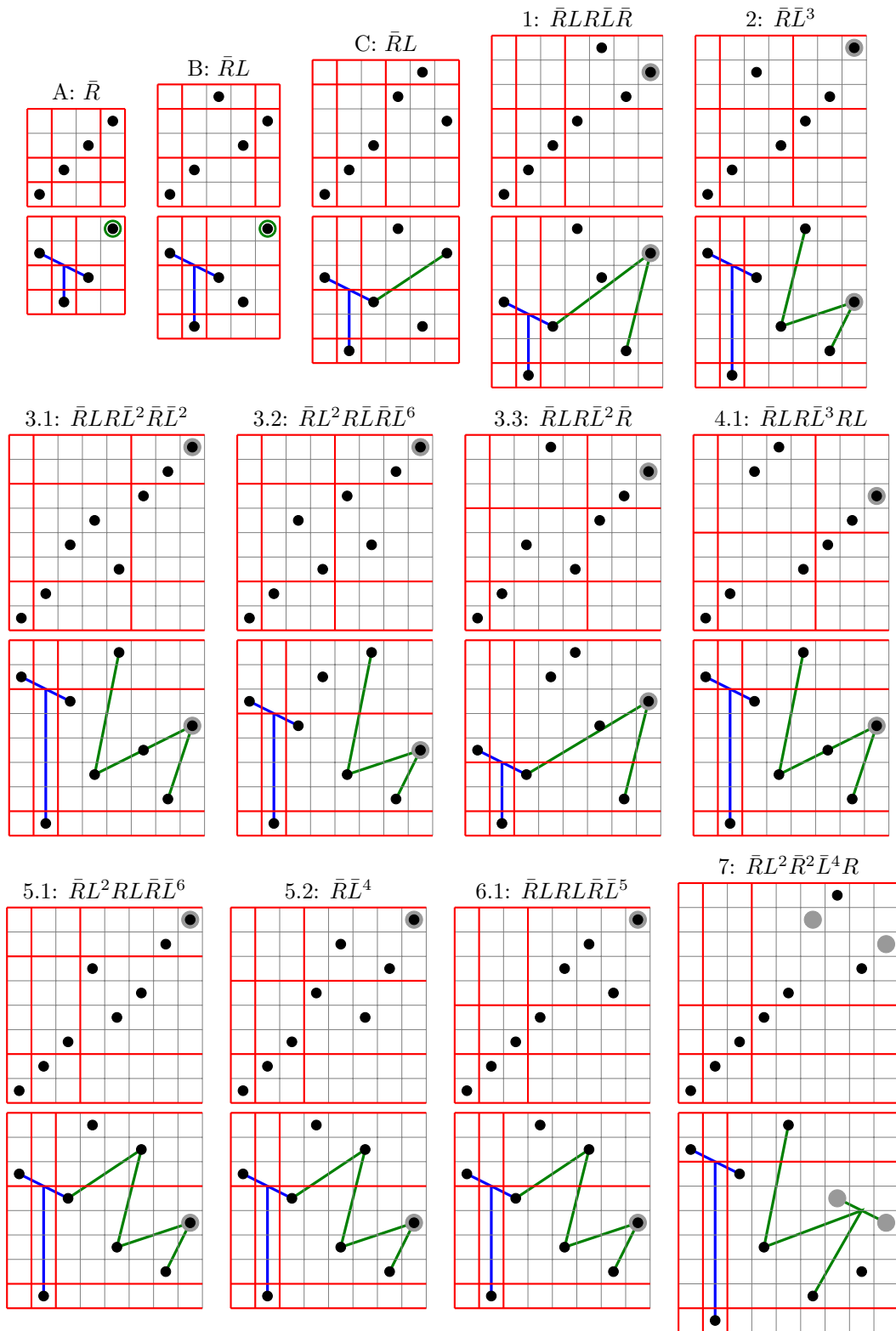


Table 5: Triples as is Proposition 5.6.

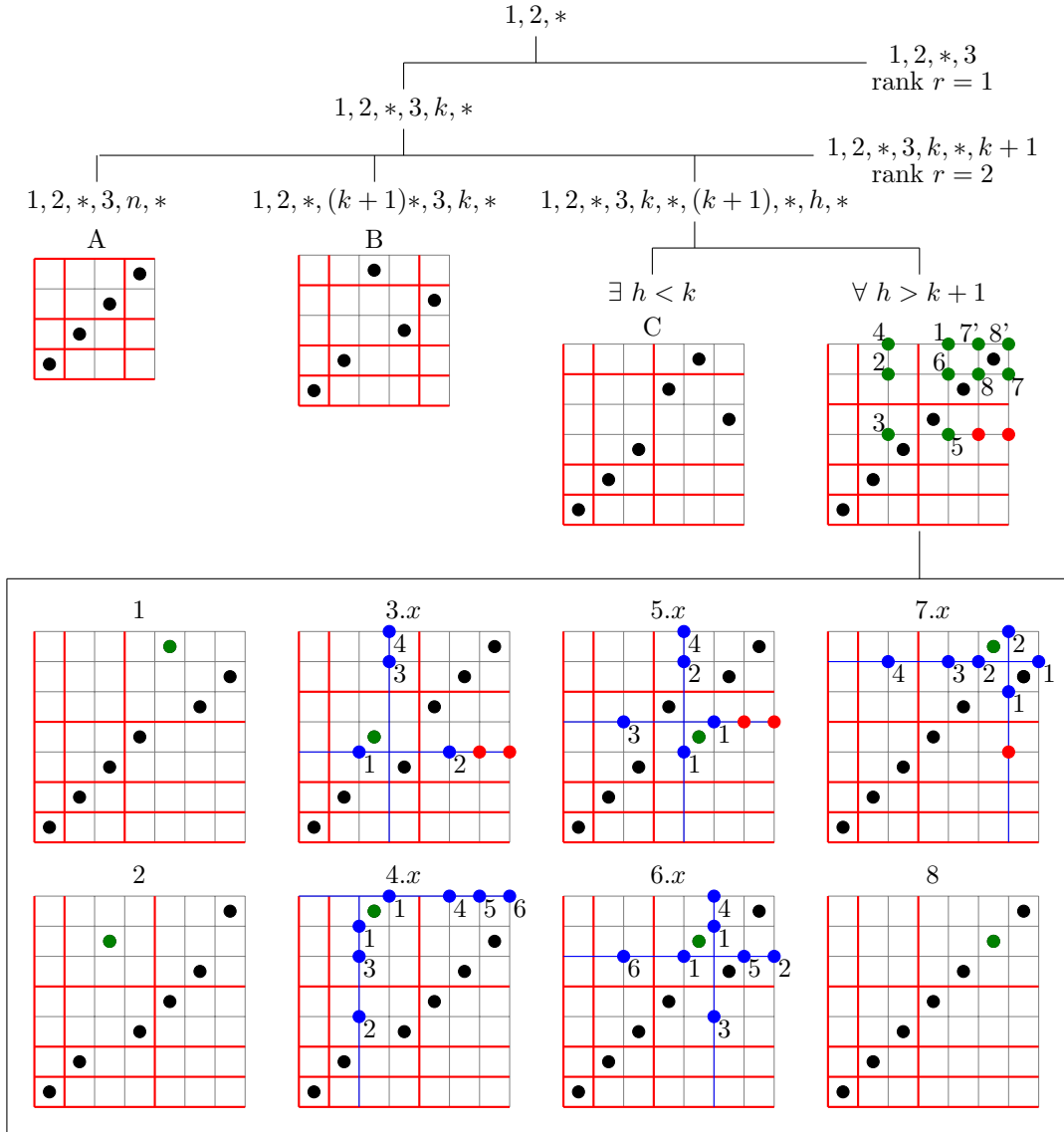


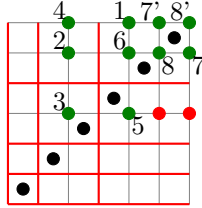
Figure 41: Decomposition of cases in the proof of Theorem 5.5. Numbers on blue bullets correspond to different values of  $x$  in case label.

of the form “given that the first  $a - 1$  blocks are empty, and the  $a$ -th one has at least one point, . . .”.

In some of these cases, adding one such block produces a pattern which may have a descent involving the black points, thus we need to further refine the analysis with a further entry certifying the absence of such descents. Although not necessary by itself (as we control the number of descents in certificates), this is important for the following reason: differently from the primitive case, at every given size there are several non-primitive exceptional standard configurations with rank at least 3, which thus would proliferate in all sorts of branches in the decomposition tree, making the analysis inconclusive. It is restriction to primitive configurations that allows to concentrate the identity configurations of all sizes into a single branch (indeed, a result of Appendix C is that  $\text{id}_n$  is the only standard permutation in  $\text{Id}_n$  starting with  $(1, 2, *)$ ).

The following picture, which is the pertinent crucial node in the tree of Figure 41,

represents the position of the blocks, by green bullets. The red bullets correspond to blocks which are certified to be empty, by the fact that, as we said, all entries at the right of  $k + 1$  are larger than  $k + 1$ .



We have ten candidate blocks, labeled  $\{1, 2, \dots, 7, 8; 7', 8'\}$ , that we now analyse. First of all, it is easily seen that cases  $7'$  and  $8'$  coincide, up to relabeling, to cases  $7$  and  $8$ , respectively. Then, cases  $1$  and  $2$  can be analysed in one stroke, by adding one entry in the corresponding block, while cases from  $3$  to  $7$  require a finer analysis in order to ensure primitivity, and thus involve the insertion of two entries, one in the corresponding block, the other one in an available block among those splitting the descent. We have thus several cases, labeled from  $3.1$  to  $7.4$  (4 cases for blocks  $3, 5, 7$  and 6 cases for blocks  $4$  and  $6$ ). The case of block  $8$  is the one that reduces to the sole configuration  $\text{id}_n$ .

All cases from  $1$  to  $7.4$  correspond to some case appearing in Proposition 5.6 (which explains the naming of cases in the proposition). Sometimes this occurs after dropping one entry. The following scheme summarizes this correspondence:

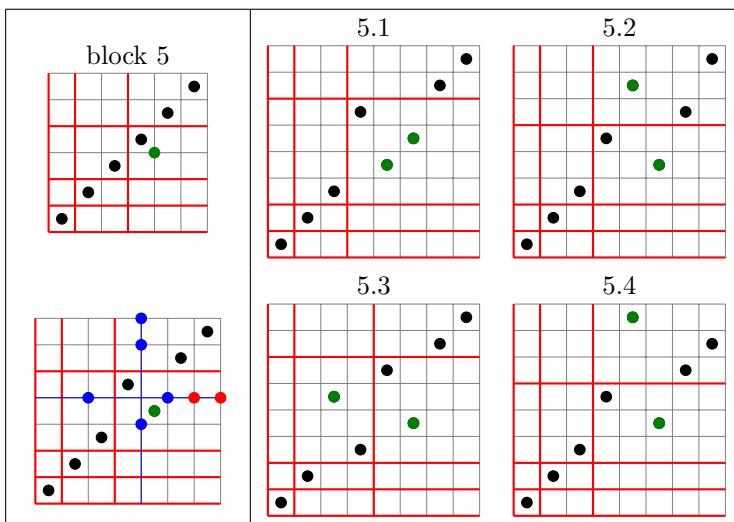
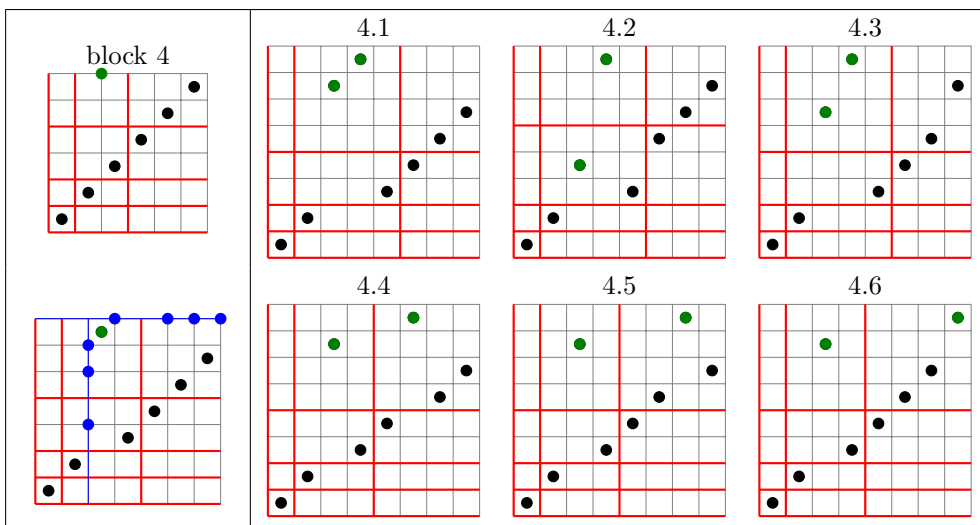
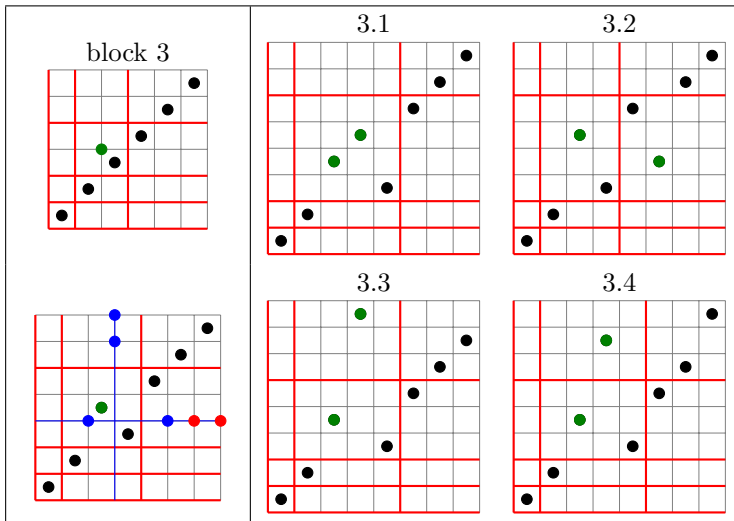
1	⟨ <b>1</b> ⟩						
2	⟨ <b>2</b> ⟩						
3	$\left\{ \begin{array}{l} 3.1 \\ 3.2 \\ 3.3 \\ 3.4 \end{array} \right.$	$\left\{ \begin{array}{l} \langle \mathbf{3.1} \rangle \\ \langle \mathbf{3.2} \rangle \\ \langle \mathbf{3.3} \rangle \\ \langle \mathbf{2} \rangle \end{array} \right.$					
4	$\left\{ \begin{array}{l} 4.1 \\ 4.2 \\ 4.3 \\ 4.4 \\ 4.5 \\ 4.6 \end{array} \right.$	$\left\{ \begin{array}{l} \langle \mathbf{4.1} \rangle \\ \langle \mathbf{3.3} \rangle \\ \langle \mathbf{2} \rangle \\ \langle \mathbf{1} \rangle \\ \langle \mathbf{2} \rangle \\ \langle \mathbf{2} \rangle \end{array} \right.$					
			5	$\left\{ \begin{array}{l} 5.1 \\ 5.2 \\ 5.3 \\ 5.4 \end{array} \right.$	$\left\{ \begin{array}{l} \langle \mathbf{5.1} \rangle \\ \langle \mathbf{5.2} \rangle \\ \langle \mathbf{3.2} \rangle \\ \langle \mathbf{1} \rangle \end{array} \right.$		
			6	$\left\{ \begin{array}{l} 6.1 \\ 6.2 \\ 6.3 \\ 6.4 \\ 6.5 \\ 6.6 \end{array} \right.$	$\left\{ \begin{array}{l} \langle \mathbf{6.1} \rangle \\ \langle \mathbf{1} \rangle \\ \langle \mathbf{5.2} \rangle \\ \langle \mathbf{1} \rangle \\ \langle \mathbf{1} \rangle \\ \langle \mathbf{2} \rangle \end{array} \right.$		
			7	$\left\{ \begin{array}{l} 7.1 \\ 7.2 \\ 7.3 \\ 7.4 \end{array} \right.$	$\left\{ \begin{array}{l} \langle \mathbf{7} \rangle \\ \langle \mathbf{7} \rangle \\ \langle \mathbf{6.4} \rangle \\ \langle \mathbf{2} \rangle \end{array} \right.$		

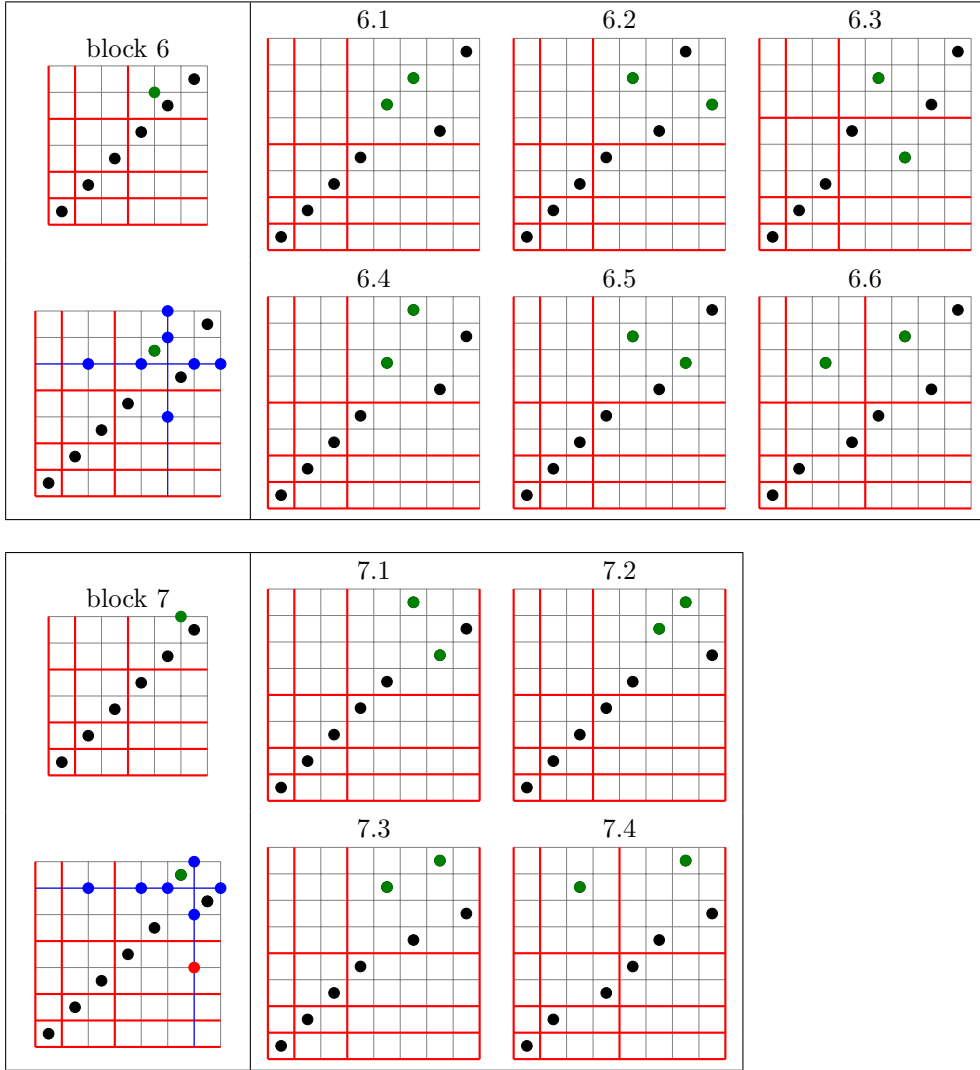
On the left column, we have the case in the decomposition. Possibly, the annotation “[drop col  $\cdot$ ]” specifies that we have to drop one entry, in the given column. In “⟨ $\cdot$ ⟩” we put the label of Table 5 (in boldface, if it is the first appearance in the list).

The two cases  $7.1$  and  $7.2$  correspond to pattern  $7$  in which one or the other gray block is certified to be non-empty, which is a sufficient condition for having a zig-zag path certificate.

The lower part of Figure 41 specifies which is which among all subcases  $3.1, \dots, 7.4$  associated to blocks  $3$  to  $7$  (the same information is also carried in a more detailed way in the tables at the end of this subsection: we remind the configuration associated to the block, analyse the possible positions for a further entry splitting the descent, using blue construction-lines, and then list the corresponding cases).

As we anticipated, if all blocks  $\{1, 2, \dots, 7; 7'\}$  are empty, and only blocks  $8$  (and  $8'$ ) are possibly non-empty, then the permutation is  $\text{id}_n$  for  $n \geq 6$ , and the theorem does not apply, since the class  $\text{Id}_n$  is exceptional.  $\square$





## 5.2 Operators $q_1$ and $q_2$

We have seen that  $\bar{T} \left( \mathfrak{S}_{n-2}^{(\text{prim})} \right) \rightarrow \mathfrak{S}_n^{(\text{prim})}|_{\text{rank}>2}$ , it is surjective on this set, and is a pullback function. In order to produce a complete decomposition, we need to introduce two more operators,  $q_1$  and  $q_2$ , such that

$$\bar{q}_1 \left( \mathfrak{S}_{n-1}^{(\text{prim})} \right) \rightarrow \mathfrak{S}_n^{(\text{prim})}|_{\text{rank}=1}; \quad \bar{q}_2 \left( \mathfrak{S}_{n-1}^{(\text{prim})} \right) \rightarrow \mathfrak{S}_n^{(\text{prim})}|_{\text{rank}=2}. \quad (52)$$

We do this in this section.

**Definition 5.7.** Let  $\sigma$  be a permutation of size  $n$ . We define  $\text{add}_i(\sigma)$  for  $i = 1, \dots, n$  to be the permutation of size  $n + 1$   $\text{add}_i(\sigma) := \sigma(1) + 1, \dots, \sigma(i - 1) + 1, 1, \sigma(i) + 1, \dots, \sigma(n) + 1$ .

I.e.,  $\text{add}_i(\sigma)$  is described by the diagrammatic manipulation below:

$$\text{add}_i \left[ \begin{array}{|c|} \hline \text{---} \\ \hline \end{array} \right] = \begin{array}{|c|} \hline \text{---} \\ \hline \end{array} \begin{array}{|c|} \hline \text{---} \\ \hline \end{array}$$

$\underbrace{\hspace{2cm}}_{i-1} \qquad \underbrace{\hspace{2cm}}_{i-1} \quad i$

The two operators  $q_1$  and  $q_2$  are defined in terms of  $\text{add}_i$ 's for suitable  $i$ 's. In order to endow them with the appropriate properties, we shall investigate the difference between the cycle

invariants of  $\sigma$  and  $\text{add}_i(\sigma)$ . This requires a case analysis based on the ‘type’ of permutations (among  $H$ - and  $X$ -type, see Definition 3.6). This is presented in Table 6, and illustrated in the following paragraph.

**Proposition 5.8.** *Let  $i \in \{1, 2\}$ . Let  $\sigma$  be a primitive permutation with invariant  $(\lambda, r)$  with  $r > i$ .*

- *If  $\sigma$  has type  $X(r, j)$  then there exists exactly one index  $\ell$  such that  $\text{rank}(\text{add}_\ell(\sigma)) = i$ .*
- *If  $\sigma$  has type  $H(r_1, r_2)$  with  $r_2 \neq i$  then there exists exactly one index  $\ell$  such that  $\text{rank}(\text{add}_\ell(\sigma)) = i$ .*
- *If  $\sigma$  has type  $H(r_1, r_2)$  with  $r_2 = i$  then there exist exactly two indices  $\{\ell, m\} = \{1, \sigma^{-1}(n)\}$  such that  $\text{rank}(\text{add}_\ell(\sigma)) = \text{rank}(\text{add}_m(\sigma)) = i$ ; moreover  $\text{add}_\ell(\sigma)$  and  $\text{add}_m(\sigma)$  are in the same class, as  $\text{add}_\ell(\sigma) = R^{-1}(\text{add}_m(\sigma))$ .*

*Proof.* This emerges from the analysis of Table 6. We discuss the three propositions one by one, with reference to the 6 rows of the table.

- If  $X(r, j)$ , it can be checked that the only possibility for having rank  $i$  is case ④ with  $s = r - i$ . The reason why we need  $r > i$  is because, e.g. if  $r = 1$ , either  $s = 0$  or  $1$ , but both eventualities are impossible, since cycles of length 0 do not exist and cycles of length 1 are not allowed in primitive permutations.
- If  $H(r_1, r_2)$  with  $r_2 \neq i$ , it can be checked that the only possibility is case ③ with  $s = r_2 - i$ , if  $r_2 > i$ , and case ① with  $s = r_1$ , if  $r_2 = 1$ . (In fact, the only case with  $r_2 < i$  is when  $i = 2$  and  $r_2 = 1$ ).
- If  $H(r_1, r_2)$  with  $r_2 = i$ , then there are exactly two possibilities: case ③ of the table with  $s = 0$ , and case ① with  $s = r_1$ . Clearly we go from one target configuration to another with the operator  $R^{\pm 1}$ , since these only differ by the edge  $(\alpha, 1)$  which is  $(1, 1)$  in case ③ and  $(\sigma^{-1}(n), 1)$  in case ①.

□

The previous proposition shows that for configurations  $\sigma$  with rank  $i$ , there exists one and only one configuration  $\tau$  and index  $\ell$  such that  $\sigma = \text{add}_\ell(\tau)$ , with an exceptional case in which there are two such configurations, which are however easily shown to be in the same class. We can thus just “break the tie” for the third situation in Proposition 5.8 (see Figure 42 for an illustration), and give the following definition:

**Definition 5.9.** *Let  $i \in \{1, 2\}$ . Let  $\tau$  be a primitive permutation with rank  $r > i$ . Define  $q_i(\tau)$  to be the unique  $\text{add}_\ell(\tau)$  such that  $\text{rank}(\text{add}_\ell(\tau)) = i$ , if we are in one of the first two situations of Proposition 5.8, and  $q_i(\tau) = \text{add}_{\tau^{-1}(n)}(\tau)$  if we are in the third situation.*

Note that the edge  $(\ell, 1)$  in  $q_i(\sigma)$  is never  $(1, 1)$ . This is true by a further investigation of the table, for the first two situations, and holds at sight for the third situation, exactly because of our choice of convention (if it were, this would mean that  $\sigma^{-1}(n) = 1$ , which implies that  $\sigma$  is reducible). Thus the edge  $(i, 1)$  is never a pivot, a fact that will be useful when we pass to a reduced dynamics after the action of a surgery operator  $q_i$ .

Now that we have defined our  $q_i$ ’s, we need to show that they satisfy the properties outlined in Section 1.7, i.e. the statement of the following lemma:

**Lemma 5.10.** *Let  $\sigma$  and  $\sigma'$  be configurations in the same class. Then  $q_i(\sigma) \sim q_i(\sigma')$  for both  $i = 1, 2$ .*

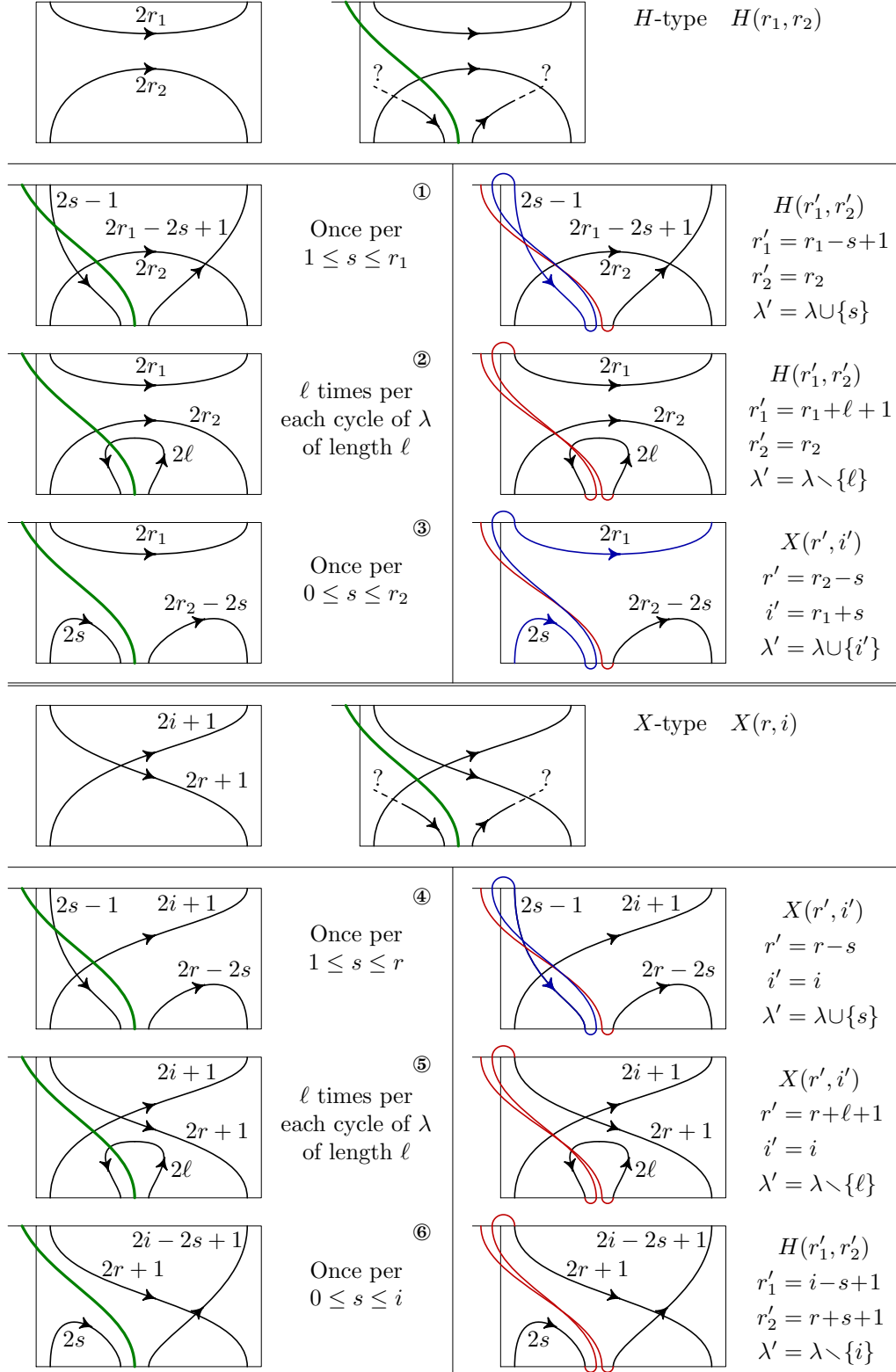


Table 6: Modification to the cycle invariant of a configuration produced by  $\text{add}_i$ . In green, the newly-added edge. In red, parts which get added to the rank path. In blue, parts which are singled out to form a new cycle.



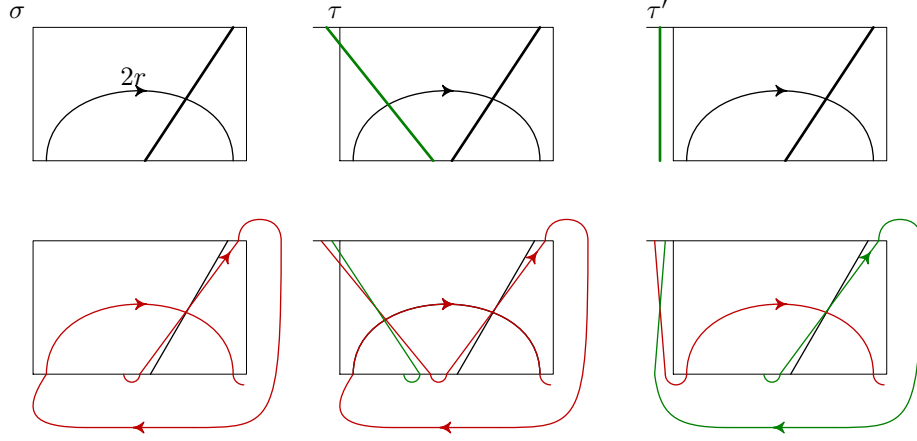


Figure 42: The two possible consistent definitions of  $q_r$  on a configuration  $\sigma$  of type  $H(r', r)$ , mentioned in the third case of Proposition 5.8. The two configurations  $\tau$  and  $\tau'$  are such that  $\tau = R\tau'$ . Our choice is to define  $q_r\sigma = \tau$ .

*Proof.* Clearly both  $q_i$ 's are injective. They are actually ‘almost bijective’, as the number of preimages is at most 2 (and, for what it matters, in large size there is a unique preimage in the majority of configurations).

Let  $\tau$  and  $\tau'$  be primitive permutations in the same class  $C$ , and let  $S$  be a sequence such that  $S(\tau) = \tau'$ . Call  $\sigma = q_i(\tau)$ . The reduced permutation of  $\sigma$  where the edge  $(\ell, 1)$  is the only gray edge is  $\tau$ . Since this edge is not a pivot, we can use the boosted dynamics and define  $\sigma' = B(S)(\sigma)$ , and we have that  $\sigma' = q_i(\tau')$ .

Indeed, by definition of  $B(S)$ , removing the edge  $(\ell', 1)$  in  $\sigma'$  gives  $\tau'$ , and  $(\ell', 1)$  is not a pivot, which coincides exactly with our characterisation of  $q_i(\tau')$  (since  $\sigma$  has rank  $i$ , so has  $\sigma'$ ). Thus  $q_i(\sigma) \sim q_i(\sigma')$ .  $\square$

As a consequence of this lemma, analogously to what we have done for the operator  $T$ , we can define the two maps  $\bar{q}_1$  and  $\bar{q}_2$  on classes.

First of all, we observe the triviality

**Lemma 5.11.**  $\bar{q}_1(\text{Id}_n) = \text{Id}'_{n+1}$ .

(this is seen by direct inspection of the canonical representatives, as  $q_1(\text{id}_n) = R^{-2} \text{id}'_{n+1}$ ).

Then, yet again, these maps have a definite behaviour for what concerns the invariants. Let us introduce the useful notation

**Notation.** Let  $\lambda$  be a cycle invariant, and let  $j \in \lambda$ . We use  $\lambda(j)$  as a shortcut for  $\lambda \setminus \{j\}$ .

Then:

**Lemma 5.12.** Let  $C$  be a class with invariant  $(\lambda, r, s)$  with  $r > 1$ . Then  $C' = \bar{q}_1(C)$  has invariant  $(\lambda \cup \{r\}, 1, s)$ .

*Proof.* The claim on the sign comes as an application of Corollary 4.9. Indeed, as seen in Proposition 4.5, the sign is a class invariant, so we can take  $\sigma \in C'$  to be standard with  $\sigma(n) = n$ . Since  $\sigma$  has rank 1, we know that  $\sigma(2) = n - 1$ . This is the permutation  $\sigma$  on the LHS of Corollary 4.9, and removing the edge  $(1, 1)$ , i.e. taking the preimage of  $R^{-1}\sigma$  under  $q_1$ , we obtain the permutation  $\tau$  on the RHS of Corollary 4.9 (indeed, we have  $q_1(\tau) = R\sigma$  because we are in the third case of the definition of  $q_1$ ).

For what concerns cycle and rank invariants, this comes from a straightforward inspection (cf. again Table 6).  $\square$

**Corollary 5.13.** *Let  $\sigma$  be a permutation with invariant  $(\lambda, 1, s)$  then either  $\tau := q_1^{-1}(\sigma)$  or  $\tau' := q_1^{-1}(R\sigma)$  or both are defined. Each of these configurations have invariant  $(\lambda(i), i, s)$  for some  $i \in \lambda$ .*

**Lemma 5.14.** *Let  $C$  be a class with invariant  $(\lambda, r, s)$  with  $r > 2$ . Then  $\bar{q}_2(C)$  has invariant  $(\lambda \cup \{r-1\}, 2, 0)$ .*

*Proof.* The claim on the sign comes as an application of Corollary 4.11. Again we can choose a standard representative with  $\sigma(n) = n$ . Then there must exist  $j$  such that  $\sigma' = R^j(\sigma)$  has  $\sigma'(n) = n$  and  $\sigma'(n-1) = n-1$ . Since  $\sigma'$  has rank 2, this configuration is of the form of the LHS permutation of Corollary 4.11, and removing the edge  $(\sigma'^{-1}(1), 1)$ , which corresponds to take the preimage of the surgery operator  $q_2$ , i.e. produces a permutation of smaller size (call it  $\tau$ ) such that  $q_2(\tau) = \sigma'$  (or  $q_2(\tau) = R(\sigma')$  if  $\sigma'^{-1}(1) = 1$ ). This proves that, regardless from the sign of  $\tau$ , the sign of  $\sigma'$  is zero.

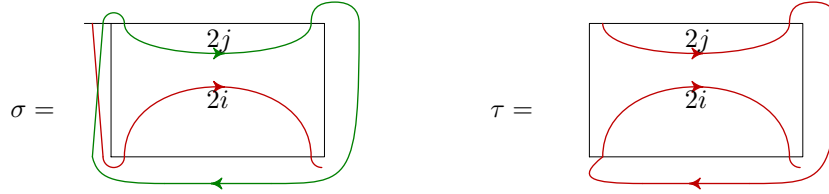
Again, for what concerns cycle and rank invariants, this comes from a straightforward inspection.  $\square$

**Corollary 5.15.** *Let  $\sigma$  be a permutation with invariant  $(\lambda, 2, 0)$  then either  $q_2^{-1}(\sigma)$  or  $q_2^{-1}(R\sigma)$  are defined. This configuration has invariant  $(\lambda(i-1), i, s)$  for some  $i \in \lambda$  and  $s \in \{-1, 0, +1\}$ , more precisely,*

- if  $\lambda(i-1)$  has a positive number of even cycles, then  $s = 0$ ;
- if  $\lambda(i-1)$  has no even cycles, then  $s = \pm 1$ .

At this point, we are left with the investigation of the pullback properties of our operators.

**Lemma 5.16.** *Let  $\sigma = (1, \sigma(2), \dots, \sigma(n))$  be a permutation of type  $X(i, j)$  with cycle and rank invariant  $(\lambda, i)$ . Then  $\tau = (\sigma(2) - 1, \dots, \sigma(n) - 1)$  has type  $H(j, i)$  and invariant  $(\lambda(j), r')$ , with  $r' = i + j - 1$ .*



*Proof.* This is the reverse implication of case ③ in Table 6, specialised to  $s = 0$ .  $\square$

**Theorem 5.17** (Pullback of  $\bar{q}_1$ ). *Let  $C$  be a class with invariant  $(\lambda, 1, s)$  then for every  $j \in \lambda$  there exists a class  $B_j$  with invariant  $(\lambda(j), j, s)$  such that  $\bar{q}_1(B_j) = C$ . In other words,  $\bar{q}_1$  is a pullback function w.r.t. the equivalence relation given by the invariant, i.e.  $C \xrightarrow{\sim} (\lambda, r, s)$ .*

*Proof.* First of all, let us remark that, by Corollary 5.13, the set of invariants  $(\lambda(j), j, s)$  coincides with the set of preimages of  $(\lambda, 1, s)$  under  $\tilde{q}_1$ .<sup>13</sup>

Now, we take a standard family of  $C$ . Then, by Lemma 3.9, for every  $j \in \lambda$  there exists  $\sigma_j = (1, \sigma_j(2) \dots)$  of type  $X(1, j)$  such that  $\tau_j = (\sigma_j(2) - 1, \dots, \sigma_j(n) - 1)$  is irreducible.

Moreover,  $\tau_j$  has invariant  $(\lambda(j), j, s)$ . We know this, for cycle and rank, from Lemma 5.16 (in the case  $i = 1$ ), and, for the sign, from Lemma 5.12, the fact that  $q_1(\tau_j) = R(\sigma_j)$ , and that  $\sigma_j$  has sign  $s$ . Thus for every  $j$  the class  $B_j \ni \tau_j$  satisfies  $\bar{q}_1(B_j) = C$ .  $\square$

For operator  $q_2$ , the facts we can establish at this point are a bit weaker, the trouble coming from the “loss of memory” on the sign, which becomes 0 regardless of what was its value on

<sup>13</sup>Where  $\tilde{\cdot}$  is the notion introduced in the definition of pullback function.

the preimage. As a result, we will need some extra work in the induction step of the next section, while at this point we establish the following:

**Theorem 5.18** (Pullback of  $\bar{q}_2$ ). *Let  $C$  be a class with invariant  $(\lambda, 2, 0)$ . Then for every  $j \in \lambda$  there exists a class  $B_j$  with invariant  $(\lambda(j), j+1, s)$ , for some  $s$ , such that  $\bar{q}_2(B_j) = C$ . In other words,  $\bar{q}_2$  is a pullback function w.r.t. the equivalence relation given by the cycle invariant, i.e.  $C \xrightarrow{\sim} (\lambda, r)$ .*

*Proof.* The proof is analogous to the one above (with the discussion of the sign left out).

By Corollary 5.15, the set of cycle invariants  $(\lambda(j), j+1)$  coincides with the set of preimages of  $(\lambda, 2)$  under  $\tilde{q}_2$ .

We take a standard family of  $C$ , then by Lemma 3.9 for every  $j \in \lambda$  there exists  $\sigma_j = (1, \sigma_j(2) \dots)$  with type  $X(2, j)$  such that  $\tau_j = (\sigma_j(2) - 1, \dots, \sigma_j(n) - 1)$  is irreducible.

Moreover,  $\tau_j$  has cycle and rank invariant  $(\lambda(j-1), j)$  by Lemma 5.16 (in the case  $i = 2$ ). Since  $q_2(\tau_j) = R(\sigma_j)$ , for every  $j$  the class  $B_j \ni \sigma'_j$  satisfies  $\bar{q}_2(B_j) = C$ .  $\square$

## 6 The induction

This section is devoted to the main induction of the paper, that implies the classification theorem. The induction mainly works at the level of non-exceptional classes, so, before doing this, we need to exclude the proliferation of distinct classes with the same invariant due to the action of our surgery operators on exceptional classes. This requires to establish ‘fusion lemmas’, i.e. lemmas of the form, for a given exceptional class  $I = \{I_n\}$ , for  $n \geq n_0$ , there exists non-exceptional classes  $C = \{C_n\}$ , such that a certain surgery operator  $X$ , acting on  $I$ , gives the same class as the action on  $C$  (in formulas,  $\exists C : X(C) \sim X(I)$ ). In the paragraph above, in principle,  $I$  may be  $\text{Id}$  or  $\text{Id}'$ , while  $X$  may be  $T$ ,  $q_1$  or  $q_2$ . However, we will see that not all of these cases need to be considered.

In proving these lemmas, we will make the ansatz that the classes  $C_n$  at different  $n \geq n_0$  have one representative with a ‘nice structure’ in  $n$ , e.g. a certain permutation of size  $n_0$  and an identity block of size  $n - n_0$  in a specific position, and that the sequence connecting this representative to a canonical representative of the exceptional class, once written in terms of dynamics operators and their inverses (so that the variable-size identity block is never broken up along the dynamics), is the same for all sizes.

In particular, we need to establish that the forementioned representative is in fact in a class  $C$  which is non-exceptional. This can be done in two ways, either by using our knowledge of the structure of *all* configurations in the special classes  $\text{Id}$  and  $\text{Id}'$ , presented in Appendix C, or by using a result, also proven in Appendix C, stating that both  $\text{Id}$  and  $\text{Id}'$  have a unique standard family (in particular, in each of these classes there is only one standard permutation  $\pi$  with  $\pi(1) = 1$  and  $\pi(n) = n$ , namely  $\pi = \text{id}_n$  for  $\text{Id}_n$  and  $\pi = \text{id}'_n$  for  $\text{Id}'_n$ ), so that, if the representative is standard, the check is straightforward. The second method is more compact, so we will adopt it in this section.

The very last lemma of this form will be based on a more general ansatz (see the pattern in the following Definition 6.10). The sequence<sup>14</sup>  $w_n \in \{L, R, \bar{L}, \bar{R}\}^*$  is not the same for all  $n \geq n_0$ , but rather has the form  $w_n = w_{\text{end}} w^{n-n_0} w_{\text{start}}$ . Indeed, instead of having a ‘large’ identity block of size  $n - n_0$ , we have two ‘large’ simple blocks, of size  $n - n_0 - k$  and  $k$ , and the iterated sequence  $S$  in the middle of  $S_n$  is used to change the value of  $k$  by one.

Such intelligible patterns allow to give unified proofs of these fusion lemmas which hold for all  $n$  large enough, as desired. We admit that these patterns could have hardly been guessed without the aid of computer search. We have been lucky in the respect that not only our ansatz holds, but also the sequences implementing our ansatz are the shortest ones connecting the two guessed representatives, so that, once the ‘good’ representatives have

<sup>14</sup>Recall that we use the shortcuts  $\bar{L}, \bar{R}$  for  $L^{-1}$  and  $R^{-1}$ .

been found by the computer at finite size, we could invent a proof just by analysing the structure of the numerically-found geodesic path in the Cayley graph.

## 6.1 Simple properties of the invariant

Here we prove a few facts on the invariants, that we have previously stated without proof. A stronger characterisation will emerge from the main induction, however it is instructive to deduce the following lemma, at the light of the previous results, and with a small extra effort.

**Lemma 6.1.** *Let  $C$  be a class with invariant  $(\lambda, r, s)$  and let  $\ell$  be the number of cycles (not including the rank). The following statements hold:*

1. *The list  $\{r, \lambda_1, \dots, \lambda_\ell\}$  contains an even number of even entries.*
2. *The sign of the class,  $s(C) = \text{Sign}(\overline{A}(C))$  can be written as  $s(C) = 2^{-\frac{n+\ell}{2}} \overline{A}(C)$ .*
3. *The sign  $s(C)$  is zero if and only if some of the entries  $r$  and  $\lambda_j$  of the cycle invariant  $(\lambda, r)$  are even.*

*Proof.* First of all, the statements can be verified for the (exceptional) class of the identity, since computing (by induction) the cycle invariant  $(\lambda, r)$  of  $id_n$  is an easy task, while the calculation of the Arf invariant was done in Corollary 4.7. The results are summarised in Table 7, top.

Then, the statements follow for the other exceptional class,  $\text{Id}'_n$ , by using the fact that  $\overline{q}_1(\text{Id}_n) = \text{Id}'_{n+1}$  (Lemma 5.11) and the action of  $\overline{q}_1$  on the Arf invariant of a class (Corollary 4.9). The results are summarised in Table 7, bottom.

Finally, the statements follow inductively for all non-exceptional classes, for the three cases of rank equal to 1, 2, or at least 3, using the pullback results for the operators  $\overline{q}_1$ ,  $\overline{q}_2$  and  $\overline{T}$  (Theorems 5.17, 5.18 and 5.5, respectively) and the action of the operators on the cycle invariant of a class (Lemma 5.12, 5.14 and 5.4 respectively), established in Section 5, and on the Arf invariant of a class (Corollary 4.9, 4.11 and 4.8 respectively), established in Section 4.

In order to illustrate how the argument works, let us analyse it in full detail in the case of operator  $T$ . Let  $C$  be a class of size  $n$  with invariant  $(\lambda, r, s)$ , with  $r \geq 3$ . Then, by the pullback theorem for  $T$  (Theorem 5.5), there exists a class  $B$  such that  $\overline{T}(B) = C$ , and  $B$  shall have invariant  $(\lambda, r - 2, s)$  in agreement with Lemma 5.4. Clearly  $T$  preserves the parity of the number of even entries in the cycle invariant (only  $r$  has changed, and by 2), so, as by induction  $B$  has an even number of even cycles, this also holds for  $C$ .

By induction we know that  $s(B) = 2^{-\frac{n-2+\ell}{2}} \overline{A}(B)$  where  $\ell = \ell(B)$  is the number of cycles in  $B$ . However, we have just noticed that  $\ell(C) = \ell(B) = \ell$ . By Corollary 4.8,  $\overline{A}(C) = 2\overline{A}(B)$ , thus  $2^{-\frac{n+\ell}{2}} \overline{A}(C) = 2 \times 2^{-\frac{n+\ell}{2}} \overline{A}(B) = 2^{-\frac{n-2+\ell}{2}} \overline{A}(B) = s(B)$ . Hence, since we have  $s(C) = s(B)$  by Lemma 5.4, we have consistently  $s(C) = \text{Sign}(\overline{A}(C)) = 2^{-\frac{n+\ell}{2}} \overline{A}(C)$ .

Finally, by induction  $s(B)$  is zero if and only if some of the entries among  $r - 2$  and  $\lambda_j$  are even. As we have just established that  $s(C) = s(B)$  and that  $C$  has as many even cycles as  $B$ , the statement holds also for  $C$ .  $\square$

The results in Table 7 imply the following simple fact

**Lemma 6.2.** *For all  $n \geq 4$ , the cycle invariants  $(\lambda, r)$  of  $\overline{T}(\text{Id}_n)$  and of  $\overline{T}(\text{Id}'_n)$  are distinct.*

*Proof.* Just combine Table 7 and Lemma 5.4.  $\square$

$n$	2	3	4	5	6	7	8	9
$(\lambda, r)$ of $\text{Id}_n$	$(\emptyset, 1)$	$(\{1\}, 1)$	$(\emptyset, 3)$	$(\{2\}, 2)$	$(\emptyset, 5)$	$(\{3\}, 3)$	$(\emptyset, 7)$	$(\{4\}, 4)$
$\bar{A}(\text{Id}_n)$	-2	-4	-4	0	8	16	16	0
$(\lambda, r)$ of $\text{Id}'_n$			$(\{1, 1\}, 1)$	$(\{3\}, 1)$	$(\{2, 2\}, 1)$	$(\{5\}, 1)$	$(\{3, 3\}, 1)$	$(\{7\}, 1)$
$\bar{A}(\text{Id}'_n)$			-8	-8	0	16	32	32

Table 7: The cycle and sign invariants of  $\text{Id}_n$  and  $\text{Id}'_n$ . The pattern of  $(\lambda, r)$  is repeated with period 2, while the pattern of  $\bar{A}$  is repeated with period 8. We include also the non-primitive classes  $\text{Id}_2$  and  $\text{Id}'_4$ , in order to illustrate the mechanism on smaller values of  $n$ .

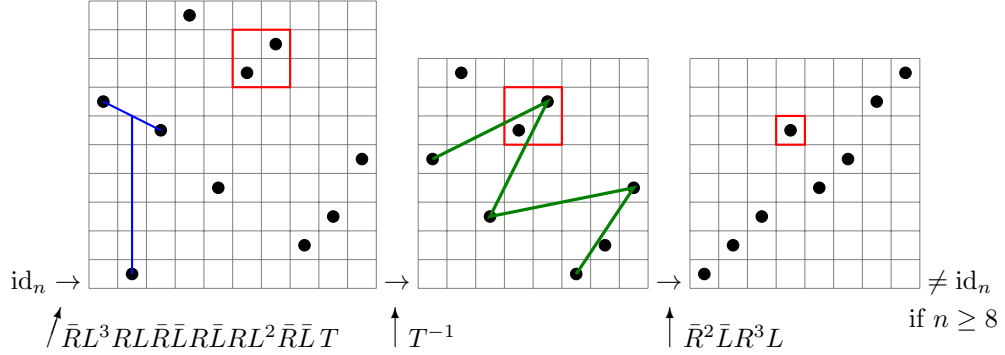


Figure 43: The three configurations involved in the proof of Lemma 6.3.

## 6.2 Fusion lemmas for $T$

**Lemma 6.3** (Fusion lemma for  $(T, \text{Id})$ ). *Let  $n \geq 8$ . There exists some non-exceptional class  $A_n$  such that  $\bar{T}(A_n) = \bar{T}(\text{Id}_n)$ .*

*Proof.* We just searched (by computer) a sequence such that  $T(\text{id}_n)$  is transformed into a  $\sigma = T(\tau)$  where  $\tau \notin \text{Id}_n$ . For  $n \geq 7$  the configuration  $\bar{R}L^3RL\bar{R}\bar{L}R\bar{L}R\bar{L}R\bar{L}^2\bar{R}\bar{L}T(\text{id}_n)$  is shown in Figure 43, left, where the red square is an identity of size  $n - 6$ . This configuration has a  $T$ -structure and its pre-image w.r.t.  $T$  is the configuration shown in Figure 43, middle. Finally, by applying the algorithm of standardization to  $\tau$ , we see that  $\tau_s = \bar{R}^2\bar{L}R^3L(\tau)$  is the standard permutation shown in Figure 43, right, where the red square is an identity of size  $n - 7$ . When this block is non-empty, this configuration has  $\tau_s(1) = 1$  and  $\tau_s(n) = n$ , but it is not  $\text{id}_n$ , from which we conclude.  $\square$

**Lemma 6.4** (Fusion lemma for  $(T, \text{Id}')$ ). *Let  $n \geq 9$ . There exists some non-exceptional class  $C_n$  such that  $\bar{T}(C_n) = \bar{T}(\text{Id}'_n)$ .*

*Proof.* We searched a sequence such that  $T(\text{id}'_n)$  is transformed into a  $\sigma = T(\tau)$  where  $\tau \notin \text{Id}'_n$ . The configuration  $\bar{R}L\bar{R}\bar{L}^2\bar{R}\bar{L}^3R\bar{L}^2R\bar{L}\bar{R}\bar{L}T(\text{id}'_n)$  is shown in Figure 44, left, where the red square is an identity of size  $n - 7$ . This configuration has a  $T$ -structure and its pre-image w.r.t.  $T$  is the configuration shown in Figure 44, middle. Finally, by applying the algorithm of standardization to  $\tau$  we see that  $\tau_s = \bar{R}^2\bar{L}^2R\bar{L}^2R(\tau)$  is the standard permutation shown in Figure 44, right, where the red square is an identity of size  $n - 8$ . When this block is non-empty, this configuration has  $\tau_s(1) = 1$  and  $\tau_s(n) = n$ , but it is not  $\text{id}'_n$ , from which we conclude.  $\square$

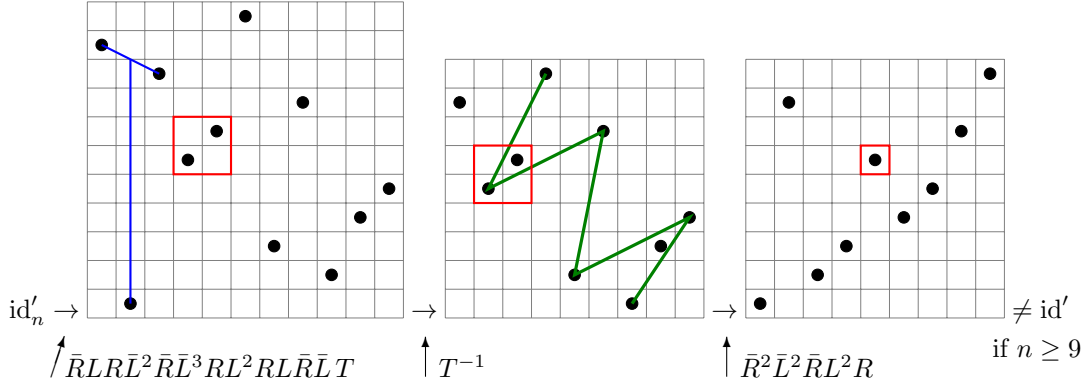


Figure 44: The three configurations involved in the proof of Lemma 6.4.

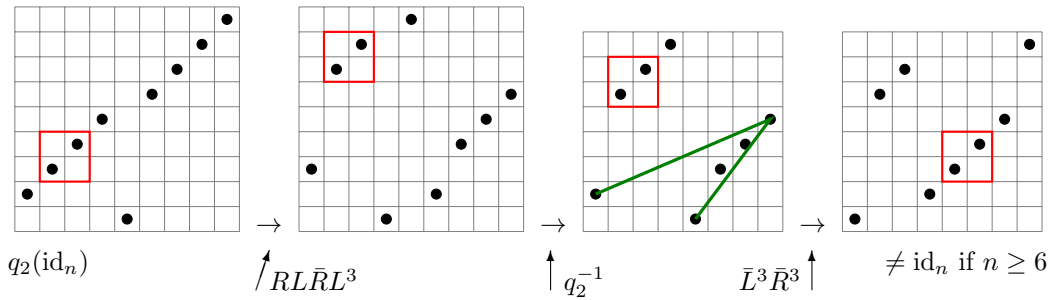


Figure 45: The four configurations involved in the proof of Lemma 6.5. Recall that, whenever  $\sigma(1) \neq 1$ ,  $q_2^{-1}\sigma$  is obtained by removing the entry of  $\sigma$  in the bottom-most row.

### 6.3 Fusion lemmas for $q_1$ and $q_2$

In this section we shall see that there is no proliferation of classes due to the action of  $q_1$  and  $q_2$  on exceptional classes of large size  $\text{Id}_n$  and  $\text{Id}'_n$ . This makes, in principle,  $2 \times 2 = 4$  cases. However, we know from Lemma 5.11 that  $\bar{q}_1(\text{Id}_n) = \text{Id}'_{n+1}$ , while neither  $q_1$  nor  $q_2$  apply to  $\text{Id}'_n$ , because these classes have rank 1, so this rules out three cases out of four, and we just need the following:

**Lemma 6.5** (Fusion lemma for  $(q_2, \text{Id})$ ). *Let  $n \geq 6$ . There exists some non-exceptional class  $B_n$  such that  $\bar{q}_2(B_n) = \bar{q}_2(\text{Id}_n)$ .*

*Proof.* We searched a sequence such that  $q_2(\text{id}_n)$  is transformed into a  $\sigma = q_2(\tau)$  where  $\tau \notin \text{Id}_n$ . The configuration  $RL\bar{R}L^3 q_2(\text{id}_n)$  is shown in Figure 45 (second image), where the red square is an identity of size  $n - 6$  (so it is possibly empty). Its pre-image w.r.t.  $q_2$  is the configuration shown in Figure 45 (third). Then, it can be easily verified that for  $n \geq 6$  the standard permutation  $\tau_s = \bar{L}^3\bar{R}^3(\tau)$  shown in Figure 45 (fourth), is neither  $\text{id}_n$  nor  $\text{id}'_n$ .  $\square$

However, we are not done still. We need to deal with the problem, anticipated in Section 5.2, that the theorem on the pullback of  $\bar{q}_2$ , Thm. 5.18, is less precise than what we need, as it does not rule out the possibility that classes of different sign remain non-connected after the application of  $q_2$  (which sets the sign to zero), in which case we would have two classes with the same invariant  $(\lambda, 2, 0)$  one coming from a sign  $s = +1$ , the other from  $s = -1$ . For this we have a trivial preparatory observation:

**Lemma 6.6.** *Let  $\lambda \cup \{2\}$  be an integer partition, with an even number of even parts. The two following facts are equivalent:*

1. There exists a value of  $j$  such that  $(\lambda \setminus j) \cup \{j+1\}$  has a positive even number of even parts.
2.  $\lambda$  does not consist of a single (even) part.

*Proof.* Clearly  $\lambda$  has at least one even part. If it has also some odd part, its value is a valid candidate for  $j$ . If it has three or more even parts, all parts of  $\lambda$  are valid candidates. On the other side, if  $\lambda = \{2k\}$ , then  $j = 2k$  is the only candidate, and results in  $(\lambda \setminus j) \cup \{j+1\} = \{2k+1\}$ .  $\square$

This is used in the following (again, we use  $\lambda(j) \equiv \lambda \setminus j$ )

**Lemma 6.7** (Fusion of sign for  $q_2$ , ordinary case). *Let  $C$  be a class with invariant  $(\lambda, 2, 0)$ . Then, if  $\lambda$  does not consist of a single cycle of even length, there exists a value of  $j$ , and a class  $B_j$  with invariant  $(\lambda(j), j+1, 0)$ , such that  $\bar{q}_2(B_j) = C$ .*

*Proof.* By Theorem 5.18 we know that, given a class with invariant  $(\lambda, 2, 0)$ , then, for all  $j \in \lambda$ , there exists a class  $B_j$  with cycle invariant  $(\lambda(j), j+1)$ , such that  $\bar{q}_2(B_j) = C$ . By the previous lemma, if  $\lambda \neq \{2k\}$ , there exists one such  $j$  with  $(\lambda \setminus j) \cup \{j+1\}$  containing even parts, thus, by Lemma 6.1, the corresponding class must also have  $s(B_j) = 0$ , as claimed.  $\square$

In light of this lemma, the only possible instance of proliferation of disjoint classes which is still open, for which we need a separate argument, corresponds to the very special partitions  $\lambda$  escaping the characterisation above, i.e., referring to notations as in Lemma 6.7, the  $\lambda$ 's consisting of a single cycle of even length. These special cases are analysed in the following Lemma 6.9. We observe the trivial fact

**Lemma 6.8.** *Define  $C'_k = \bar{T}^{k-1}(\text{Id}_4)$  and  $C''_k = \bar{T}^{k-2}(\text{Id}_6)$ . Then  $C'_k$  has invariant  $(\emptyset, r = 2k+1, -1)$  and  $C''_k$  has invariant  $(\emptyset, r = 2k+1, +1)$ .*

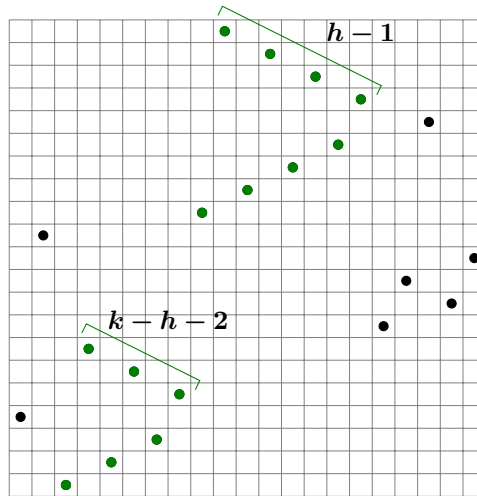
*Proof.* By corollary 4.7  $\text{Id}_4$  has invariant  $(\emptyset, 3, +1)$  while  $\text{Id}_6$  has invariant  $(\emptyset, 5, -1)$ . Then, the statement follows from the properties of  $\bar{T}$  implied by Corollary 4.8.  $\square$

Then we have

**Lemma 6.9** (Fusion of sign for  $q_2$ , special case). *For  $k \geq 3$ , define  $C'_k = \bar{T}^{k-1}(\text{Id}_4)$  and  $C''_k = \bar{T}^{k-2}(\text{Id}_6)$ , and similarly  $c'_k = T^{k-1}(\text{id}_4)$  and  $c''_k = T^{k-2}(\text{id}_6)$ . We have  $q_2(c'_k) \sim q_2(c''_k)$ , i.e.  $\bar{q}_2(C'_k) = \bar{q}_2(C''_k)$ .*

We split the proof in a few lemmas. We start with a definition.

**Definition 6.10.** *For  $k \geq 3$  and  $0 \leq h \leq k-3$ , call  $C_{k,h}$  the following configuration*



We have

**Proposition 6.11.**

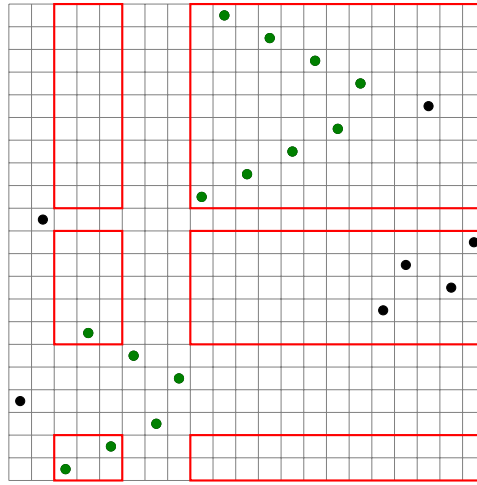
$$\begin{array}{|c|c|c|c|} \hline & a & & b \\ \hline \bullet & e & & d \\ \hline & & \bullet & \\ \hline \bullet & & & \\ \hline & e & \bullet & f \\ \hline \end{array} \xrightarrow{\bar{R}LR\bar{L}\bar{L}} \begin{array}{|c|c|c|c|} \hline & & a & \bullet \\ \hline & & \bullet & e \\ \hline & & & \bullet \\ \hline \bullet & & & e \\ \hline & & & f \\ \hline \end{array} \tag{53}$$

Note, the sequence above does *not* require to be boosted. In other words, the exponents in the boosted sequence are  $\alpha_j \in \{\pm 1\}$ .<sup>15</sup>

**Corollary 6.12.** For  $k \geq 4$  and  $0 \leq h < k - 3$ ,

$$C_{k,h} \xrightarrow{\bar{R}LR\bar{L}\bar{L}} C_{k,h+1}$$

It suffices to identify the blocks  $a, \dots, f$  in the boosted dynamics of Proposition 6.11 as follows:



□

Then we have the technical verifications

**Proposition 6.13.**

$$\bar{R}\bar{L}R^2L\bar{R}^3\bar{L}\bar{R}\bar{L}\bar{R}\bar{L}\bar{R}\bar{L}^2R^2q_2(c'_k) = C_{k,0}.$$

**Proposition 6.14.**

$$\bar{L}R^2L\bar{R}^2\bar{L}^4\bar{R}\bar{L}C_{k,k-3} = q_2(c''_k).$$

(the configurations involved in these two propositions are shown in Figure 46), which, together with Corollary 6.12, imply Lemma 6.9.

## 6.4 Classification of Rauzy classes

We are now ready to collect the large number of lemmas established so far into a proof of Theorem 1.13.

*Proof of Theorem 1.13.* By the results of Appendix C, we have a full understanding of the two exceptional classes  $\text{Id}_n$  and  $\text{Id}'_n$  (and, of course, we know their invariant), so that we can concentrate solely on (primitive) non-exceptional classes.

We proceed by induction. The theorem is established by explicit investigation for classes up to  $n = 8$ . Then, for the inductive step, we suppose that non-exceptional classes of size

<sup>15</sup>Also note that the green bullets on the right-hand-side are not the image of those on the left, they are just coloured for use in the following statement.



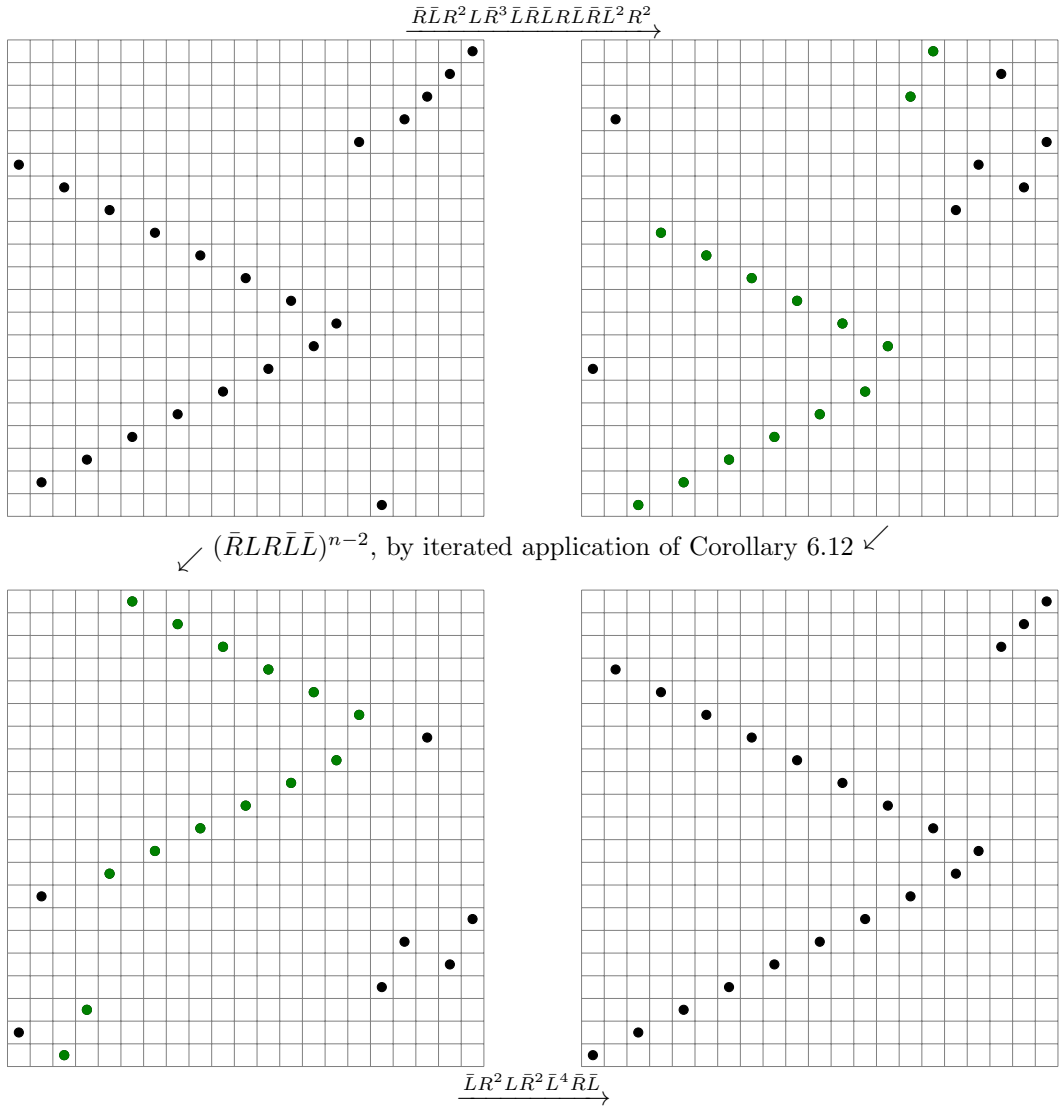


Figure 46: Illustration of Lemma 6.9. The configuration on the top left is  $q_2T^n(id_6)$ , and the one on the bottom right is  $\bar{L}q_2T^{n+1}(id_4)$ , for  $n = 7$ .

$n - 1$  and  $n$  are completely characterized by  $(\lambda, r, s)$ , in agreement with the statement of Theorem 1.13, and investigate classes at size  $n + 1$ .

Figure 47, in three copies for the three surgery operators  $\bar{T}$ ,  $\bar{q}_1$  and  $\bar{q}_2$ , illustrates a partition of the set of classes according to certain properties of the cycle invariant. This partition, despite containing ‘only’ 5 blocks for non-exceptional cases, is fine enough so that classes within the same block have a consistent behaviour w.r.t. all of our three surgery operators. These behaviours are represented through arrows. Recall that the operator  $\bar{T}$  increases the size by 2, while operators  $\bar{q}_{1,2}$  increase it by 1. The pullback theorems (Theorem 5.17, 5.18 and 5.5) of Section 5.1 and 5.2 justify the fact that, in order to prove that there exists *at least* one non-exceptional class per invariant, for the invariants listed in the theorem statement, it suffices to observe that, in the layer of largest size, all blocks of the partition have positive in-degree (when the three copies are considered altogether). This is steadily verified on the image.

For blocks which have in-degree higher than 1, we need our fusion lemmas to conclude that there exists *exactly* one non-exceptional class per invariant, for the invariants listed in

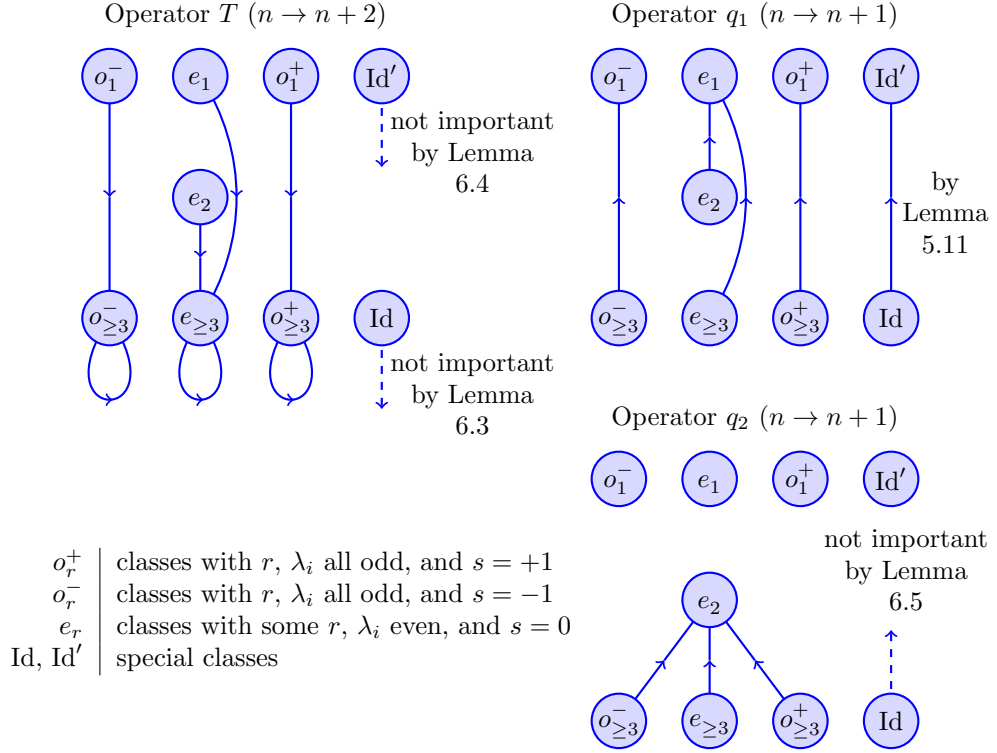


Figure 47: Inductive scheme for the application of operators  $T$ ,  $q_1$  and  $q_2$ .

the theorem statement.

In the following paragraph we recall which lemma justifies which arrow of the diagram, and how the fusion lemmas are used. We analyse the arrows in some order, according to the rank of the image of the operator.

We start with rank at least 3. By Theorem 5.5,  $\bar{T}$  is a surjection from classes of size  $n-1$  to classes of size  $n+1$  with rank at least 3 other than  $\text{Id}_{n+1}$ . Notice however that the classes of size  $n-1$  include  $\text{Id}_{n-1}$  and  $\text{Id}'_{n-1}$ . Nonetheless, by the ‘fusion’ Lemmas 6.3 and 6.4, there exist two non-exceptional classes,  $C_1$  and  $C_2$ , of size  $n-1$ , such that  $\bar{T}(\text{Id}_{n-1}) = \bar{T}(C_1)$  and  $\bar{T}(\text{Id}'_{n-1}) = \bar{T}(C_2)$ , thus  $\bar{T}$  provides a natural bijection from the set of non-exceptional classes of size  $n-1$  to the set of non-exceptional classes of size  $n+1$  with rank at least 3.

Now we pass to rank 1. By (the easy) Lemma 5.11  $\bar{q}_1(\text{Id}_n) = \text{Id}'_{n+1}$ , furthermore  $\bar{q}_1$  cannot be applied to  $\text{Id}'_n$  since  $\text{Id}'_n$  has rank 1. Thus the case of exceptional classes has been dealt with. By Theorem 5.17, if there exist two classes  $C_1$  and  $C_2$  with invariant  $(\lambda, 1, s)$  of size  $n+1$ , then this would imply that, for some  $i$  a part of  $\lambda$ , there exist also two classes of size  $n$  with invariant  $(\lambda(i), i, s)$ . So the induction step is proved for classes of rank 1.

Finally, we analyse classes of rank 2. Again the exceptional classes are ruled out, since  $\text{Id}'_n$  has rank 1, and, by the fusion Lemma 6.5, there exists  $C_1$  such that  $\bar{q}_2(\text{Id}_n) = \bar{q}_2(C_1)$ . So we are left only with the issue of the pullback of  $\bar{q}_2$ , among non-exceptional classes.

Theorem 5.18 tells us that for every  $C$  with invariant  $(\lambda, 2, 0)$ , for every  $j \in \lambda$  there exists some class  $B_j$  with invariant  $(\lambda(j), j+1)$  such that  $\bar{q}_1(B_j) = C$ , so there are two cases:

- One of these  $B_j$  has invariant  $(\lambda(j), j+1, 0)$ . In this case, as was above with  $q_1$ ,  $C$  is the only class with invariant  $(\lambda, 2, 0)$ .
- None of these  $B_j$  has invariant  $(\lambda(j), j+1, 0)$ . In this case it could be that all the classes  $B_j^+$  with invariant  $(\lambda(j), j+1, 1)$  give a class  $C^+$  with invariant  $(\lambda, 2, 0)$  and all the classes  $B_j^-$  with invariant  $(\lambda(j), j+1, -1)$  give a class  $C^-$ , distinct from  $C^+$ ,

with invariant  $(\lambda, 2, 0)$ . We need to rule out this possibility now, because this was not still excluded by the ‘weak’ Lemma 5.18.

Indeed, at this point we have all the elements to conclude that this does not happen: by Lemma 6.7, if no  $B_j$  has invariant  $(\lambda(j), j + 1, 0)$  then  $\lambda$  consists of a single cycle of even length (say, of length  $2k$ ), so the two candidate classes  $B^+$  and  $B^-$  must have invariant  $(\emptyset, 2k + 1, +1)$  and  $(\emptyset, 2k + 1, -1)$  respectively. By the induction and Lemma 6.8 we know that  $B^+ = \bar{T}^{k-2}(\text{Id}_6)$  and  $B^- = \bar{T}^{k-1}(\text{Id}_4)$ , and by Lemma 6.9 we know that for  $n$  large enough  $\bar{q}_2(B^+) = \bar{q}_2(B^-)$ .

This proves the induction step for classes of rank 2, and allows to conclude.  $\square$

Table 8 illustrates a typical step of the induction, at a size sufficiently large that all fusion lemmas are already in place, and all typical situations do occur.

Figure 48 shows the top-most part ( $4 \leq n \leq 8$ ) of the full decomposition tree associated to the action of  $T$ ,  $q_1$  and  $q_2$  operators on the classes. At difference with Table 8, this part is quite lacunary w.r.t. the general pattern. The relevant fact is that, for  $n > 8$ , there are no more exceptions (cf. the statements in Section 6.2 and 6.3, which hold under the hypotheses  $n \geq n_0$  for certain values of  $n_0$  all at most 8), so that this picture encompasses all of the small-size exceptional behaviour.

## 6.5 Classification of extended Rauzy classes

In this section we show how, by a crucial use of Lemma 3.9, the classification theorem for  $\mathcal{S}_n^{\text{ex}}$ , Theorem 1.14 descends from the one for  $\mathcal{S}_n$ , Theorem 1.13, as a rather straightforward corollary.

The idea is that, by including more operators for the dynamics on the same set of configurations, we may only join classes. As, in fact, most of the invariants for  $\mathcal{S}_n$  survive in  $\mathcal{S}_n^{\text{ex}}$  (essentially, only the rank is lost), as a matter of fact, and as we shall prove, there is no residual lack of connectivity: all classes of  $\mathcal{S}_n$  with the same structure of invariants except for the rank ultimately join together in  $\mathcal{S}_n^{\text{ex}}$ .

Let us define two involutions on  $\mathfrak{S}_n$ ,  $S$  and  $\bar{S}$ . The first one is defined as  $S\sigma = \sigma^{-1}$ , i.e., in matrix representation, it acts as a reflection along the main diagonal, and, in diagram representation, as a reflection along the horizontal axis. The operator  $S$  intertwines between the four operators in the  $\mathcal{S}_n^{\text{ex}}$  dynamics, i.e.  $SLS = L'$  and  $SRS = R'$ . Analogously, we have  $\bar{S}\sigma = \tau$  for  $s(i) = j \Leftrightarrow \tau(n + 1 - i) = n + 1 - j$ . Then,  $\bar{S}$  acts on permutations in matrix representation as a reflection along the main anti-diagonal, and on permutations in diagram representation as a reflection along the vertical axis, and intertwines between the four operators in the  $\mathcal{S}_n^{\text{ex}}$  dynamics as  $\bar{S}L\bar{S} = R'$  and  $\bar{S}R\bar{S} = L'$ .

Recall that, in Section 3.3, we defined permutations of type  $X$  and  $H$ , and the *principal cycle* in a type- $X$  permutation as the cycle passing through the ‘ $-1$  mark’. It is easy to establish

**Proposition 6.15.** *Let  $\sigma$  be an irreducible permutation of type  $H$ , with invariant  $(\lambda, r, s)$ . Then  $\sigma^{-1} = S\sigma$  is an irreducible permutation of type  $H$ , with invariant  $(\lambda, r, s)$ .*

*Let  $\sigma$  be an irreducible permutation of type  $X$ , with invariant  $(\lambda, r, s)$ , and principal cycle of length  $\bar{r}$ . Let  $\bar{\lambda} = \lambda \setminus \{\bar{r}\} \cup \{r\}$ . Then  $\sigma^{-1} = S\sigma$  is an irreducible permutation of type  $X$ , with invariant  $(\bar{\lambda}, \bar{r}, s)$  and principal cycle of length  $r$ .*

This follows from the diagrammatic construction of the invariants, which is symmetric w.r.t. the involution  $S$ , up to exchanging the lengths of the rank and of the principal cycle in type- $X$  permutations.  $\square$

Recall that we define  $\lambda' = \lambda \cup \{r\}$ , and that we have determined that  $\lambda'$  is invariant in the  $\mathcal{S}_n^{\text{ex}}$  dynamics.

For the proof Theorem 1.14 we need two ingredients. On one side, we need to deal with exceptional classes. For  $\text{Id}'_n$ , it is especially easy: this class has rank 1 at all  $n$ , thus it is not primitive in the  $\mathcal{S}^{\text{ex}}$  dynamics, and shall be discarded. So we are left to prove that the class

		$n = 9, 10$	$n = 11$
			new $((5), 5, -); \text{Id}$
by Lemma 6.3		$((2), 6, 0);$	$\bar{T} \rightarrow ((2), 8, 0);$
		$((3), 5, +);$	$\bar{T} \rightarrow ((3), 7, +);$
		$((3), 5, -);$	$\bar{T} \rightarrow ((3), 7, -);$
		$((4), 4, 0); \text{Id}$	$\bar{T} \rightarrow ((4), 6, 0);$
		$((4), 4, 0);$	
		$((5), 3, +);$	$\bar{T} \rightarrow ((5), 5, +);$
		$((5), 3, -);$	$\bar{T} \rightarrow ((5), 5, -);$
		$((6), 2, 0);$	$\bar{T} \rightarrow ((6), 4, 0);$
by Lemma 6.4		$((2, 2, 2), 2, 0);$	$\bar{T} \rightarrow ((2, 2, 2), 4, 0);$
		$((7), 1, +);$	$\bar{T} \rightarrow ((7), 3, +);$
		$((7), 1, +); \text{Id}'$	
		$((7), 1, -);$	$\bar{T} \rightarrow ((7), 3, -);$
		$((3, 2, 2), 1, 0);$	$\bar{T} \rightarrow ((3, 2, 2), 3, 0);$
		$((3, 2), 4, 0);$	$\bar{q}_2 \rightarrow ((3, 3, 2), 2, 0);$
by Lemma 6.9	$((3, 3), 3, +);$		
	$((3, 3), 3, -);$		
	$((2, 2), 5, 0);$	$\bar{q}_2 \rightarrow ((4, 2, 2), 2, 0);$	
	$((4, 2), 3, 0);$		
by Lemma 6.5	$((), 9, +);$	$\bar{q}_2 \rightarrow ((8), 2, 0);$	
	$((), 9, -);$		
	$((), 9, -); \text{Id}$		
by Lemma 5.11	$((), 9, +);$	$\bar{q}_1 \rightarrow ((9), 1, +);$	
	$((), 9, -);$	$\bar{q}_1 \rightarrow ((9), 1, -);$	
	$((), 9, -); \text{Id}$	$\bar{q}_1 \rightarrow ((9), 1, -); \text{Id}'$	
	$((5, 2), 2, 0);$	$\bar{q}_1 \rightarrow ((5, 2, 2), 1, 0);$	
	$((2, 2), 5, 0);$		
	$((4, 3), 2, 0);$		
	$((4, 2), 3, 0);$	$\bar{q}_1 \rightarrow ((4, 3, 2), 1, 0);$	
	$((3, 2), 4, 0);$		
	$((3, 3), 3, +);$	$\bar{q}_1 \rightarrow ((3, 3, 3), 1, +);$	
	$((3, 3), 3, -);$	$\bar{q}_1 \rightarrow ((3, 3, 3), 1, -);$	

Table 8: A typical step of the induction, at a size sufficiently large that all fusion lemmas are already in place, and all typical situations do occur. All classes at size  $n = 11$  (right column), except for  $\text{Id}_{11}$ , are obtained from classes at  $n = 9$ , under the action of  $\bar{T}$ , and classes at  $n = 10$  and rank large enough, under the action of  $\bar{q}_1$  (on classes with  $r \geq 2$ ) and  $\bar{q}_2$  (on classes with  $r \geq 3$ ). For comparison, the list of classes for  $n \leq 8$ , and their construction through surgery operators, is shown in figure 48.

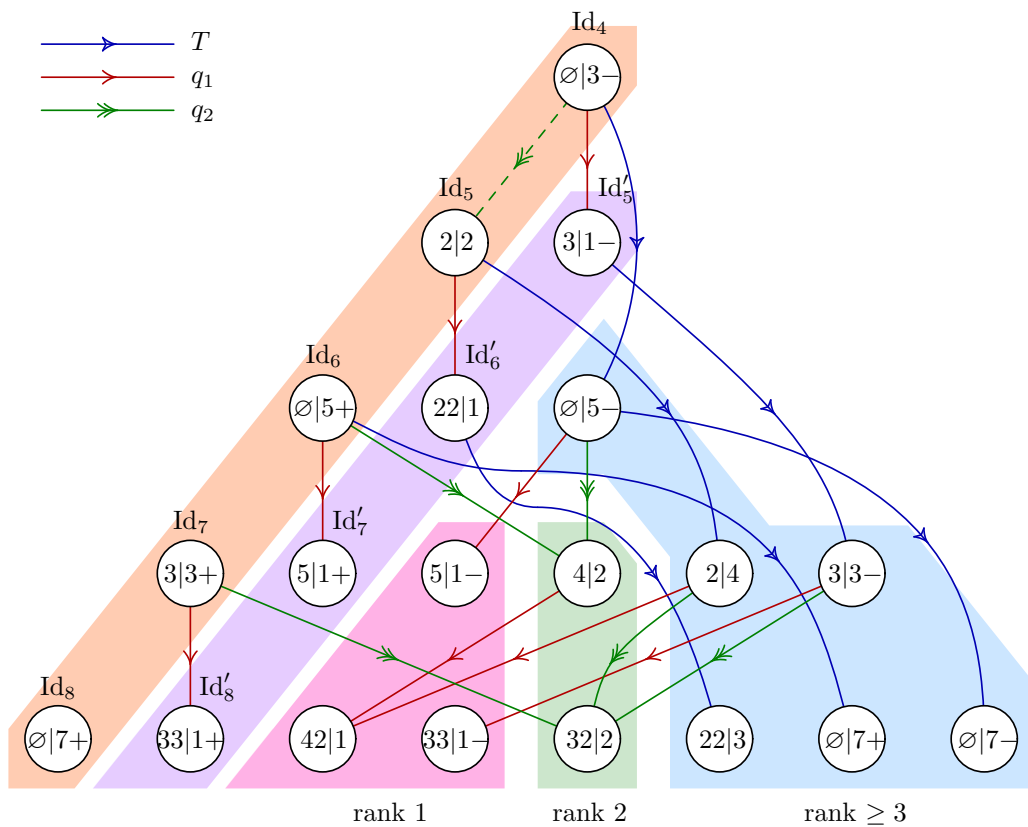


Figure 48: Full decomposition tree up to  $n = 8$ . Each balloon denotes a class, and contains its cycle and sign invariant, in the form  $\lambda_1 \lambda_2 \cdots \lambda_\ell |rs$ , with  $s \in \{+, -\}$  and omitted if zero.

$\text{Id}_n$  is not connected to other classes by the two further operators  $L'$  and  $R'$  of the dynamics. This is easily evinced from the results of Appendix C.1, in particular the organisation of the configurations in  $\text{Id}_n$  in a complete binary tree. The involution  $\bar{S}$  acts just as the vertical symmetry on this tree. As a result, the class  $\text{Id}_n$  is closed under the action of  $L$ ,  $R$  and  $\bar{S}$ , which, as  $L' = \bar{S}R\bar{S}$  and  $R' = \bar{S}L\bar{S}$ , implies closure under the action of  $L$ ,  $R$ ,  $L'$  and  $R'$ .

On the other side, we shall prove that all the non-exceptional classes of  $\mathcal{S}_n$  with same sign invariant, and cycle invariant  $(\lambda' \setminus \{\lambda'_i\}, \lambda'_i)$ , for  $i$  running over the different cycles of  $\lambda'$ , are connected by the extended dynamics. A first example occurs at size 7, where we shall show that the classes of  $\mathcal{S}_7$  with invariant  $(\{2\}, 4, 0)$  and  $(\{4\}, 2, 0)$  merge into a unique class with invariant  $(\{2, 4\}, 0)$ .

In fact, we shall prove an even stronger statement:

**Theorem 6.16.** *Any two configurations  $\sigma, \sigma'$  in the same class for the dynamics  $\mathcal{S}_n^{\text{ex}}$  are connected by a word of the form  $w = w_1(L')^k w_2$ , with  $k$  an integer, and  $w_1, w_2$  words in the  $\mathcal{S}_n$  dynamics.*

*Proof.* In other words, let  $\lambda' = \lambda \cup \{r_1, r_2\}$ , with  $r_1 \neq r_2$ . We want to prove that the classes  $C_1$  and  $C_2$  of  $\mathcal{S}_n$ , with invariants  $(\lambda \cup \{r_2\}, r_1, s)$  and  $(\lambda \cup \{r_1\}, r_2, s)$ , respectively, are connected in  $\mathcal{S}_n^{\text{ex}}$ , and through a word  $w$  of the type above.

Let  $\sigma \in C_1$  be a configuration in a standard family, and of type  $H(r'_1, r''_1)$  (thus with  $r'_1 + r''_1 = r_1$ ). From our classification theorem for  $\mathcal{S}_n$  we can restrict to such configurations with no loss of generality. It is easily seen that  $S\sigma$  is also standard, and has the same invariant in  $\mathcal{S}_n$  (by Proposition 6.15), thus  $\sigma \sim S\sigma$  in the  $\mathcal{S}_n$  dynamics.

By Lemma 3.9, for all  $r_2 \in \lambda$  there exists  $i$  such that  $L^i\sigma$  has form  $X(r_1, r_2)$ , and thus (by Proposition 6.15)  $SL^i\sigma = (L')^i S\sigma$  has form  $X(r_2, r_1)$ , and is thus in class  $C_2$ . This completes our proof.  $\square$

As remarked above, the stronger Theorem 6.16 implies Theorem 1.14 as a corollary.

## A Representation of Cayley graphs

This short appendix deals with a graphical convention on the representation of the dynamics.

Given a group dynamics with  $h + k$  generators  $\{\iota_1, \dots, \iota_h, \kappa_1, \dots, \kappa_k\}$ , of which  $h$  involutive and  $k$  non-involutive, a *Cayley (di)graph* can be constructed, with one connected component per equivalence class. Vertices  $v_x$  are associated to configurations  $x$ . The edges are labeled by a generator. They are unoriented in the case of involutive generators, and oriented otherwise. We have the unoriented edge  $(v_x, v_y)$  with label  $\iota_a$  if  $\iota_a x = y$ , and the oriented edge  $(v_x, v_y)$  with label  $\kappa_a$  if  $\kappa_a x = y$ . As a result, each vertex has overall degree  $h + 2k$ .

For dynamics with two (non-involutive) generators, such as  $\mathcal{S}_n$  and  $\mathcal{M}_n$ , the Cayley graph has thus degree 4. Even for relatively small classes, this makes a too complex structure for being visualised in an effective way. In this section we introduce a notation that, through an embedding on a two-dimensional grid, allows to omit to draw a fraction of the edges with no loss of information. As a result of this pruning, some of the Cayley graphs of classes are reduced to regular intelligible structures, this being in particular the case for exceptional classes, discussed in Appendix C. From this point on, we concentrate on the case of non-involutive generators.

Clearly, such an enhancement cannot be made for graphs in general, and we shall use the specialties coming from the fact that these graphs are Cayley graphs of a group action.

The iterated application of a single generator partitions a Cayley graph into cyclic orbits. Let us embed our graph in dimension  $d \geq 2$ , and choose a direction  $\theta_a$ , in the sphere of dimension  $d - 1$ , for each generator  $\kappa_a$ . If we take care of representing a directed edge with label  $\kappa_a$  as oriented in the direction  $\theta_a$ , then one edge per orbit can be omitted without loss of information: an orbit of length  $\ell$  is turned into a linear chain with  $\ell$  vertices and  $\ell - 1$  collinear oriented edges, and it will be understood without ambiguities that the image of the

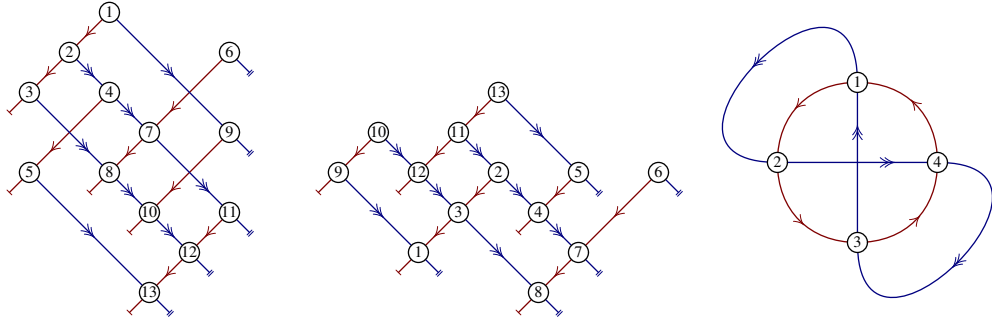


Figure 49: Left: Straight representation of a digraph. This representation is *not* planar. Middle: a planar straight representation of the same digraph. Right: a digraph which is not straight: the four vertices are in the same red and blue orbit, and cannot be simultaneously collinear along  $x$  and along  $y$ , on two distinct directions and in the given cyclic orderings, while staying distinct.

last vertex of the chain under the operator is the first vertex of the chain. In fact, edges can be omitted completely, and only the angles  $\theta_a$  be specified, at the condition that no other vertices, besides those in the orbit, lay on the line in  $\mathbb{R}^d$  associated to the orbit. If  $d = k$ , the directions  $\kappa_a$  can be taken to constitute the canonical basis without loss of generality.

The most useful application of this strategy is when there are two generators, and thus the graph is conveniently represented on a plane. In this special case, we will use edges with a single- or double-arrow, and in red or blue, for the two generators, and add a small tag on the last vertex of any chain, for further enhancing the visualisation.

See Figure 49, left, for an example of representation of such a digraph.

We say that a Cayley graph admitting a representation with these properties is *straight*, and if it admits a representation with these properties, and such that the edges do not cross, it is *straight planar*.

It is easy to see that if a graph is straight, it also allows a straight representation in which all vertices are distinct vertices of  $\mathbb{Z}^2$ , and different orbits are in different rows/columns of the grid, thus straight digraphs are also representable as finite subsets of  $\mathbb{Z}^2$ , and a list of rational numbers (one per generator) associated to the slopes.

It is also easy to see that not all digraphs are straight. See Figure 49, right, for a simple counter-example.

## B Non-primitive classes

In this appendix we discuss how the classification theorem on primitive classes implies, with a small amount of further reasoning, a classification theorem for all classes, including non-primitive ones. More generally, we prove how even the full structure of the Cayley graph of a non-primitive class can be evinced from the Cayley graph of the associated primitive class. This result is announced in Section 1.4.3.

Recall that we announced, in Corollary 1.12, that the map  $\text{prim}(\cdot)$  is a homomorphism for the dynamics, so that, as a result of the analysis performed below, if  $\sigma \in C$ , we can naturally define the *primitive*  $C' = \text{prim}(C)$  as the class containing  $\text{prim}(\sigma)$  for any  $\sigma \in C$ .

We start by discussing the most basic example of irreducible non-primitive class, namely the set of classes  $T_n$ , of size  $n \geq 2$ , such that  $\text{prim}(T_n) = \text{Id}_2$ .<sup>16</sup>

We claim that the class  $T_n$  has cardinality  $\binom{n}{2}$ , and that the Cayley graph admits an especially simple straight planar representation, illustrated in Figure 50, namely a triangular

<sup>16</sup>This is the smallest example among irreducible configurations, as if  $\text{prim}(\sigma) = \text{id}_1$  and  $\sigma \neq \text{id}_1$ , then  $\sigma$  is reducible.

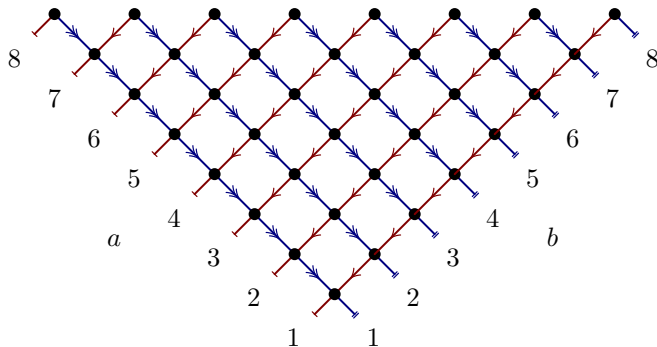


Figure 50: The straight representation of the Cayley graph of the class  $T_n$ . Here  $n = 9$ .

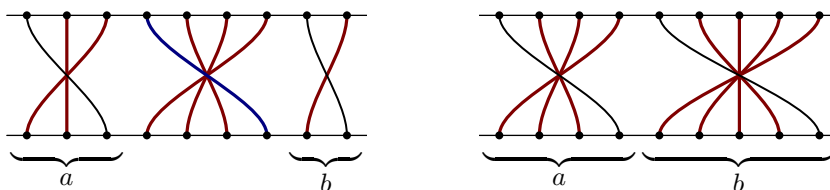


Figure 51: Left, the configuration with coordinate  $(a, b) = (3, 2)$  in  $T_9$ , composed of three bundles of crossing edges, and having a special descent. Right, the configuration with coordinate  $(a, b) = (4, 5)$  in  $T_9$ , composed of two bundles of crossing edges, and having no special descent.

portion of the square grid.

More precisely, w.r.t. the coordinates  $a$  and  $b$  shown in figure, we claim that the configurations with coordinate  $(a, b)$  are composed of three bundles, and have a special descent, if  $a + b < n$ , and are composed of two bundles, and have no special descent, if  $a + b = n$ , as shown in Figure 51. These facts are easily verified.

For a permutation  $\sigma$  of size  $n$ , with no special descent, call  $\tilde{\sigma}$  the permutation of size  $n + 1$  in which the special descent has been added:



Now we want to illustrate how the structure of classes  $T_n$  is sufficiently general to describe the local structure of non-primitive classes  $C$  in terms of the one of the class  $C' = \text{prim}(C)$ . Let  $n$  and  $n'$  be the sizes of classes  $C$  and  $C'$ . Let  $\sigma \in C$ , without a special descent, and  $\tau = \text{prim}(\sigma)$ . The configuration  $\sigma$  thus consists of  $n'$  bundles of crossing edges. Let  $\mathbf{m} = (m_1, \dots, m_{n'})$  be the cardinalities of these bundles (so that  $m_i \geq 1$  and  $m_1 + \dots + m_{n'} = n$ ). In particular, we single out the multiplicities of the two pivots, i.e.,  $\mathbf{m} = (m_1, \dots, m_{\tau^{-1}(n')}, \dots) =: (m_L, \dots, m_R, \dots)$ . The datum of the pair  $(\tau, \mathbf{m})$  is of course equivalent to  $\sigma$ . The following properties are easily verified:

- For  $i < m_L$ ,  $L^i \sigma$ , gives the permutation associated to  $(\tilde{\tau}, (m_L - i, \dots, i, m_R, \dots))$ . Similarly, for  $i < m_R$ ,  $R^i \sigma$  gives  $(\tilde{\tau}, (m_L, \dots, i, m_R - i, \dots))$ .
- $L^{m_L} \sigma$  gives  $(L\tau, (\dots, m_L, m_R, \dots))$ .
- Similarly,  $R^{m_R} \sigma$  gives  $(R\tau, (m_L, \dots, m_R, \dots))$ .



As a corollary, if  $m_L \geq 2$  we have that  $R^{-1}L\sigma$  gives  $(\tau, (m_L - 1, \dots, m_R + 1, \dots))$ , and if  $m_R \geq 2$  then  $L^{-1}R\sigma$  gives  $(\tau, (m_L + 1, \dots, m_R - 1, \dots))$ , which implies

$$(\tau, (m_L, \dots, m_R, \dots)) \sim (\tau, (m_L + c, \dots, m_R - c, \dots)) \quad \forall \quad -m_L + 1 \leq c \leq m_R - 1. \quad (54)$$

More generally, combining the remarks above, we have

$$\begin{aligned} (\tau, (m_L, \dots, m_R, \dots)) &\sim (\tilde{\tau}, (m_L - a, \dots, a + b, m_R - b, \dots)) \\ &\quad \forall a \leq m_L - 1, b \leq m_R - 1, a + b \geq 0 \\ &\sim (L\tau, (\dots, m_L + c, m_R - c, \dots)) \\ &\quad \forall -m_L + 1 \leq c \leq m_R - 1 \\ &\sim (R\tau, (m_L + c, \dots, m_R - c, \dots)) \\ &\quad \forall -m_L + 1 \leq c \leq m_R - 1. \end{aligned} \quad (55)$$

In other words, a portion of the Cayley graph for  $C$ , containing  $\sigma = (\tau, (m_L, \dots, m_R, \dots))$ , is isomorphic to a large patch of the class  $T_{m_L+m_R}$  represented in Figure 50, with the identification of parameters  $(a, b) = (m_L, m_R)$ , up to an important difference. For the class  $T_k$  in itself, according to the notation introduced in Appendix A, when we exit the straight-planar representation of  $T_k$  from one boundary, we come back to a vertex on another boundary of the same class. The portion of  $T_n$  within  $C$ , instead, is such that when we exit from the boundary of its planar representation, we enter into a different copy  $T_{k'}$ , and associated to a different set of omitted parameters  $(\tau', \mathbf{m}' \setminus \{m'_L, m'_R\})$ .

It is a fortunate coincidence that the simple straight representation of the class  $T_k$  presented above has the orbits cut exactly at the position at which the different copies of  $T_k$ 's are patched together.

*Proof of Proposition 1.11.* As another application of Lemma 3.12, we see that

$$(\tau, (m_1, m_2, \dots, m_n)) \sim (\tau, (m'_1, m'_2, \dots, m'_n))$$

whenever  $\sum_i m_i = \sum_i m'_i$ , and all  $m_i, m'_i$  are strictly positive. This implies the statement for  $\sigma$  having no special descent. A configuration  $\sigma'$  with a special descent is always at alternating distance 1 from a  $\sigma$  with no special descent, this allowing to complete the reasoning.  $\square$

The clarification of the Cayley graph of  $C$  in terms of the Cayley graph of  $C'$  has a corollary on the size of these graphs. Let  $C$  be a class of size  $n + k$ , with  $k$  descents. Then  $C'$  is a class of size  $n$ . Let  $\tau \in C'$ . Consider the number of configurations  $\sigma \in C$  which can be written as  $\sigma = (\tau, (m_L, \dots, m_R, \dots))$  (if  $\sigma$  has no special descent) or as  $\sigma = (\tilde{\tau}, (m_L, \dots, m_{\text{pivot}}, m_R, \dots))$  (if  $\sigma$  has a special descent). Identify  $(\tau, (m_L, \dots, m_R, \dots)) \equiv (\tilde{\tau}, (m_L, \dots, 0, m_R, \dots))$ , and consider the list  $(m_L - 1, m_2 - 1, \dots, m_{\text{pivot}} - 1, m_R - 1, \dots, m_n - 1) =: (k_1, \dots, k_{n+1})$ . At fixed  $\tau \in C'$ , each list with  $k_i \geq 0$  and  $\sum_i k_i = k$  is obtained from a single  $\sigma \in C$ , and lists not satisfying the properties above are never obtained. As a result, we have

**Proposition B.1.** *With notations as above,*

$$|C| = \binom{n+k}{n} |C'|. \quad (56)$$

A version of this proposition, for the case of the extended dynamics, has been first established by Delecroix in [Del13, Thm. 2.4]. His derivation is quite different in spirit, as it results from the analysis of a complicated general formula for  $|C|$ , instead of deriving directly the weaker (and easier) result on  $|C|/|C'|$ .

## C Exceptional classes

In this appendix we describe the structure of the Cayley graph of the classes  $\text{Id}_n$  and  $\text{Id}'_n$ , which we have called *exceptional classes* in the main text. This structure is so rigid that,

for any permutation  $\sigma$ , it is ‘easily’ tested if  $\sigma \text{Id}_n$ ,  $\sigma \in \text{Id}'_n$  or none of the two (by ‘easily’ we mean, in particular, that this can be tested in a time  $\sim n$ , instead of the naïve upper bound  $\sim 2^n$  based on the cardinality of these classes). This result is of crucial importance for our classification theorem, as the latter is based on a result of the form “a list of invariants for the dynamics is complete”. Our main invariants are the cycle (with the rank) and the sign. We have painfully proven that these invariants distinguish non-exceptional classes, however at generic  $n$  each of the two exceptional classes have the same cycle and sign invariant of one non-exceptional class, so that the complete list of invariants must include the boolean ‘exceptionality’ invariant, i.e. the outcome of the forementioned membership testing algorithm.

In this appendix, when using a matrix representation of configurations, it is useful to adopt the following notation: The symbol  $\epsilon$  denotes the  $0 \times 0$  empty matrix. The symbol  $\blacksquare$  denotes a square block in a matrix (of any size  $\geq 0$ ), filled with an identity matrix. A diagram, containing these special symbols and the ordinary bullets used through the rest of the paper, describes the set of all configurations that could be obtained by specifying the sizes of the identity blocks. In such a syntax, we can write equations of the like

$$\text{id} := \blacksquare = \epsilon \cup \begin{array}{|c|c|} \hline \blacksquare & \bullet \\ \hline \bullet & \blacksquare \\ \hline \end{array} = \epsilon \cup \begin{array}{|c|c|} \hline \bullet & \blacksquare \\ \hline \blacksquare & \bullet \\ \hline \end{array}; \quad \text{id}' := \begin{array}{|c|c|c|c|} \hline & & & \bullet \\ \hline & \bullet & & \\ \hline & & \blacksquare & \\ \hline \bullet & & & \\ \hline \end{array}. \quad (57)$$

The sets  $\text{id}$  and  $\text{id}'$  contain one element per size,  $\text{id}_n$  and  $\text{id}'_n$ , for  $n \geq 0$  and  $n \geq 3$  respectively.

The two exceptional classes  $\text{Id}_n$  and  $\text{Id}'_n$  contain the configurations  $\text{id}_n$  and  $\text{id}'_n$ , respectively (and are primitive for  $n \geq 4$  and  $n \geq 5$ , respectively).

## C.1 Classes $\text{Id}_n$

The structure of the classes  $\text{Id}_n$  is summarised by the following relation:

$$\text{Id} := \bigcup_n \text{Id}_n = \left( \bigcup_{k \geq 1} (X_{RL}^k \cup X_{LR}^k \cup X_{LL}^k \cup X_{RR}^k) \right) \cup \text{id} \quad (58)$$

where the configurations  $X_{\cdot\cdot}^k$  are defined as in figure 52 (discard colours for the moment).

In other words, we claim that the configurations in classes  $\text{Id}_n$  are partitioned into five disjoint sets: the identity configurations  $\text{id}_n$ , and those contained in the four sets  $X_{\cdot\cdot}^k$ , with  $\cdot = R, L$  and total size  $n$ . More in detail, the configuration  $\sigma_{RL}^{n;(i_1, j_1, \dots, i_k, j_k)} := R^{j_k+1} \dots L^{i_2+1} R^{j_1+1} L^{i_1+1} \text{id}_n$  is in  $X_{RL}^k$  whenever  $i_1 + j_1 + i_2 + \dots + j_k = n - 2k - 2 + \delta$ , with  $\delta \geq 0$ , and it is represented exactly as in figure 52, bottom-left, with red blocks having size  $i_1, i_2, \dots, i_k$ , (from bottom-right to top-left), blue blocks having size  $j_1, j_2, \dots, j_k$  (still from bottom-right to top-left), and the violet box having size  $\delta$ . The other three sets have similar definitions.

We also claim that the class  $\text{Id}_n$  has a straight planar representation (in the sense of Appendix A) consisting of a complete binary tree of height  $n - 2$  (and, in particular,  $|\text{Id}_n| = 2^{n-1} - 1$ ). An illustration of this fact for  $\text{Id}_6$  is presented in Figure 53. The root configuration of the tree is  $\text{id}_n$ . All the vertices of the tree can be described in terms of the unique path that reaches them starting from the root. When we have a vertex such that the corresponding path starts with  $i_1 + 1$  left-steps, followed by  $j_1 + 1$  right steps, followed by  $i_2 + 1$  left-steps, and so on, and finally terminating with  $j_k + 1$  right step, the corresponding configuration is the forementioned  $\sigma_{RL}^{n;(i_1, j_1, \dots, i_k, j_k)}$ . The other three cases are described analogously.

In order to see why this correspondence holds, we have to verify that the action of  $R$  and  $L$  on these configurations is consistent with this straight representation. The relations

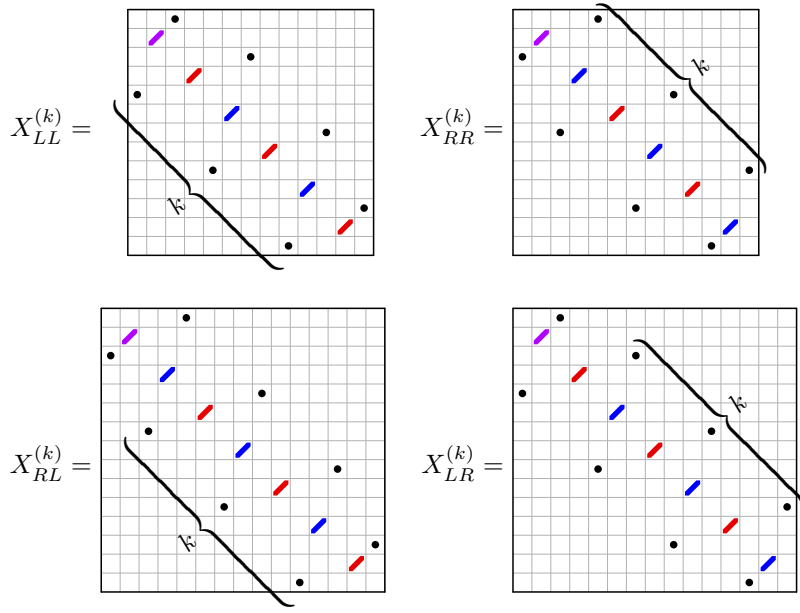


Figure 52: Description of the structure of configurations in the identity class  $\text{Id}_n$ , besides the configuration  $\text{id}_n$ .

implied by the straight representation as a binary tree are

$$L\sigma_{RL}^{n;(i_1, j_1, \dots, i_k, j_k)} = \begin{cases} \sigma_{LL}^{n;(i_1, j_1, \dots, i_k, j_k, 1)} & \delta \geq 1 \\ \sigma_{RL}^{n;(i_1, j_1, \dots, i_k, j_k)} & \delta = 0 \end{cases} \quad (59a)$$

$$R\sigma_{RL}^{n;(i_1, j_1, \dots, i_k, j_k)} = \begin{cases} \sigma_{RL}^{n;(i_1, j_1, \dots, i_k, j_k+1)} & \delta \geq 1 \\ \sigma_{LL}^{n;(i_1, j_1, \dots, i_k)} & \delta = 0 \end{cases} \quad (59b)$$

Similarly we have

$$L\sigma_{LL}^{n;(i_1, j_1, \dots, i_k)} = \begin{cases} \sigma_{LL}^{n;(i_1, j_1, \dots, i_k+1)} & \delta \geq 1 \\ \sigma_{RL}^{n;(i_1, j_1, \dots, j_k-1)} & \delta = 0 \end{cases} \quad (60a)$$

$$R\sigma_{LL}^{n;(i_1, j_1, \dots, i_k)} = \begin{cases} \sigma_{RL}^{n;(i_1, j_1, \dots, i_k, 1)} & \delta \geq 1 \\ \sigma_{LL}^{n;(i_1, j_1, \dots, i_k)} & \delta = 0 \end{cases} \quad (60b)$$

(the other two cases are treated analogously). Recalling that the graphical description of the dynamics, in matrix representation, is given by figure 2, we find that these equations are verified, as is illustrated in Figure 54 for equations (60) (the other cases are treated analogously)

The characterisation of  $\text{Id}_n$  has a couple of interesting consequences. A first one is the fact that  $\text{Id}_n$  has a unique standard family, containing  $\text{id}_n$  (this comes from the direct inspection of figure 52). The second one is the following

**Corollary C.1.** *We can decide in linear time if  $\sigma \in \text{Id}_n$ .*

*Proof.* It is easily seen that we can check in linear time if  $\sigma$  has one of the four structures of figure 52. In fact, for each of the two sets  $\text{id} \cup X_{RL} \cup X_{LL}$  and  $\text{id} \cup X_{LR} \cup X_{RR}$ , the test takes  $\sim 2n$  accesses to the matrix, if successful, and less than this if unsuccessful.

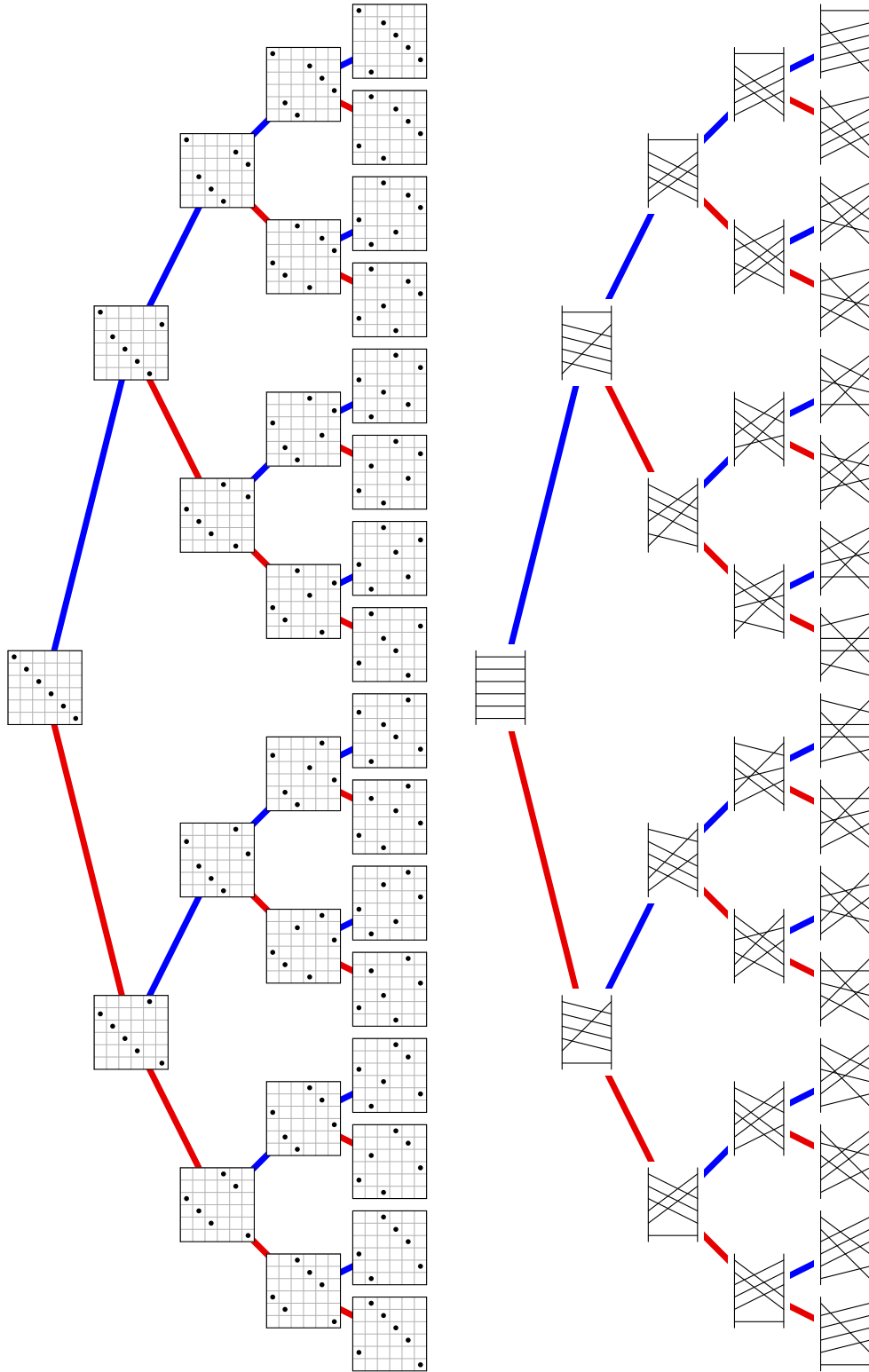


Figure 53: The Cayley graph of  $Id_6$ , with configurations in matrix and diagram representation. The image shall be observed rotated by 90 degrees (i.e., the root of the tree is on top). Red and blue edges correspond to actions of  $L$  and  $R$  respectively, and are omitted with the same rules of straight representations.

Another way of seeing this is to use a linear-time standardisation algorithm, and the uniqueness of the standard family. However, the naïve standardisation algorithm is quadratic in time. A linear algorithm exists, but we postpone its description to future work.

## C.2 Classes $\text{Id}'_n$

This class is somewhat more complicated than  $\text{Id}_n$ , however, within its exponential cardinality, the vast majority of configurations and transitions follow the same basic mechanism of  $\text{Id}_n$  (and are arranged into complete binary trees), the new ingredients being confined to a number, linear in  $n$ , of special configurations, with a simple structure (i.e., at generic  $n$ , described by a finite number of bullets and identity blocks).

We use again a straight representation of the Cayley graph. This could be represented in a planar way (with some edges being very stretched), but we will instead use a non-planar representation, illustrated in Figure 55 for the case of  $\text{Id}'_6$ .

Figure 56 illustrates the general structure of the class  $\text{Id}'_n$ . We observe four families of configurations:

- The three configurations  $\text{id}'$ ,  $L\text{id}'$  and  $R\text{id}'$ , which are on the top part of our straight

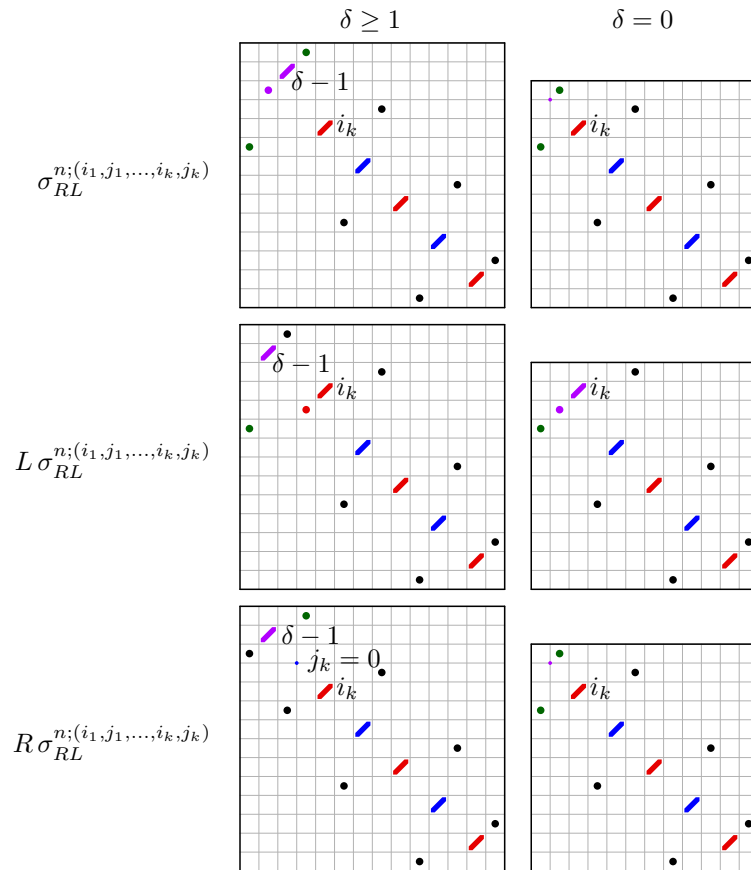


Figure 54: Action of the dynamics on a configuration in  $\text{Id}_n$ . We analyse separately the cases of  $\delta \geq 1$  (in this case we can single out one point in the top-right identity block) and  $\delta = 0$  (in this case we can omit the top-right identity block). In all the four cases we obtain a configuration in one of the four forms considered in figure 52, and all the sizes of the identity blocks, except for a finite number of blocks on the top-left corner, are left unchanged, this allowing for the analysis of a generic configuration.

representation of the Cayley graph.

- Two linear families of configurations, related one another by the symmetry of reflection along the diagonal, and denoted in green in the figures 55 and 56. An index  $1 \leq i \leq n - 3$  is associated to the size of one of the two diagonal blocks.
- One linear family of configurations, which are symmetric, and denoted in orange in the figures. Again, an index  $1 \leq i \leq n - 3$  is associated to the size of one of the two diagonal blocks.
- Two linear families, related one another by the symmetry, of subgraphs of the Cayley graph, isomorphic to the graph of  $\text{Id}_{n-i-2}$  except for one transition (interpret  $\text{Id}_0$  as an empty graph). These are denoted by the cyan triangles in the figures. In figure 56, the restriction to the yellow blocks of these configurations coincides with the corresponding configurations in  $\text{Id}_{n-i-2}$ .

At the light of the results of the previous section on the structure of  $\text{Id}$ , it is easy to verify that this Cayley graph indeed describes the dynamics on this class.

**Corollary C.2.**  $\text{Id}'_n$  has size  $2^{n-2} + n - 2$ .

*Proof.* We have the three configurations  $\text{id}'$ ,  $L\text{id}'$  and  $R\text{id}'$ , then  $2(n - 3)$  ‘green’ configurations (w.r.t. the colours of Figure 55),  $n - 3$  ‘orange’ ones, and  $2 \sum_{i=1}^{n-3} (2^{i-1} - 1) = 2^{n-2} - 2n + 4$  for the ‘cyan’ ones. Collecting all the summands gives the statement.

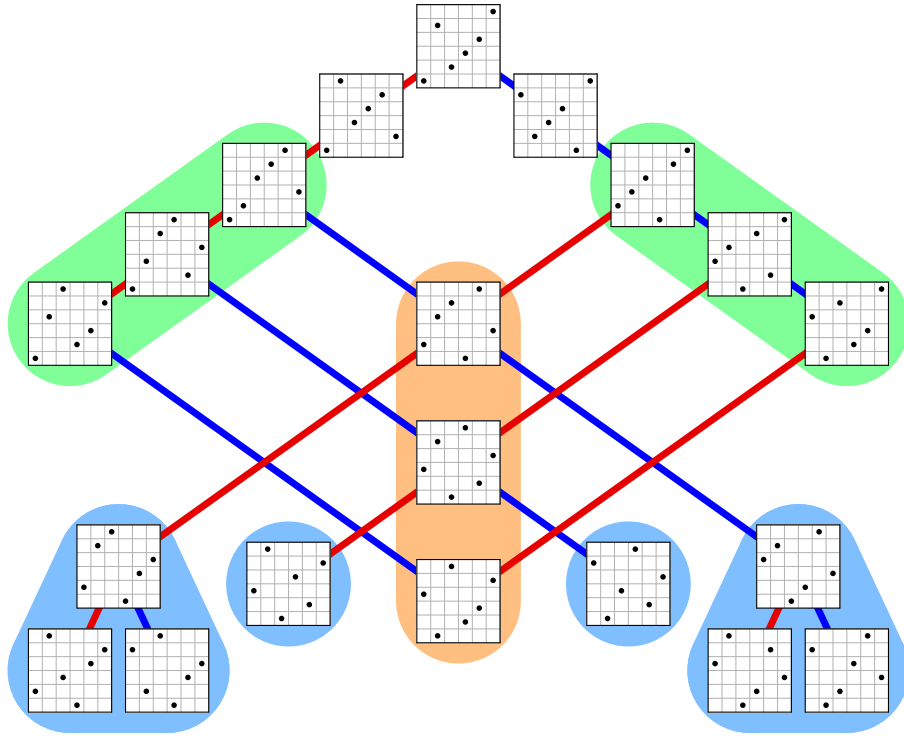


Figure 55: The Cayley graph of  $\text{Id}'_6$ , with configurations in matrix representation. Red and blue edges correspond to actions of  $L$  and  $R$  respectively, and are omitted with the same rules of straight representations. Green, orange and cyan blocks of configurations correspond to configurations with different structure, illustrated in the text. In particular, the cyan blocks are isomorphic to classes  $\text{Id}_k$ , except for the action of  $L^{-1}$  (or  $R^{-1}$ , depending on the position w.r.t. the vertical axis) on the root of the binary tree, and the action of  $L$  (resp.  $R$ ) on the left-most leaf of the tree (resp. right-most).

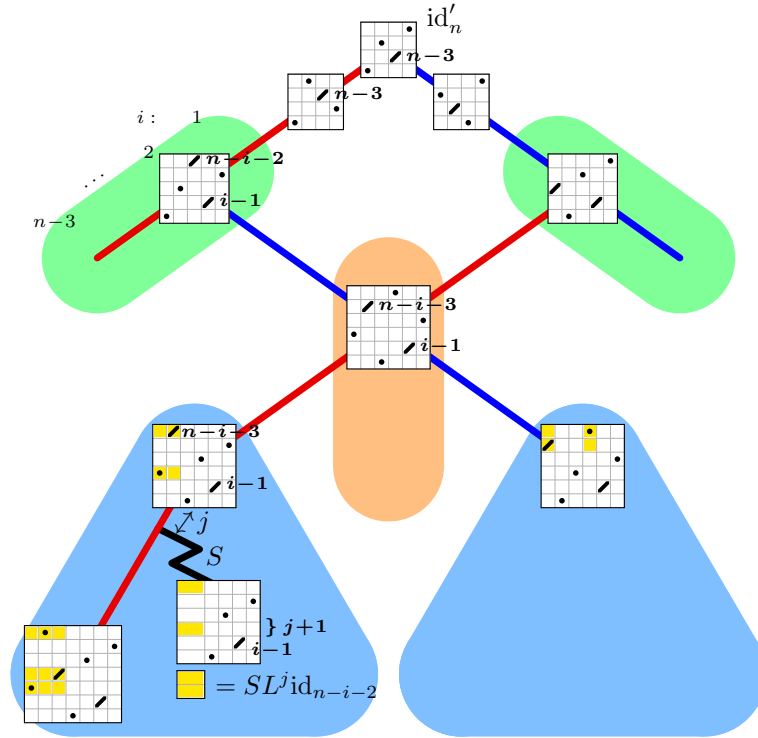


Figure 56: A schematisation of the Cayley graph of  $\text{Id}'_n$ , with configurations in matrix representation. Only a few branches are represented (the full structure is evinced from comparison with Figure 55). The configuration on the bottom-left corner has been added for clarity, in order to illustrate its ‘anomalous behaviour’ under the application of  $L$ , w.r.t. the copy of  $\text{Id}_{n-i-2}$  in which it is contained.

**Corollary C.3.** *We can decide in linear time if  $\sigma \in \text{Id}'_n$ .*

*Proof.* All configurations in  $\text{Id}'_n$  have either a structure described by a finite number of bullets and identity blocks, within the finite list of Figure 56, or a structure of this form, plus a block which is in the class  $\text{Id}_k$  for some  $k$ . With an argument similar to the one of Corollary C.1, and in light of the latter, we can thus conclude.

### C.3 Synthetic presentation of classes $\text{Id}_n$ and $\text{Id}'_n$

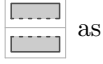
Instead of using the explicit descriptions of figures 52 and 56, we can describe the sets  $\text{Id}$  and  $\text{Id}'$  in a synthetic recursive way. To this aim we need a few definitions.

**Definition C.4.** *A configuration  $\sigma \in \text{Id}_n$  is of type  $(L, j)$  if  $\sigma(n) = j > \sigma^{-1}(1)$ , and it is of type  $(R, j)$  if  $\sigma(n) < j = \sigma^{-1}(1)$ . We denote by  $\text{Id}_n^{(L, j)}$  and  $\text{Id}_n^{(R, j)}$  the corresponding sets.*

**Proposition C.5.** *The configurations in  $\text{Id}_n$  are the disjoint union of  $\text{id}_n$ , configurations of type  $(L, j)$  for  $2 \leq j \leq n-1$ , and configurations of type  $(R, j)$  for  $2 \leq j \leq n-1$ . The set  $\text{Id}_n^{(R, j)}$  consists of the transpose of matrices in set  $\text{Id}_n^{(L, j)}$ .*

For compactness of the following expressions, we do the identification  $\text{id} \equiv \text{Id}_n^{(L, 1)} \equiv \text{Id}_n^{(R, 1)}$ , and we introduce  $\text{Id}_n(L) = \cup_{j \geq 1} \text{Id}_n^{(L, j)}$ , and similarly for  $\text{Id}_n(R)$ .

Define also recursively the family of square matrices divided into two rectangular blocks



$$\begin{array}{|c|} \hline \text{---} \\ \hline \text{---} \\ \hline \end{array} = \begin{array}{|c|c|} \hline \text{---} & \text{---} \\ \hline \text{---} & \text{---} \\ \hline \end{array} = \epsilon \cup \begin{array}{|c|c|} \hline \text{---} & \text{---} \\ \hline \text{---} & \text{---} \\ \hline \end{array} \quad (61)$$

Then the set  $\text{Id}$  defined as

$$\text{Id} = \text{Id}(L) \cup \text{Id}(R); \quad \text{Id}(L) \cap \text{Id}(R) = \text{id}; \quad (62)$$

$$\text{Id}(L) := \begin{array}{|c|c|} \hline \text{---} & \bullet \\ \hline \text{---} & \\ \hline \text{---} & \\ \hline \end{array}; \quad \text{Id}(R) := \begin{array}{|c|c|} \hline \text{---} & \\ \hline \text{---} & \bullet \\ \hline \text{---} & \\ \hline \end{array}; \quad (63)$$

consists of configurations of size  $\leq 3$ , which are not primitive, and the union of  $\text{Id}_n$  for  $n \geq 4$ .

Similarly, the set  $\text{Id}'$  defined as follows

$$\text{Id}' = \text{Id}'(L) \cup \text{Id}'(R) \cup \text{Id}'(T); \quad \text{Id}'(R) = (\text{Id}'(L))^T; \quad (64)$$

$$(\text{Id}'(L) \cup \text{Id}'(R)) \cap \text{Id}'(T) = \emptyset; \quad \text{Id}'(L) \cap \text{Id}'(R) = \text{id}'; \quad (65)$$

$$\text{Id}'(T) = \begin{array}{|c|c|c|} \hline \bullet & & \bullet \\ \hline \bullet & \diagup & \bullet \\ \hline & & \bullet \\ \hline \bullet & \diagdown & \\ \hline & & \bullet \\ \hline \end{array}; \quad \text{Id}'(L) = \begin{array}{|c|c|} \hline \bullet & \bullet \\ \hline \bullet & \diagup \\ \hline \bullet & \bullet \\ \hline \end{array} \cup \begin{array}{|c|c|} \hline \bullet & \bullet \\ \hline \bullet & \diagdown \\ \hline \bullet & \bullet \\ \hline \end{array} \cup \begin{array}{|c|c|} \hline \text{---} & \text{---} \\ \hline \bullet & \bullet \\ \hline \bullet & \bullet \\ \hline \end{array}; \quad (66)$$

consists of configurations of size 3 and 4, which are not primitive, and the union of  $\text{Id}'_n$  for  $n \geq 5$ .

Note that, with respect to the notations of Section C.1, we have  $\text{Id}(L) = \text{id} \cup X_{RL} \cup X_{LL}$  and  $\text{Id}(R) = \text{id} \cup X_{LR} \cup X_{RR}$ , and with respect to the notations of Section C.2 we have that  $\text{Id}'(T)$  contains the orange configurations, and  $\text{Id}'(L)$ ,  $\text{Id}'(R)$  both contain  $\text{id}'$ , and for the rest contain each half of the configurations which are not symmetric w.r.t. reflection along the diagonal.

## References

- [Ati71] Michael F. Atiyah. Riemann surfaces and spin structures. *Annales scientifiques de l'École Normale Supérieure*, 4(1): 47–62, 1971.
- [BL09] Corentin Boissy and Erwan Lanneau. Dynamics and geometry of the Rauzy–Veech induction for quadratic differentials. *Ergodic Theory and Dynamical Systems*, 29(3): 767–816, 006 2009.
- [BL12] Corentin Boissy and Erwan Lanneau. Pseudo-Anosov homeomorphisms on translation surfaces in hyperelliptic components have large entropy. *Geom. Funct. Anal.*, 22 (2012), no. 1, p. 74-106.
- [Boi12] Corentin Boissy. Classification of Rauzy classes in the moduli space of abelian and quadratic differentials. *Discrete Contin. Dyn. Syst.*, 32(10): 3433–3457, 2012.
- [Boi13] Corentin Boissy. Labeled Rauzy classes and framed translation surfaces. *Annales de l'Institut Fourier*, 63(2): 547–572, 2013.



- [Boi15] Corentin Boissy. Connected components of the strata of the moduli space of meromorphic differentials. *Comment. Math. Helv.*, 90: 255–286, 2015.
- [Del13] Vincent Delecroix. Cardinalités des classes de Rauzy. *Ann. Inst. Fourier*, 63(5): 1651–1715, 2013.
- [EMZ03] Alex Eskin, Howard Masur, and Anton Zorich. Moduli spaces of abelian differentials: the principal boundary, counting problems, and the Siegel–Veech constants. *Publications Mathématiques de l’IHÉS*, 97: 61–179, 2003.
- [Fic16] Jon Fickenscher. A combinatorial proof of the Kontsevich–Zorich–Boissy classification of Rauzy classes. *Discrete Contin. Dyn. Syst.*, 36(4): 1983–2025, 2016.
- [FM14] Giovanni Forni and Carlos Matheus. Introduction to Teichmüller theory and its applications to dynamics of interval exchange transformations, flows on surfaces and billiards. *Journal of Modern Dynamics*, 8(3/4): 271–436, 2014.
- [Yoc07] Jean-Christophe Yoccoz. Interval exchange maps and translation surfaces. In *Homogeneous Flows, Moduli Spaces and Arithmetic*, Clay Mathematics Proceedings, 2007.
- [Joh80] Dennis Johnson. Spin structures and quadratic forms on surfaces. *Journal of the London Mathematical Society*, s2-22(2): 365–373, 1980.
- [KZ03] Maxim Kontsevich and Anton Zorich. Connected components of the moduli spaces of abelian differentials with prescribed singularities. *Inventiones mathematicæ*, 153(3): 631–678, 2003.
- [Lan08] Erwan Lanneau. Connected components of the strata of the moduli spaces of quadratic differentials. *Annales scientifiques de l’École Normale Supérieure*, 41(1): 1–56, 2008.
- [Mas82] Howard Masur. Interval exchange transformations and measured foliations. *Ann. Math. (2)*, 115: 169–200, 1982.
- [Rau79] Gérard Rauzy. Échanges d’intervalles et transformations induites. *Acta Arithmetica*, 34(4): 315–328, 1979.
- [Vee82] William A. Veech. Gauss measures for transformations on the space of interval exchange maps. *Ann. Math. (2)*, 115: 201–242, 1982.
- [Zor06] Anton Zorich. Flat surfaces. In *Frontiers in Number Theory, Physics, and Geometry I*, pages 439–585. Springer, 2006.
- [Zor08] Anton Zorich. Explicit Jenkins–Strebel representatives of all strata of Abelian and quadratic differentials. *Journal of modern dynamics*, 2(1): 139–185, 2008.